Grant agreement no. 776479

COACCH

CO-designing the Assessment of Climate CHange costs

H2020-SC5-2016-2017/H2020-SC5-2017-OneStageB

D2.7. Macroeconomic, spatially-resolved impact assessment

Work Package:	2
Due date of deliverable:	M 32 (July/2020)
Actual submission date:	22/10/2020 – rev 07/03/2022
Start date of project: 01/DEC/2017	Duration: 42 months
Lead beneficiary for this deliverable:	CMCC
Contributors:	Francesco Bosello (CMCC), Gabriele Standardi (CMCC), Ramiro Parrado (CMCC), Shouro Dasgupta (CMCC), Gianni Guastella (FEEM), Massimiliano Rizzati (FEEM), Stefano Pareglio (FEEM), Jessie Schleypen (CA), Esther Boere (IIASA), Miroslav Batka (IIASA), Hugo Valin (IIASA), Benjamin Bodirsky (PIK), Daniel Lincke (GCF), Timothy Tiggeloven (VU), Kees van Ginkel (Deltares)

Dissemination Level		
PU	Public	X
CO	Confidential, only for members of the consortium (including the Commission Services)	
CI	Classified, as referred to in Commission Decision 2001/844/EC	

Disclaimer

The content of this deliverable does not reflect the official opinion of the European Union. Responsibility for the information and views expressed herein lies entirely with the author(s).

Suggested citation

Table of contents

Version log

Version	Date	Released by	Nature of Change
0.1	30/October/18	All partners	Request for input
0.2	29/June/20	CMCC	First draft
0.3	29/September/20	CMCC	Second draft
0.4	22/October/2020	CMCC	Final check by the coordinator
0.5	January/2022	CMCC	Updated with further simulations, robustness checks and uncertainty analysis
0.6	7/March/2022	CMCC	Last version incorporating suggestions by the reviewer

Summary

This deliverable assesses the higher order economic implications of climate change impact previously assessed by COACCH sectoral impact models, applying the ICES macroeconomic computable general equilibrium (CGE) model. Once computed, EU regional GDP performances in the presence of climate change, quantified by the ICES model, are further detailed at a higher spatial resolution applying statistical downscaling techniques. The analysis is completed by assessing potential distributional implications of the economic impacts.

Macroeconomic impacts are determined in the nine SSP-RCP scenario combinations used as reference in the COACCH project and, to fully characterize the uncertainty space, are specified for a low, a medium and a high impact case. The range is obtained using as input to the macroeconomic model, for each impact, in each year, in each region, the highest and the lowest value produced by the sectoral impact assessment exercises. These, on their turn, depend mostly upon the different climate models used to perturb the sectoral impact model. Given its relevance in a regional (sub national) context as examined, also two alternative specifications of investment mobility across EU areas, "high" and "low" are considered. In the first case there is a higher, in the second a lower, investment sensitivity to inter regional differentials in the rate of return to capital. This has a direct influence on how impacts propagate across regions, especially when the regional capital stock is affected. This applies mostly to sea-level rise and river flooding assessments. Under "high investment mobility" there is a higher transmission of negative shocks. Under "low investment mobility", losses tend to remain more confined in the region of origin.

In the majority of EU regions climate change impacts can become larger than 1-2% of regional GDP already by mid-century. As expected, this is more evident in the "high impact case" and in scenarios with the stronger climate signal: RCP6.0 and RCP8.5. This is evident in the high investment mobility case where impacts on GDP are exacerbated. Nonetheless, this result, even though partly moderated, is confirmed in the "low" and "medium impact" cases and also in the low investment mobility case. In the "high impact case" there are regions, mostly located in southern, but also western European countries where the loss is close to or larger than 5%. In Latvia the loss can potentially exceed 10%. Until 2050 macro-economic effects are quite similar across the SSP-RCP combinations. The ampler difference in the results indeed originates more by the choice of the impact forcing data, whether they are taken from the low, medium, or high impact case, or by investment mobility assumptions than by the different SSP-RCP combination.

In 2070 GDP impacts and their variability increase. There is an evident difference across the low and high investment mobility cases. Although losses prevail in both specifications, and the geographical distribution of macroeconomic effects is robust across setups, in the former, losses are smaller, and more regions may gain under a lower climate signal (either from lower warming scenarios or lower climate sensitivity). The divergence is almost entirely due to the behaviour of two impacts: primarily sea-level rise and partly riverine floods. These two impacts affect the regional capital assets. Investment reactions to capital return are thus one of the main drivers of systemic macroeconomic effects. Accordingly, the way in which investment mobility is modelled can play a large role. In the specific case, sea-level rise losses are considerably smaller and less widespread under low investment mobility. Given that sea-level rise costs are also among the larger sources of economic losses, this explains the width of difference.

The following dynamics can be further described:
- The low impact case highlights potential gains in agriculture, forestry, and fisheries in many EU regions. At the same time, negative impacts from other drivers are small. This eventually originates the possibility of net GDP gains in regions generally located in the central and northern EU, but also in some southern European countries where the local economic activity is particularly oriented to these sectors. Gains are however moderate (mostly lower than 1% of GDP) with just the exception of Bulgaria close to 5% of regional GDP in SSP1-RCP2.6. On average, over the sample of EU regions, losses prevail over gains. When present, losses are more widespread in southern EU regions, nonetheless they can affect northern areas mostly because of sea-level rise.
- Gains from agriculture, forestry and fishing that increase with climate change can originate, in some regions, lower net losses (or higher net gains) in a stronger climate signal scenario like RCP8.5 than in a more moderate one like RCP4.5.
- The main drivers of macroeconomic impacts from climate change are sea-level rise (especially in the high investment mobility case), riverine floods and crop

yield changes. Impacts on fishery and forestry (that in the majority of EU regions originate GDP gains), roughly comparable in magnitude with impacts on labour productivity, energy supply and demand (the latter inducing GDP losses), follow. Less relevant in terms of GDP effects (with some regional exceptions) are interruptions of road networks. On the one hand these can be good news as we demonstrated in sub section 2.2.4 that adaptation can deal cost-effectively with one of the most concerning of these climate change impact: sea level rise. On the other hand, less optimism is induced noting that positive GDP impacts in low and moderate warming scenarios, are due to investment mobility patterns or indirect trade effects for natural resource dependent sectors such as agriculture, forestry, and fishing. Some caution needs to be taken because of the high uncertainty associated with these dynamics and sectors, and because there may be other constraints.

An "analysis of variance" ANOVA was performed to quantify the role of the different uncertainty sources in determining the macroeconomic results. The larger are associated with investment mobility, closely followed by "impact model sensitivity", then by the choice of the climate scenarios and finally by the social economic scenarios. This analysis conveys important messages. It stresses the possibility to experience high economic losses also in low climate change scenarios. Uncertainty associated with the impact models, which in our case often coincides with climate sensitivity, is indeed a larger driver of economic losses than climate scenarios themselves.

Disaggregating this information to a higher geographical resolution would nonetheless allow to map the climate impacts more precisely, and to help the policymaker to develop more tailored and cost-effective actions. In this work, we apply statistical downscaling techniques to map the ICES scenarios results to a 1-Km resolution spatial grid that covers all the regions included in the ICES model. The projections for each year of each region's GDP, either baseline or following a climate impact, are distributed in the grid map according to each grid cell's share of projected artificial areas. Following the literature on the topic, we condition the projections of these artificial areas to each grid's cell level of total population. To obtain this variable, we downscale the total country-level population through a share of growth procedure based on the growth rates available for each SSP scenario. The impact of the grid's population changes influences then the prediction of the artificial area. We model this impact with a nested linear mixed model, which is regressed on satellite-based data available for the starting years of the ICES model and controlled by the inclusion of several auxiliary variables. This results in a collection of geographically explicit datasets at the grid's level that includes the downscaled GDP level for each baseline and each climate impact level projections. While useful for highlighting the most impacted areas and to compare the different scenarios, this methodology could further act as a starting point to model explicit spatial variations in the GDP distribution over time following climate impacts of different types.

The distributional analysis suggests that regions with the largest projected GDP loss in 2050 are the same regions with the lowest GDP per capita, the lowest share of the population with tertiary education, and the lowest life expectancy, historically, among the EU-27 + UK countries. The top GDP gainers are NUTS2 regions grouped under the cluster showing the highest projected GDP growth, the lowest population density, and below-average current mean temperature. In this sense climate change is amplifying inequality. At the same time improvement in health and higher education relates to higher GDP in the future, despite climate change impacts. The correlation to development indicators is, however, weak.

Furthermore, we do not see a clear pattern in relation to the largest GDP *gains* due to climate change.

Peer reviewed publications related to the deliverable:

Italian Ministry of Infrastructures and Sustainable Mobility (2022), "Cambiamenti Climatici, Infrastrutture e Mobilità". Available at: https://www.mit.gov.it/nfsmitgov/files/media/notizia/2022-02/Rapporto_Carraro_Mims.pdf

Spano D., et al. (2021), "G20 Climate Risk Atlas. Impacts, policy and economics in the G20", available at: https://www.cmcc.it/g20

United Nations Environment Programme (2021). Adaptation Gap Report 2021: The gathering storm – Adapting to climate change in a post-pandemic world. Nairobi. Available at: https://www.unep.org/resources/adaptation-gap-report-2021

Global Center on Adaptation (2021) State and Trends in Adaptation Report 2021: Africa, How Adaptation Can Make Africa Safer, Greener and More Prosperous in a Warming World, Conference Edition. Available at: https://gca.org/reports/state-and-trends-in-adaptation-report-2021/

1 Introduction and method (CMCC)

This deliverable operationalizes the second part of COACCH task 2.7: "Multi-scale cross-sectoral macroeconomic assessment". It assesses the higher order economic implications of climate change impact following the sectoral assessment delineated in task 2.7 by applying COACCH sectoral impact models (results reported in COACCH D2.2, D2.3, D2.4) and the ICES macroeconomic computable general equilibrium (CGE) model developed by CMCC that details with a subnational resolution (NUTS 0-2 level) the EU.

D2.7 is placed at the final step of the impact chain assessment methodology described in D2.1: "Protocol of information exchange flow and model integration" and summarized in Figure 1.
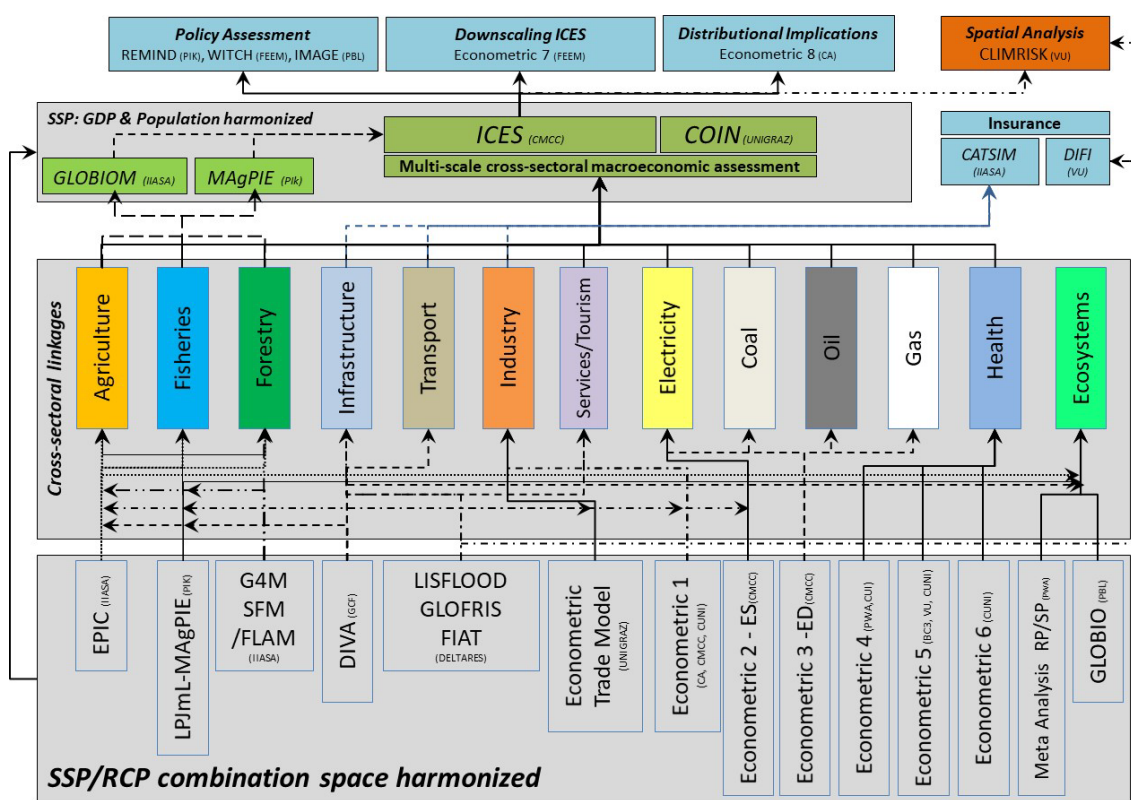

Figure 1. Representation of the vertical and horizontal integrated information exchange flows within the COACCH project

NUTS 2 results from the macroeconomic assessment are further downscaled at a higher resolution applying statistical downscaling techniques. The analysis is completed by assessing potential distributional implications of the economic impacts.

The organization of the deliverable is the following: section 2 describes the methodology used to conduct the macroeconomic assessment, and its results; section 3 presents the method and results of the downscaling procedure applied to detail at a 1 Km resolution spatial grid for the EU28, the ICES model results. Finally, section 3 discusses distributional implications of the macroeconomic impacts.

2 Macroeconomic assessment of climate change at regionalized scale

2.1 Macroeconomic assessment methodology

The description of the Intertemporal Computable Equilibrium System (ICES) model and of its application can be found in deliverable D2.2 of the COACCH project (Bosello and Parrado 2018), while the calibration procedure in milestone 8 (Bosello et al., 2019). The main feature of the model is to provide a multi-country, multi sector representation of the global economic system, developing for the EU a sub national description. As typical in CGE models, in ICES markets (or economic sectors) are connected, domestically and internationally, by trade flows of goods and services. These flows are governed by changes in prices determined by the interaction between demand and supply claims originated by profit maximizing representative firms and utility maximizing representative households. In doing so, price determination and exchanges across sectors are fully endogenous. Said differently: the model can track how a "shock" be it a policy signal (a tax or a quota) or climate change induced (a change in factors of production availability or "quality"; or shift in household expenditures) may affect the economic performance of a country or region , its sectoral production and commodity prices. The application of CGE models to the economic assessment of climate change impacts is quite consolidated in the literature. Recent examples are the efforts from the OECD (Dellink et al 2019), Feyen et al. (2020). The use of CGE models offers an alternative to the application of "hard linked" integrated assessment models like the DICE-RICE model family initiated by Nordhaus (Nordhaus , 2011) and represented in the COACCH project by models like CLIMRISK, WITCH, REMIND, and FAIR. This last category of models is characterized by the application of reduced-form climate change damage functions. In practice, a (most often quadratic) function translates temperature increases into GDP loss. This methodology is very appealing for its simplicity of application and allows the study of very complex climate policy decision processes like, for instance, strategic behaviour in international agreements, or choice in the presence of catastrophic uncertainty. It is however weaker in representing impacts on and from trade and, more in general, "market driven adaptation" i.e. how economic agents can react facing new price (i.e. scarcity) signals triggered by climate change shocks.

In what follows, the different categories of climate change impacts assessed in COACCH deliverables D2.2, D2.3, and D2.4 are translated into inputs for the ICES CGE model through appropriate changes in sectoral supply and demand schedules. The economic model then evaluates how these perturbations transform into regional gross domestic product (RGDP) changes once market have adjusted.

Macroeconomic impacts are determined in the nine SSP-RCP scenario combinations used as reference in the COACCH project and, to fully characterize the uncertainty space, are specified for a low, a medium and a high impact case. The range is obtained using as input to the macroeconomic model, for each impact, in each year, in each

region, the highest and the lowest value produced by the sectoral impact assessment exercises. These, on their turn, depend mostly upon the different climate model used to perturb the sectoral impact model. One of the distinctive features of COACCH is to provide a macroeconomic assessment of climate change impacts at the sub-national level for the EU. An important driver of macroeconomic impacts is how investment moves inter-regionally. Therefore, to offer a further robustness check of our findings, all results are also provided considering two different assumptions on investment mobility across EU regions. The first, called "high investment mobility" treats each EU region as all the other countries in the model: investment is free to move internationally and inter-regionally seeking the highest return. The second, called "low investment mobility", introduces a slightly different mechanism: international investment flows are firstly allocated across countries according to the usual rule of pursuing the highest return, but then are allocated inter-regionally following a proportionality criterion. In the first case there is a higher, in the second a lower, investment sensitivity to inter regional differentials in the rate of return to capital. This has a direct influence on how impacts propagate across regions, especially when the regional capital stock is affected. This applies mostly to sea-level rise and river flooding assessments. Under "high investment mobility" there is a higher transmission of negative shocks. Under "low investment mobility", losses tend to remain more confined in the region of origin. Each assumption is feasible and therefore presented to illustrate the potential range of economy-wide impacts, while we believe the actual behaviour lies in the middle.

2.2 Sectoral impact assessment

2.2.1 Agriculture

i. Source data and impact implementation in the CGE modelling

Data for the macroeconomic assessment of climate change impacts in the agricultural sector have been originated in COACCH D2.2 (Boere et al. 2019). Input information for the CGE model are yield changes that are implemented as changes in the productivity of the land primary production factor used by the representative agricultural firms in each of the ICES region.

Yield changes derive from two different assessments. One is performed by IIASA. It is based on the application of the biophysical model EPIC (Balkovič et al., 2013) whose gridded outputs are aggregated to the ICES regional resolution and crop categories with the GLOBIOM model (Havlík et al, 2011). The data has been generated based on 10 Global Circulation Models (GCMs) as detailed in Table 1.

The second input data for the macroeconomic assessment has been produced by PIK computing yield changes applying the biophysical model LPJmL (Bondeau et al., 2007). Data from PIK are based on 4 GCMs: HadGEM2-ES GCM, IPSL-CM5A-LR, GFDL-ESM2M, NorESM1-M. Only HadGEM2-ES provides information for all RCPs while the other GCMs include data only for RCP 4.5.

The yields effects computed do include the CO2 fertilization effect.

Table 1 reports the global circulation models applied in the IIASA and PIK assessments to detail impacts under the different climate scenarios.

Table 1 GCM and climate scenarios analyzed with the EPIC and LPJML models

Project	GCM	RCP2.6	RCP4.5	RCP6.0	RCP8.5
Euro-Cordex	RACMO22E-EC-EARTH		I		I
Euro-Cordex	RCA4-EC-EARTH	I	I		I
Euro-Cordex	RCA4-HadGEM2-ES		I		I
Euro-Cordex	REMO2009-MPI-ESM-LR	I	I		I
Euro-Cordex	IPSL-WRF33-CM5A		I		
ISIMIP FT	HadGEM2-ES	I, P	I, P	I, P	I, P
ISIMIP FT	IPSL-CM5A-LR	I	I, P	I	I
ISIMIP FT	GFDL-ESM2M	I	I, P	I	I
ISIMIP FT	MIROC-ESM-CHEM	I	I	I	I
ISIMIP FT	NorESM1-M	I	I, P	I	I

I = considered by IIASA impact assessment; P = considered by PIK impact assessment

IIASA data have been organized according to a "minimum", "maximum" and "medium" level of impact on yields, where the range was determined by the space spanned by the climate models used to perturb the crop model. This has been done for each SSP-RCP combination considered by the COACCH project.

Data from PIK have been used to offer a comparison across crop models and assess model uncertainty. This has been done just in the SSP2-RCP4.5 scenario combination and using the information from the 4 GCMs that both PIK and IIASA used.

ii. Simulation results

In the economic assessment of climate change impact on agriculture, the assumption on investment mobility plays a minor role, that is detectable only in 2070. Impacts, both positive and negative, are slightly smaller with low investment mobility, and qualitatively identical (see Figure 2, and Figure 3). According to yield data from the EPIC model, the overall GDP effects of climate change impacts on agriculture start to be detectable, in the EU, by mid-century, but mostly when yield losses are taken from the high damage estimates (Figure 2). In the medium damage case, regional GDP gains and losses range roughly between the -0.5 and the +1% in 2050 and between -1.8% and +2.4% in 2070. It is important to recall that the change in yields, input to the macroeconomic assessment, does take into account the CO_2 fertilization effect that smooths yield losses and often transforms them into gains. This is more evident in 2070. In many regions, the GDP losses in the high climate signal scenario RCP8.5, are smaller and less widespread than in RCP2.6 or 4.5. Losses also show a rather clear West-East pattern with especially the north-western part of France severely hit (Figure 3). There, GDP decline is between 1 and 2% in the medium damage case, irrespectively of the climate scenario. It can reach the 7.5-10% of regional GDP in the high damage case in the SSP55-RCP8.5 scenario combination. The vulnerability of southern EU is anyway partly confirmed with southern Spain and some southern Italian regions showing losses ranging from 2.5 to 5% of GDP.

Should impacts on yield fall in the low end of estimates, the EU is in fact projected to experience generalized gains in roughly all SSP-RCP scenario combination. The gains will be lower than the 5% of regional GDP.
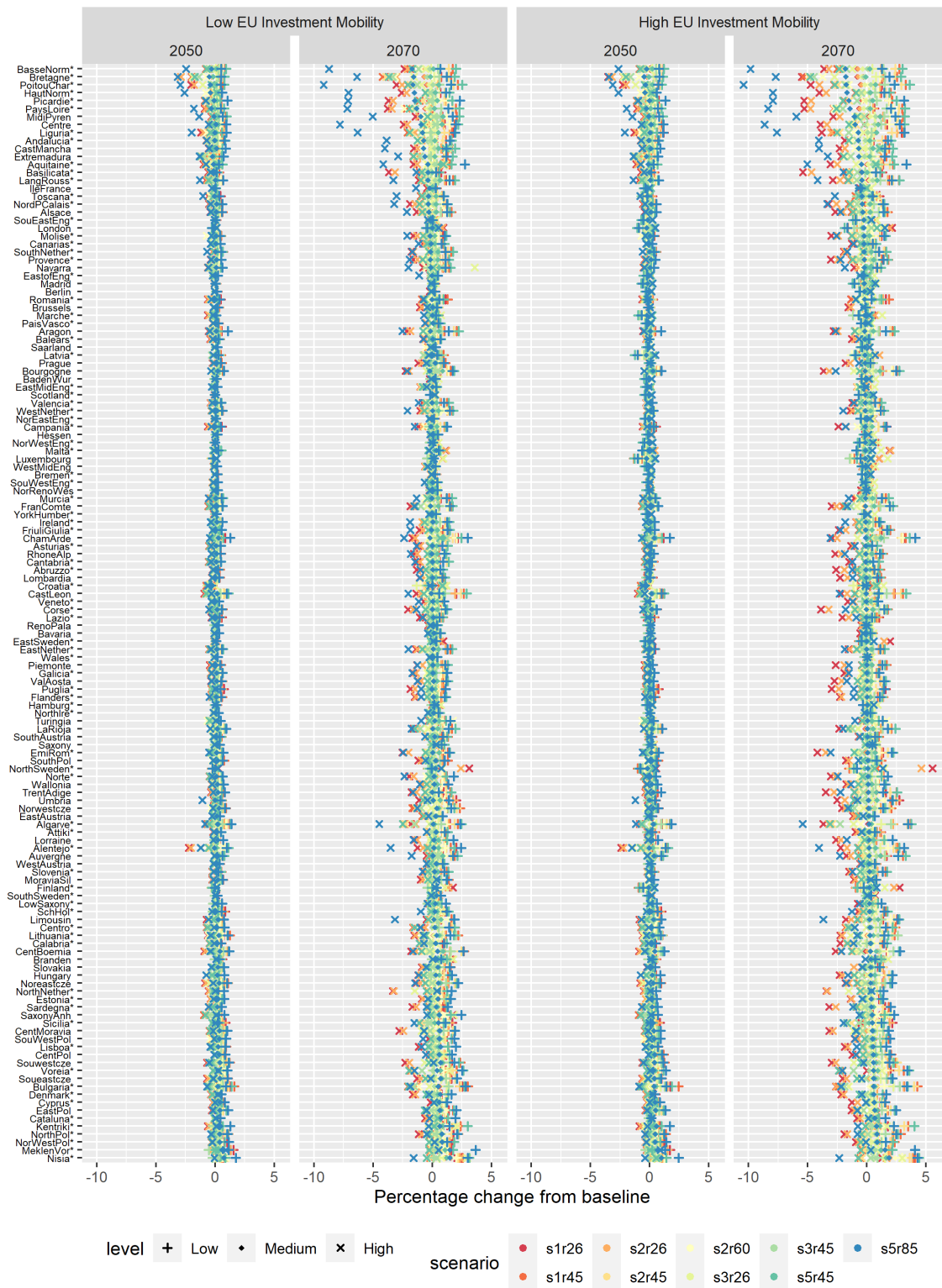
Figure 2. Climate change impacts on agriculture in the EU: GDP effects by region, scenario combination, climate sensitivity and assumption on interregional investment mobility for 2050 and 2070. Values are percentage changes from the baseline.
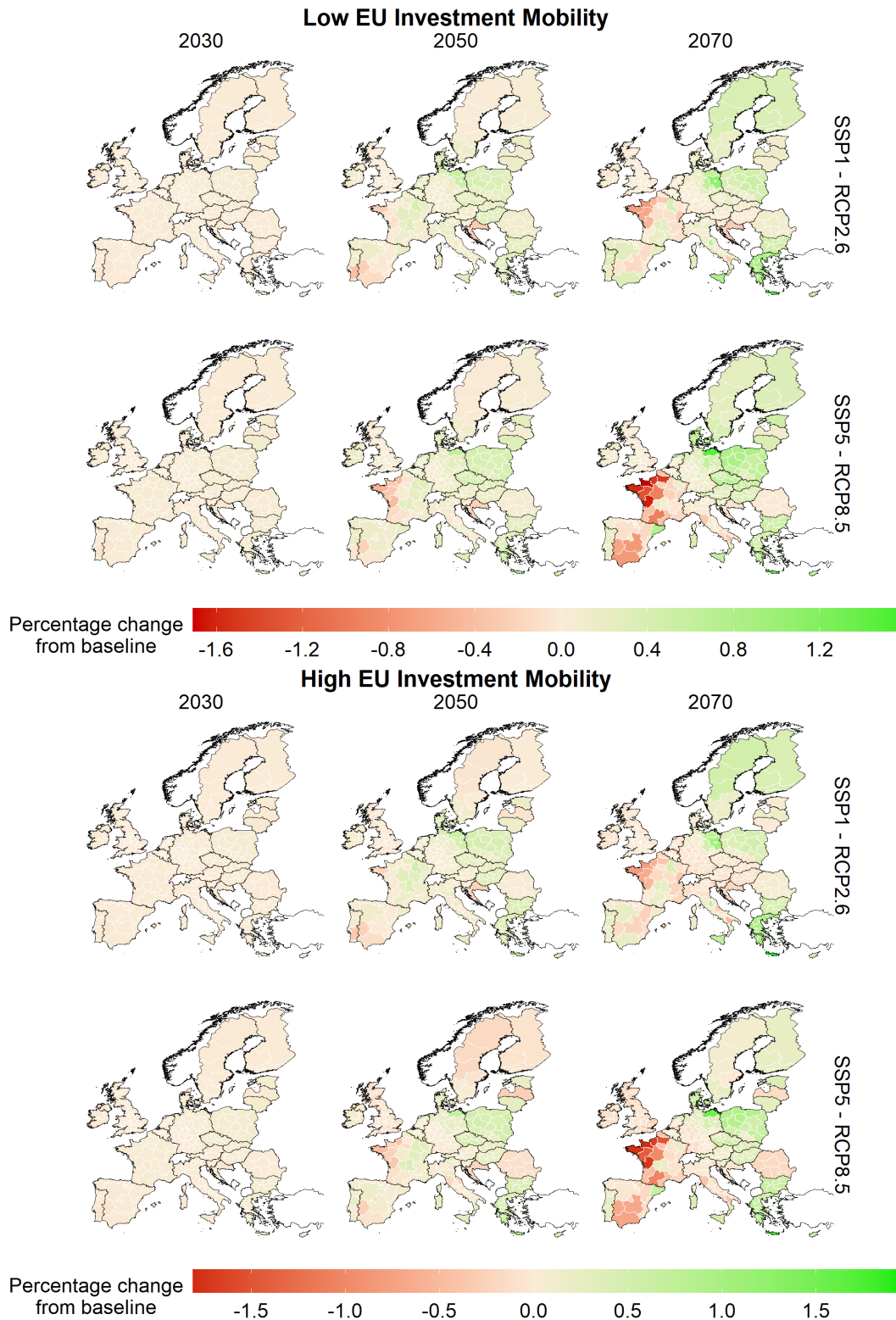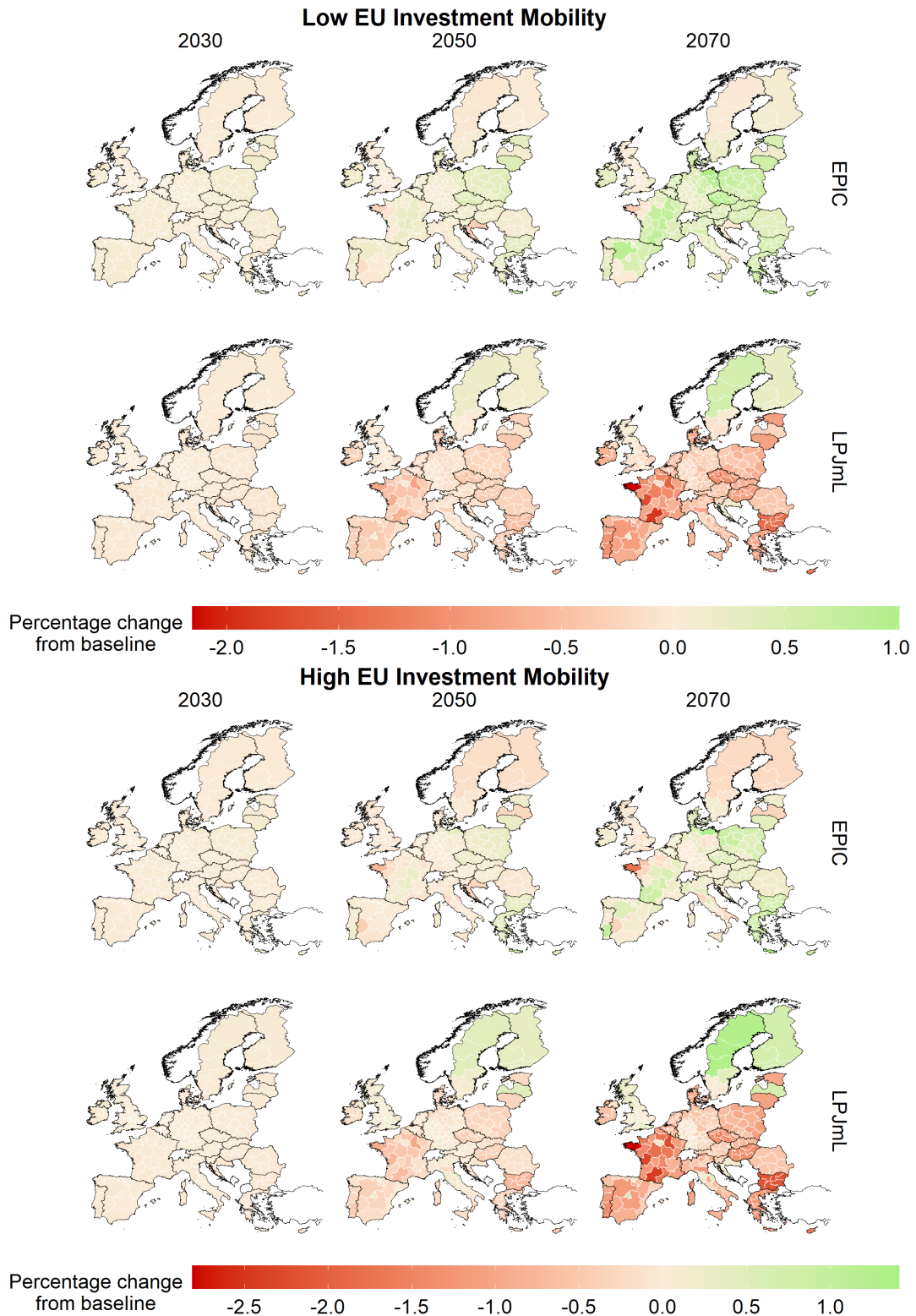
Figure 3 Climate change impacts on agriculture: GDP impacts by region in 2030, 2050 and 2070 in the MEDIUM impact-on-yield case, SSP1-RCP2.6 and SSP5-RCP8.5 comparison. Low investment mobility upper panel, high investment mobility lower panel. Values expressed in percentage change from the baseline.

Impact on yields from the LPJmL model are more clearly negative and, accordingly, regional GDP losses are larger. Figure 4 reports the EPIC vs LPJmL model comparison. Data for the SSP2-RCP4.5 scenario combination in the medium impact-on-yield case are reported (low and high cases in Figure 39 and Figure 40 of Appendix 1). Inputs from both models lead to a relatively higher vulnerability to economic losses from impacts on agriculture in the north western part of France, southern Spain, and Italy. In LPJmL however regional GDP losses are larger and more EU widespread. The EPIC and LPJmL models originate economic impacts with opposite sign in the Northern EU regions with LPJmL also depicting a clearer north-south pattern in regional GDP losses than EPIC.

Low EU Investment Mobility

High EU Investment Mobility

Figure 4. Climate change impacts on agriculture: GDP effects by region in 2030, 2050 and 2070 in the MEDIUM impact-on-yield case, SSP2-RCP4.5 scenario combination. EPIC, LPJmL comparison. Low investment mobility, upper panel, high investment mobility lower panel. All data expressed in percentage change from the baseline.

Figure 5 summarizes in a compact format all simulation results, for all the world regions of the ICES model, using EPIC inputs. In the low and medium impact-on-yield case, effects on GDP are mildly positive until 2050 in all the SSP-RCP combinations. In 2070, in the medium impact case GDP changes range between -4 and + 4%. In the high impact on yield case, GDP is impacted mostly negatively since 2030. It can be also appreciated that, due to the CO2 fertilization effect, low climate signal scenarios like RCP2.6 and 4.5 originate losses comparable to that of RCP8.5. The variance of results increases along time and especially moving from the low to the high impact case. In 2070 there are more regions experiencing a GDP loss between 5 and 10% than in other scenarios, even though other scenarios may show some regions with higher losses.
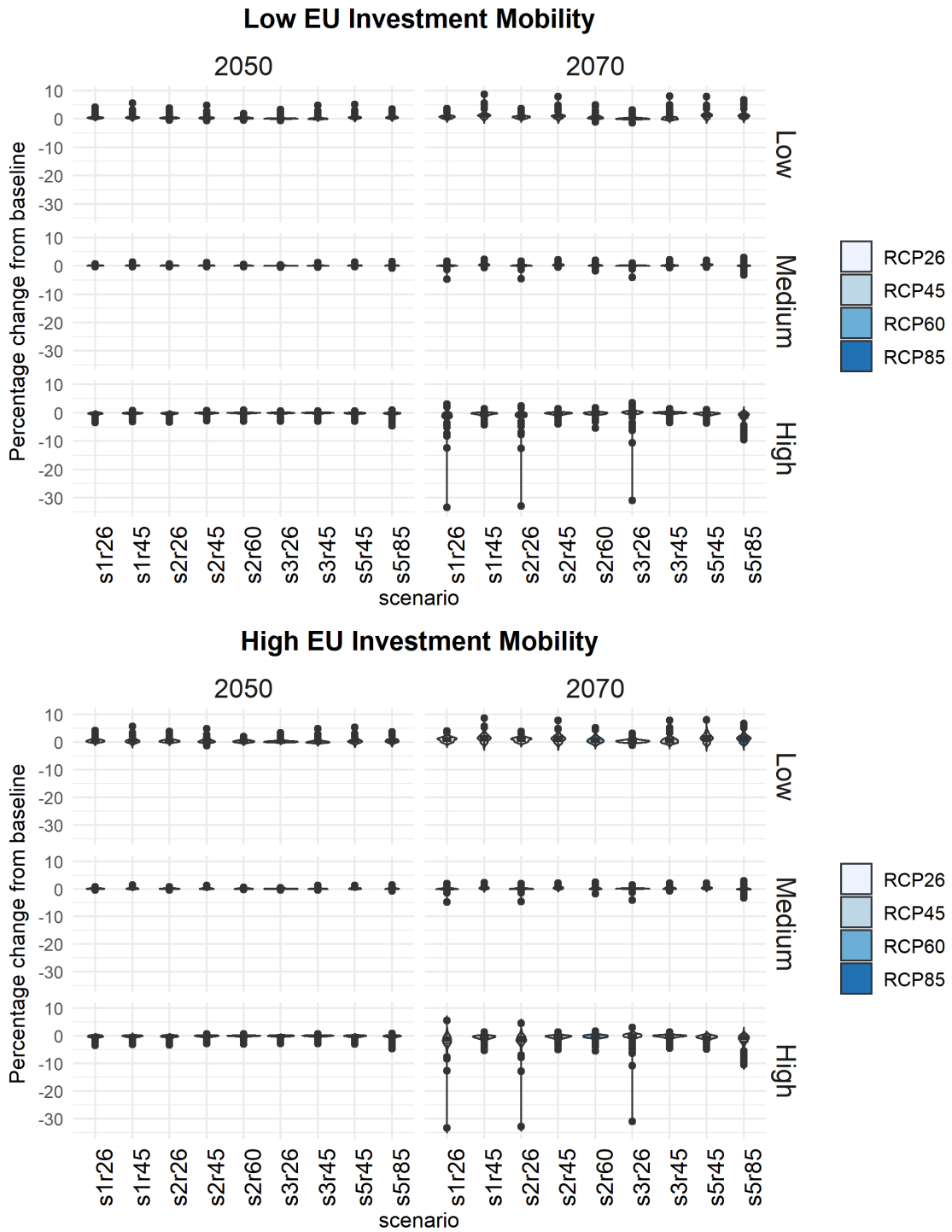
Figure 5 Climate change impacts on agriculture: distribution of GDP impacts across all regions of the ICES model in 2050 and 2070, all scenario combinations, low, medium and high impact on yield cases. Low investment mobility upper panel, high investment mobility lower panel. All data expressed in percentage change from the baseline.

2.2.2 Forestry

i. Impact modelling

Data for the macroeconomic assessment of climate change impacts in the forestry sector have been originated in COACCH D2.2 (Boere et al. 2019). Changes in net physical wood production per hectare are derived from the biophysical G4M model (Kindermann et al. 2008).

The GLOBIOM model has then been used to translate the grid resolution of G4M to the regional resolution of the ICES economic model.

For these simulations, only one GCM, the HadGEM2-ES model, has been used. Accordingly, it was not possible to characterize a high, low and medium range for impacts. Estimates have to be considered as a central or medium case. They are specified for the four RCPs 2.6, 4.5, 6.0 and 8.5.

Changes in forest yields are implemented in ICES as changes in the productivity of the natural resource input used by the regional representative timber (logging) industry.

Macroecomomic impacts are computed for all nine SSP-RCP scenario combinations considered by the COACCH project.

ii. Simulation results

Albeit the forestry sector builds a small percentage of value added in EU country economies (the highest are close to 4% in Alentejo and North Sweden), for some countries and regions, especially in the northern part of the EU, climate change impacts on forest productivity can be particularly troublesome in the SSP5-RCP8.5 scenario combination (Figure 6 and Figure 7). The results are partly driven by the relevance of the forestry sector in those regions, but also by a specific feature of the model baseline calibration process. The price of timber and fish resources has been calibrated to match projections from ECORYS (2012) for the fishery and timber sectors. According to projections, the price of these resources is expected to increase over the years more than that of capital and labour. Fish and wood resources are therefore becoming progressively more important in relative terms in value added. Accordingly, when these resources are hit negatively or positively by climate change impacts, effects on regional GDP can be substantive. This however occurs in the long term, when the "scarcity" of these resources is pronounced enough and the direct impacts on the resource are also substantive. The SSP5-RCP8.5 scenario combination in 2070 depicts well this situation marking a quite evident difference with respect to the other scenarios (Figure 8). Until 2050 GDP effects remain modest in all regions with the partial exception of Finland, Northern Sweden and Latvia that show losses slightly larger than the 1% of their regional GDP. Also in this case, economic impacts that mostly derive from effect on the natural resource stock, are quite insensitive to different assumptions of inter-regional investment mobility. Still, with lower mobility negative impacts tend to be slightly smaller.
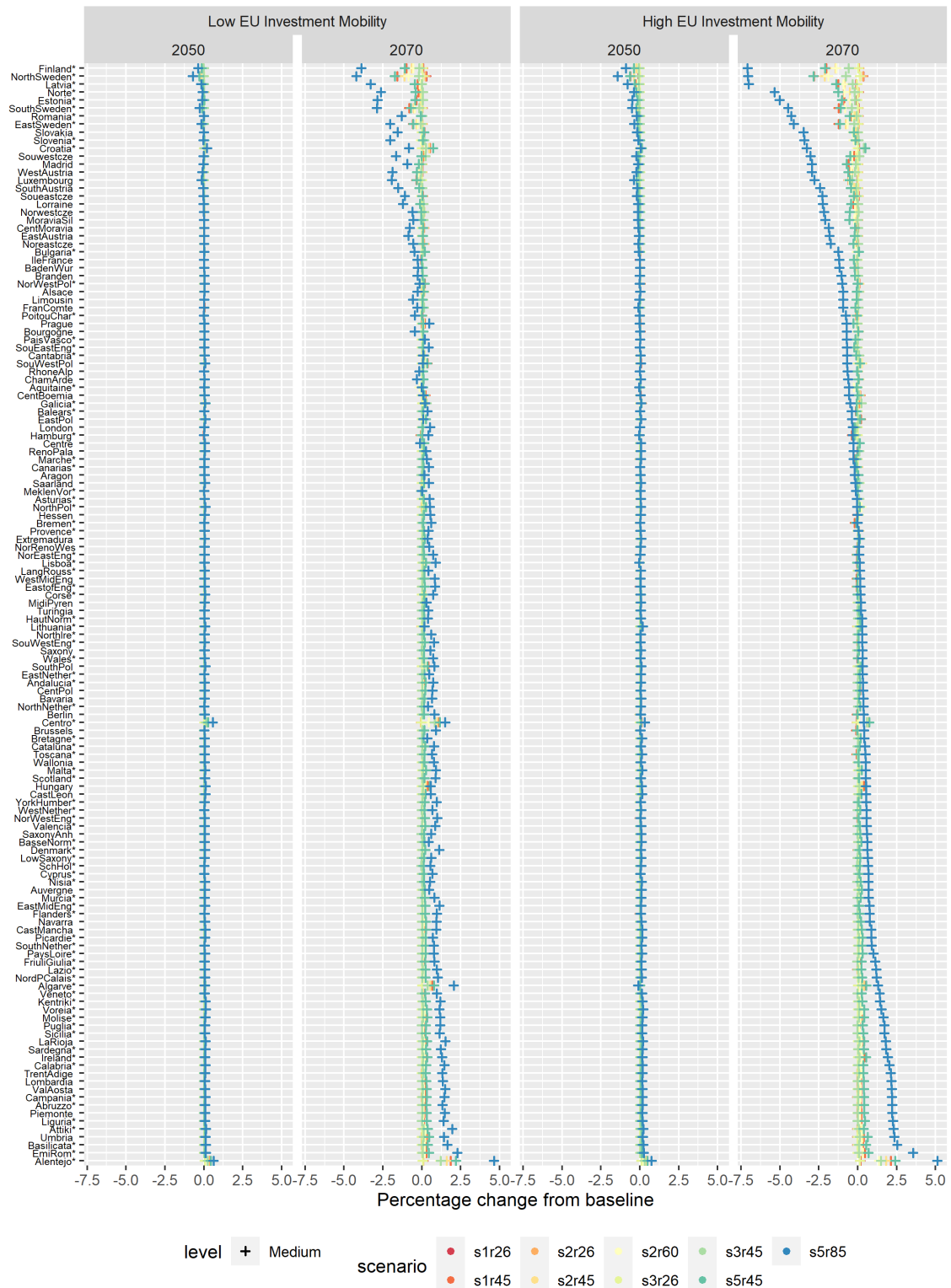
Figure 6 Climate change impacts on forestry in the EU: GDP effects by region, scenario combination, and assumption on interregional investment mobility for 2050 and 2070. Values are percentage changes from the baseline.
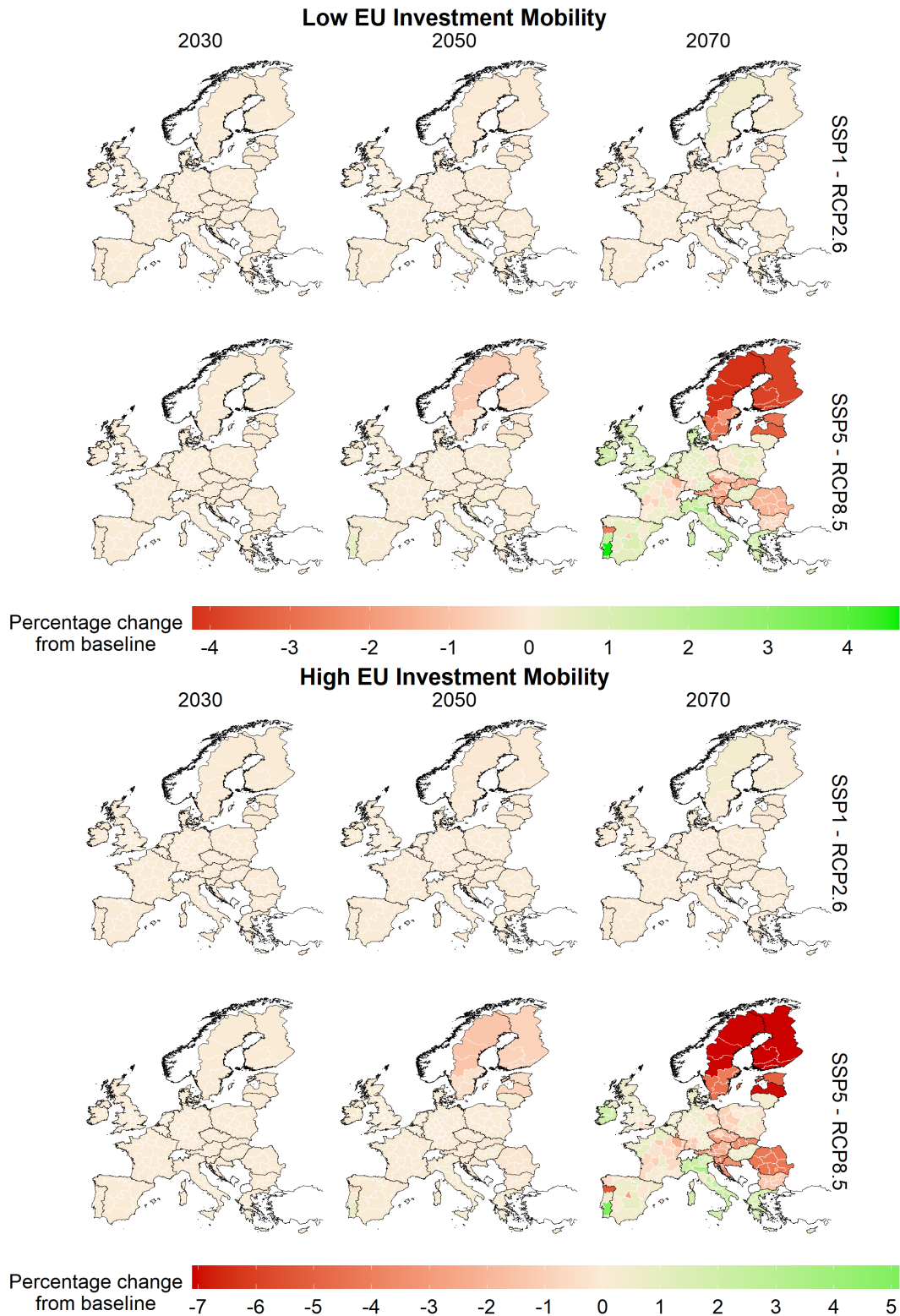
Figure 7 Climate change impacts on forestry: GDP effects by region and scenario combination in 2030, 2050 and 2070. SSP1-RCP2.6 and SSP5-RCP8.5 comparison. Values are percentage changes from the baseline.
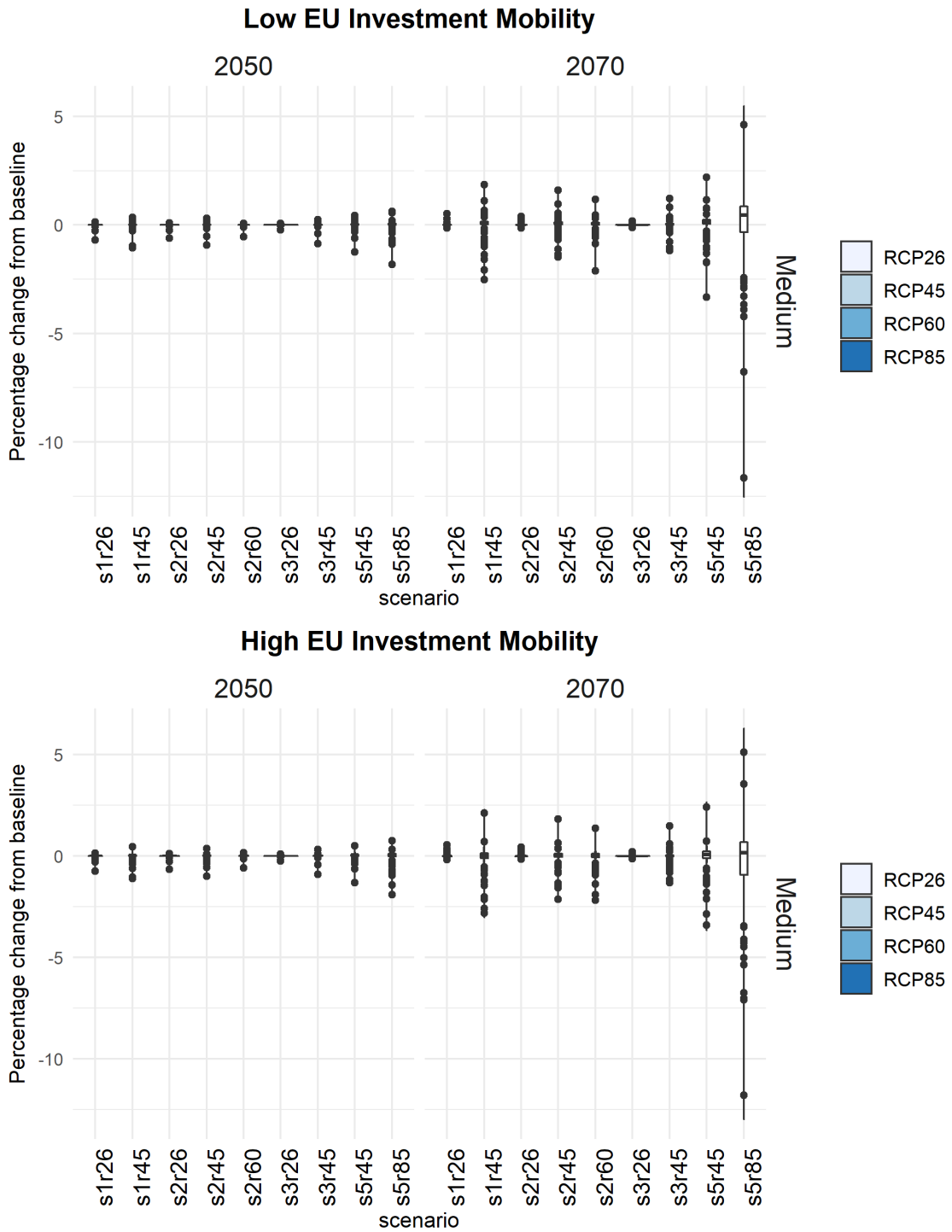
Figure 8 Climate change impacts on forestry: distribution of GDP impacts across all regions of the ICES model by year and scenario combinations; medium impact on forest productivity case. Low investment mobility upper panel, high investment mobility lower panel. Values are percentage changes from the baseline.

2.2.3 Fisheries

i. Impact modelling

Data for the macroeconomic assessment of climate change impacts on fisheries have been originated in COACCH D2.2 (Boere et al. 2019). The effects on the fish stock are assessed applying two bio-physical models: the Dynamic Bioclimate Envelope Model (DBEM) (Cheung et al., 2016) and the Dynamic Size-based Food web model (DSFM) (Blanchard et al., 2012). Results are available at the national level and for the RCP2.6 and RCP 8.5 climate change scenarios. The effect on freshwater fish is not examined.
Potential impacts on catches in RCP 4.5 and 6.0 have been reconstructed for every country by linear interpolation between RCP 2.6 and RCP 8.5 assuming these two RCPs as the two extremes of the interpolation.
Once computed, changes in catches have been implemented into the ICES model as changes in the productivity of the natural resource input of the representative regional fish industry. Only coastal regions are affected directly by the impact. Furthermore, data are available at the national and not at the NUTS level. Accordingly, the same shock on the fish stock productivity has been imposed to all coastal regions belonging to the same country.

ii. Simulation results

As shown in Figure 9, particularly evident in 2070 under RCP 8.5 and in the high impact scenario, EU regions can, with few exceptions, experience gains in the order of roughly 1-2% of the regional GDP. It is important to stress that the direct impact of climate change on the fish stock in the RCP 8.5 and high impact case are negative across all the coastal regions. Accordingly, the positive GDP performances are due to trade effects. EU regions can experience lower productivity loss than other non-EU producers and become eventually more competitive. It is also worth noting that EU land locked regions which are not directly affected by the negative productivity shock on the fish resource, gain.
A similar finding is highlighted also in Boere et al (2019). Indeed, according to the partial equilibrium MAgPIE model simulation, perturbed with the same biophysical changes in the fish resource, climate change can produce a mildly positive effect on commercial fish catches in the EU. The largest negative GDP impact is felt in Latvia. The huge losses are driven by a strong drop in investment dynamics. These are not only driven by the direct impacts on the fishery sector. Indeed, we note that, in Latvia, the productivity loss is comparable to that of other EU regions, while its fishing sector builds a comparable share of value added. Therefore, alone, these impacts cannot explain the GDP result. Indirect trade effects play an important role and in models with such a high sub-national detail, small regions, like Latvia can be particularly sensitive. Also in this case, economic impacts that mostly derive from effect on the natural resource stock, are quite insensitive to different assumptions of inter-regional

investment mobility. Still, when the mobility is lower negative impacts tend to be slightly smaller.
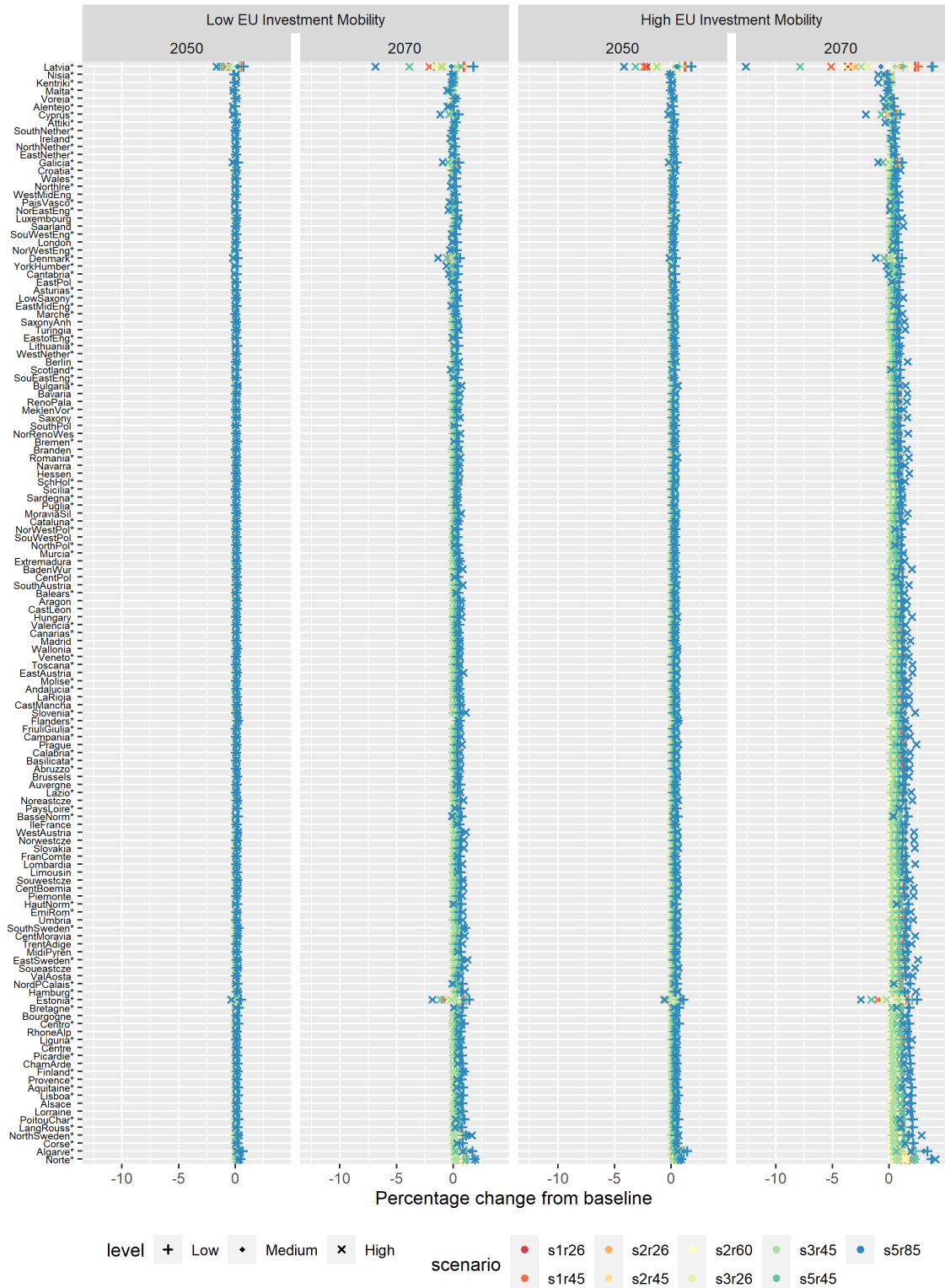
Figure 9 Climate change impacts on fisheries in the EU: GDP effects by region, scenario combination, climate sensitivity, investment mobility for 2050 and 2070. Values are percentage changes from the baseline. The "*" after the region name indicates the regions where an impact has been imposed.
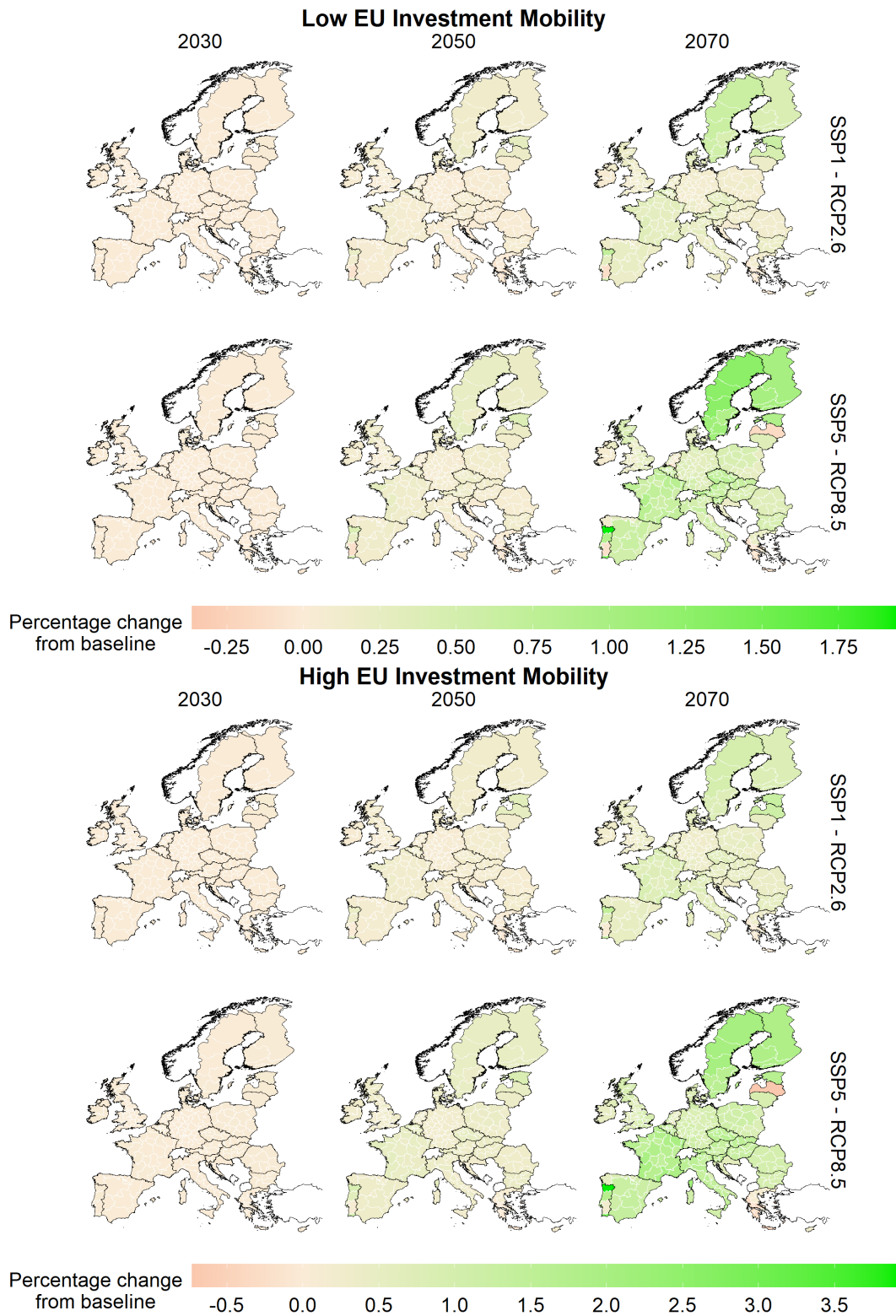
Figure 10 Climate change impacts on fisheries: GDP effects by region in 2030, 2050 and 2070 in the MEDIUM impact-on-fish stock case, SSP1-RCP2.6 and SSP5-RCP8.5 comparison, Low interregional

investment mobility upper panel, high interregional investment mobility lower panel. Values are percentage changes from the baseline.
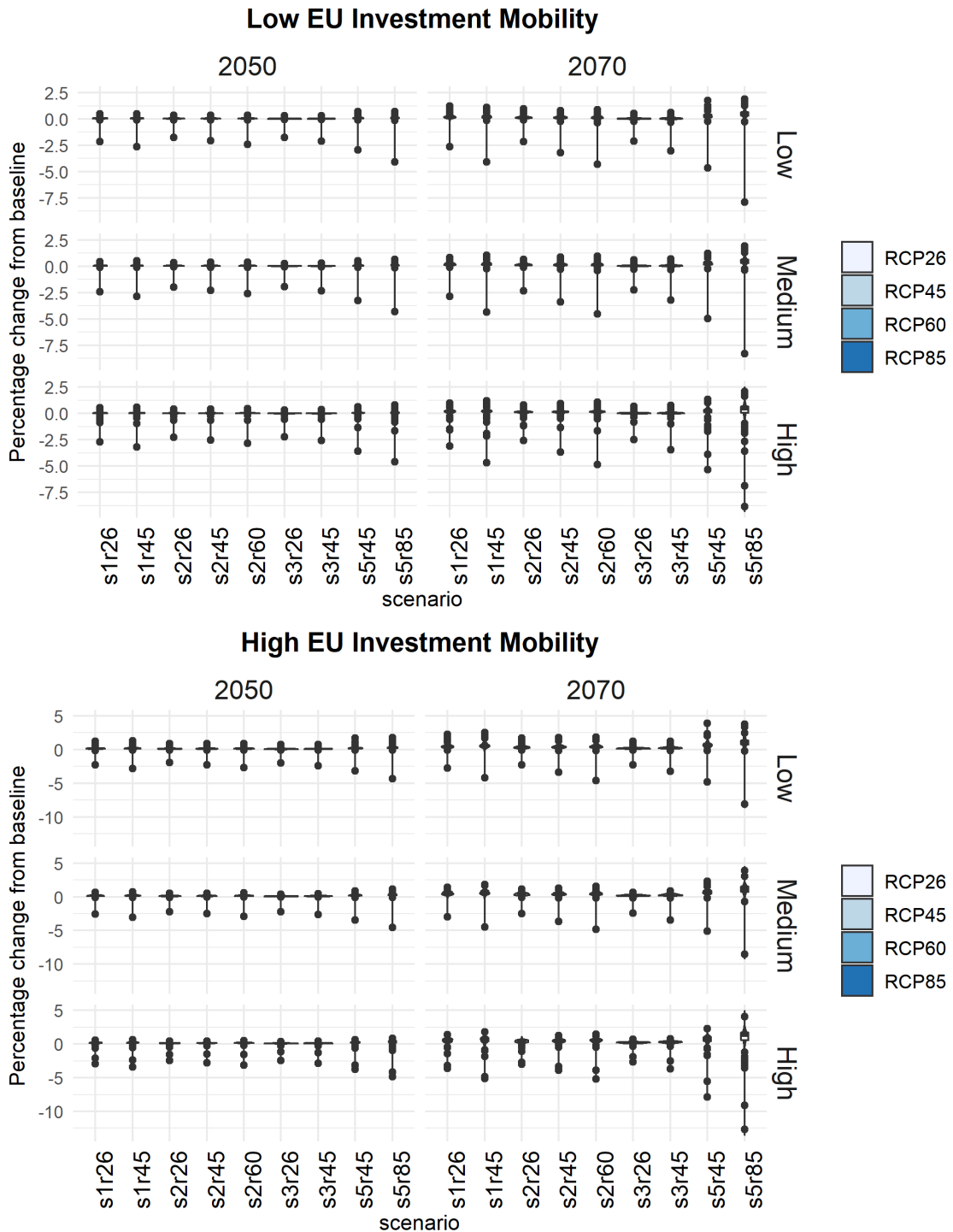

Figure 11 Climate change impacts on fisheries: distribution of GDP impacts across all regions of the ICES model in 2050 and 2070, all scenario combinations, low, medium and high impact on fish stock case. Low investment mobility upper panel, high investment mobility lower panel. Values are percentage changes from the baseline.

2.2.4 Sea level rise

i. Impact and adaptation modelling

The direct damage costs of SLR and of coastal protection (building of sea dikes) are derived from the DIVA model (Hinkel et al. 2014; Hinkel et al. 2013; Hinkel et al. 2012; Hinkel and Klein 2009) applied in D2.3 (Lincke et al. 2019).

Direct impacts and adaptation costs are computed for a "No additional adaptation scenario", assuming constant protection at 1995 levels and for a "With adaptation scenario", where the demand for safety increases with increasing affluence and higher dikes are built with rising sea-levels. The costs of coastal protection include construction and annual maintenance costs. Information is available in 5-year time steps.

For each combination of SLR and socio-economic scenario the following DIVA model outputs were used as input to the ICES economic model:

a) Annual land loss due to submergence (km²/year): land is considered to be unusable, and thus lost, if it is situated below the 1-in-1 year flood water level and not protected by a dike.

b) Expected annual damages to assets by sea floods (million US$/year).

c) Expected annual number of people flooded per year (thousands/year).

d) Annual protection costs including construction of new dikes, raising of existing dikes, and maintenance of existing dikes (million US$/year).

For a consistent flow of information across the two models, all values from DIVA, expressed in US$ PPP (Purchasing Power Parity) were converted to US$ MER (Market Exchange Rate), the ICES reference, using the conversion factors from the World Development Indicators (World Bank 2017). The physical and economic data of the spatially resolved DIVA model were aggregated to match the ICES regions. Then we calculated the losses on land, capital, and labour productivity using the DIVA aggregated data to find consistent values to be applied to the ICES model.

As in previous CGE assessments (Bosello et al. 2007; Bosello et al., 2012a; Bosello et al., 2012b), we assume that SLR impacts affect regional performances through land loss, labour productivity loss, and capital loss:

a) The first is implemented in ICES decreasing the stock of productive land available to agriculture assuming this coincides with submerged land, which is commonly observed.

b) Labour productivity is reduced assuming that people flooded are not able to work for 2 working weeks per year.[1]

---

[1] This value derives from assumptions made in Bosello et al (2012b) on the period of time that people will not be able to work after being affected by river floods. Parrado et al (2020) control for the weight of this assumption with a sensitivity analysis considering 1, 2, 4 and 6 weeks for the No Adaptation scenario with high SLR. Applying these periods does not change the final

c) Capital stock is decreased according to the expected annual damages to assets by sea floods. This presupposes that all countries of the world would experience in every year a flood that provokes exactly the expected damage. We keep this assumption for simplicity noting that our results, under this respect, can be placed in the high range of damage estimates.

Adaptation costs are modeled in a quite stylized manner. Regional expenditures for coastal protection over time are implemented as a proportional reduction of the regional endowment of capital stock. This may seem counterintuitive as more protection infrastructure is supposed to increase the capital asset of a region. However, this procedure is consistent with the structure of the macroeconomic model. Capital stock accumulation process is one of the engines of economic growth in the recursive dynamic ICES model. Therefore, the idea behind the reduction of capital stock is to capture the opportunity costs of coastal protection that diverts resources from economic growth to sea-level rise damage prevention. The gains from coastal protection are instead measured by the lower damages to assets and population enabled by dike building. Richer modelization of coastal protection expenditure is possible. For instance, Bosello et al, (2007) examine the investment/consumption effects of public expenditure, while Parrado et al. (2020) account for the difference in dike building costs and maintenance and operational costs and relate those to public budget sustainability. However, modelling adaptation as a pure capital loss is a way to represent the highest possible adaptation cost thus giving a conservative estimate in the following cost benefit assessment.

ii.   Simulation results

In the case of sea-level rise, an impact that transmits macro-economic losses primarily through effects on the regional capital stock and its return, while land and labour productivity losses are marginal, assumptions on interregional investment mobility are particularly important. Assuming adaptation stays constant at its current level, sea-level rise can determine huge GDP losses. When investment is "highly" mobile inter-regionally, GDP contractions, not only affect coastal regions, but also spread over EU land locked areas (Figure 12, Figure 13). The mechanism at play is as follow: the loss of capital due to sea-level rise induces higher return to capital in flooded regions that drains investments from other areas that experience lower growth. In the high-end sea-level rise case, in 2050, Latvia, Malta, Veneto, Tuscany and Marche in Italy can experience a regional GDP loss beyond or close to 2.5% also in a moderate warming scenario like the RCP4.5. In 2070 damages amplify. Latvia, with contractions of 15%, Malta, Veneto, Tuscany and Marche are still the top GDP losers. Anyway, the majority of EU regions demonstrates losses larger than 2, 2.5% of their regional GDP. Two

outcome of estimates. There is some variability on impacts at the aggregate level for North Europe and Asian countries, but these variations do not change the overall results of that study. As a final remark, it has to be noted that the labour productivity effect in Parrado et al. (2020) represents a minor share (1% to 16%) of the total impact.

aspects are worth highlighting (see also COACCH D3.3 (Bachner et al., 2020) and COACCH D3.4 (Botzen et al., 2020)):

- Regions that in the different countries are particularly interconnected economically, not only with coastal areas, but also with the overall economic trade flows, which often coincide with regions where the capital cities are, show losses of comparable magnitude with coastal areas. The cases of Piedmont and Lombardy in Italy, of the Ile de France in France, Madrid in Spain and of central Germany are emblematic.

- Particularly evident in the high sea-level case, the SSP3 scenario coupled with the lower climate signal RCPs 4.5 demonstrates in many regions higher GDP losses than the SSP5-RCP8.5 combination. This may appear counter intuitive not only because more sea-level rise is expected in RCP 8.5, but also because the SSP5 storyline features higher GDP than SSP3 and, accordingly, may also suggest a higher exposure. This outcome is however driven by the different parameterization of the SSPs in the model. In particular, SSP3, the "fragmented world", is characterized, among other, by a lower substitutability between domestic and imported commodities. This factor, introducing higher friction in international trade, induces more rigidity in market adjustment to external shocks. What shown, is that a more "flexible" system can eventually experience lower macroeconomic costs than a more "rigid" one, even though the former is more exposed to climate change impacts.

The picture can be quite different when lower investment mobility is assumed. In this case macroeconomic losses tend to remain within coastal areas. On the one hand a much lower capital "drain" is observed, on the other hand, international trade acts as an impact smoothing factor. The regions less damaged increase their production to compensate losses in sea-level rise exposed regions. Accordingly, a smaller number of regions, mostly coastal, exhibit losses, while moderate gains are common. Some robust findings can be anyway highlighted: Latvia, Malta, and Veneto remain top losers and the SSP3-RCP4.5 scenario combination confirms to be the more economically concerning.
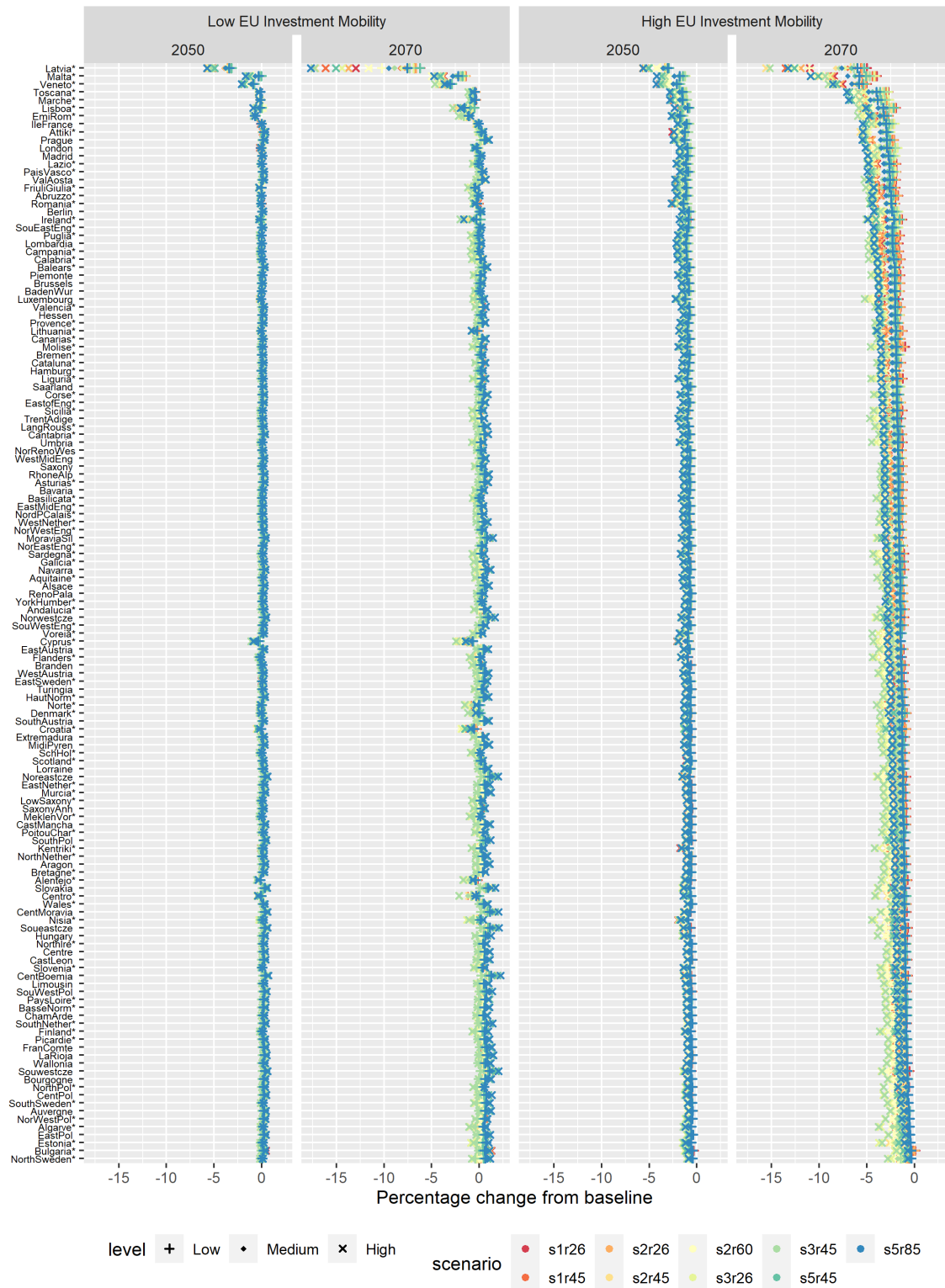
Figure 12: Climate change impacts on sea-level rise in the EU: GDP effects by region, scenario combination, climate sensitivity, investment mobility for 2050 and 2070. Values are percentage changes from the baseline.
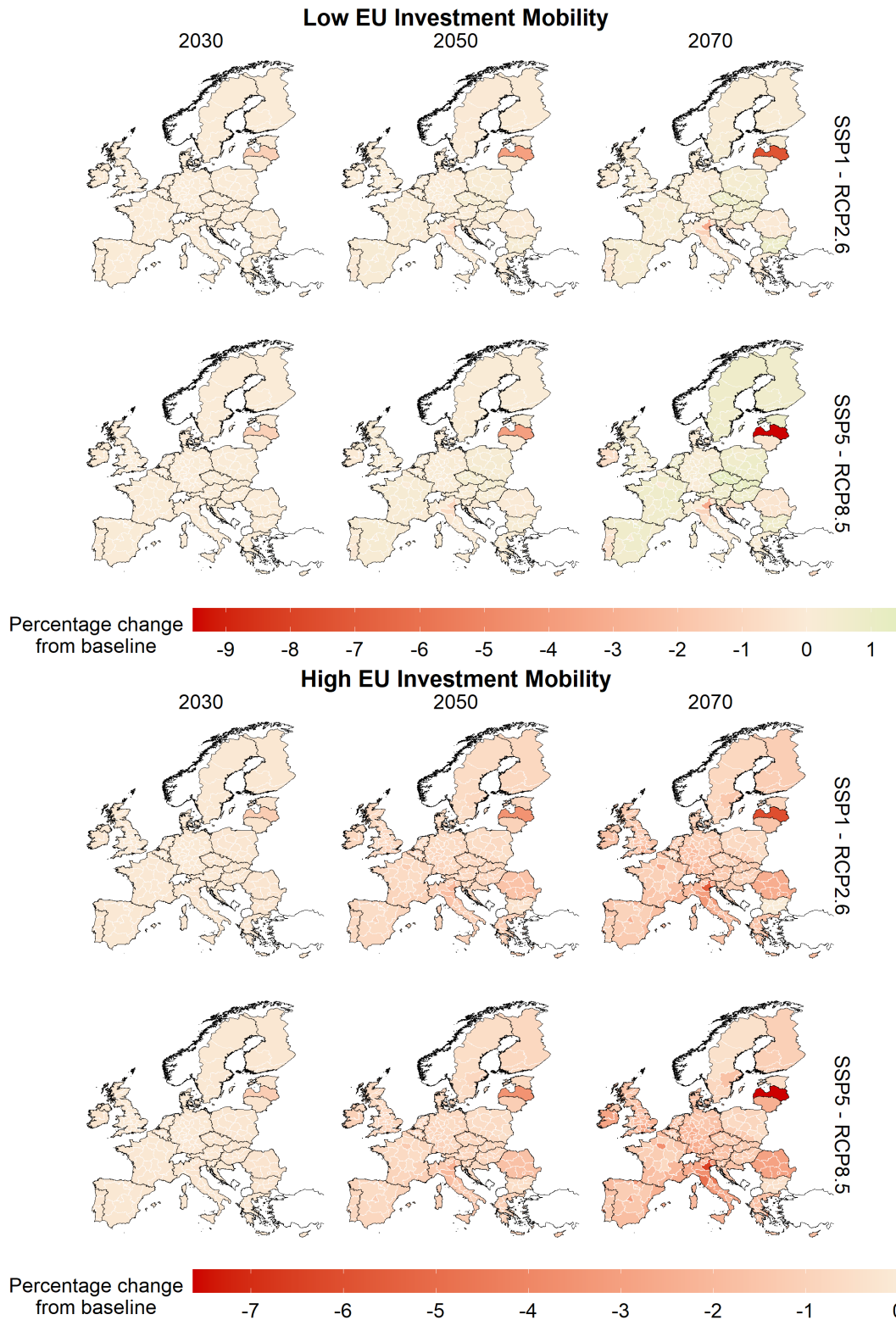
Figure 13 Climate change impacts on sea-level rise: GDP effects by region in 2030, 2050 and 2070 in the MEDIUM impact case, SSP1-RCP2.6 and SSP5-RCP8.5 comparison, low interregional investment mobility upper panel, high interregional investment mobility lower panel. Values are percentage changes from the baseline.

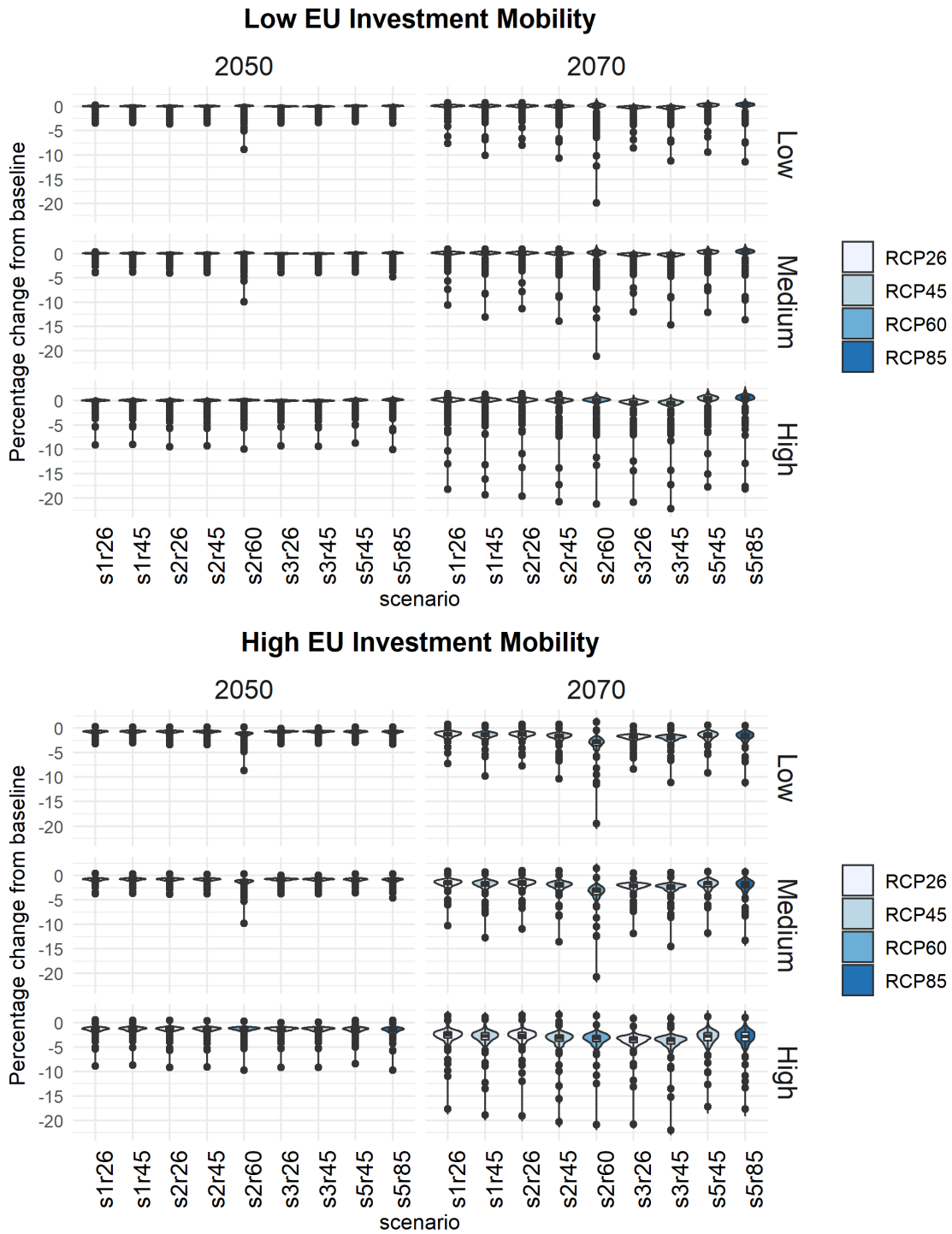**Figure 14 Climate change impacts on sea-level rise: distribution of GDP impacts across all regions of the ICES model in 2050 and 2070, all scenario combinations, low, medium and high impact case. Low investment mobility upper panel, high investment mobility lower panel. Values are percentage changes from the baseline.**

The introduction of adaptation changes substantively the picture (Figure 15 depicts the SSP2-RCP6.0 scenario combination that features the highest GDP impacts from sea-level rise).

Incremental adaptation, although entailing non marginal costs (see Lincke et al. 2019), determines an expenditure much smaller than the avoided damage. Residual damages are also marginal. Eventually, in all the SSP-RCP scenario combinations, in all EU coastal regions, and in all EU regions, GDP costs in the presence of incremental coastal protection (that is what is expected to occur in reality or the "business as usual case") are significantly lower than without adaptation (i.e. when adaptation is kept at the current level). Given that sea-level rise is one of the major drivers of macroeconomic impacts from climate change and that coastal protection seems to offer high benefit to cost ratios, it is an adaptation strategy that is worth prioritizing.

When investment mobility is low, adaptation still removes most effects of sea-level rise. On the one hand this is highly positive for sea-level rise exposed regions. On the other hand, this originates the somehow paradoxical result of removing the GDP gains experienced in land locked areas without increased coastal protection.
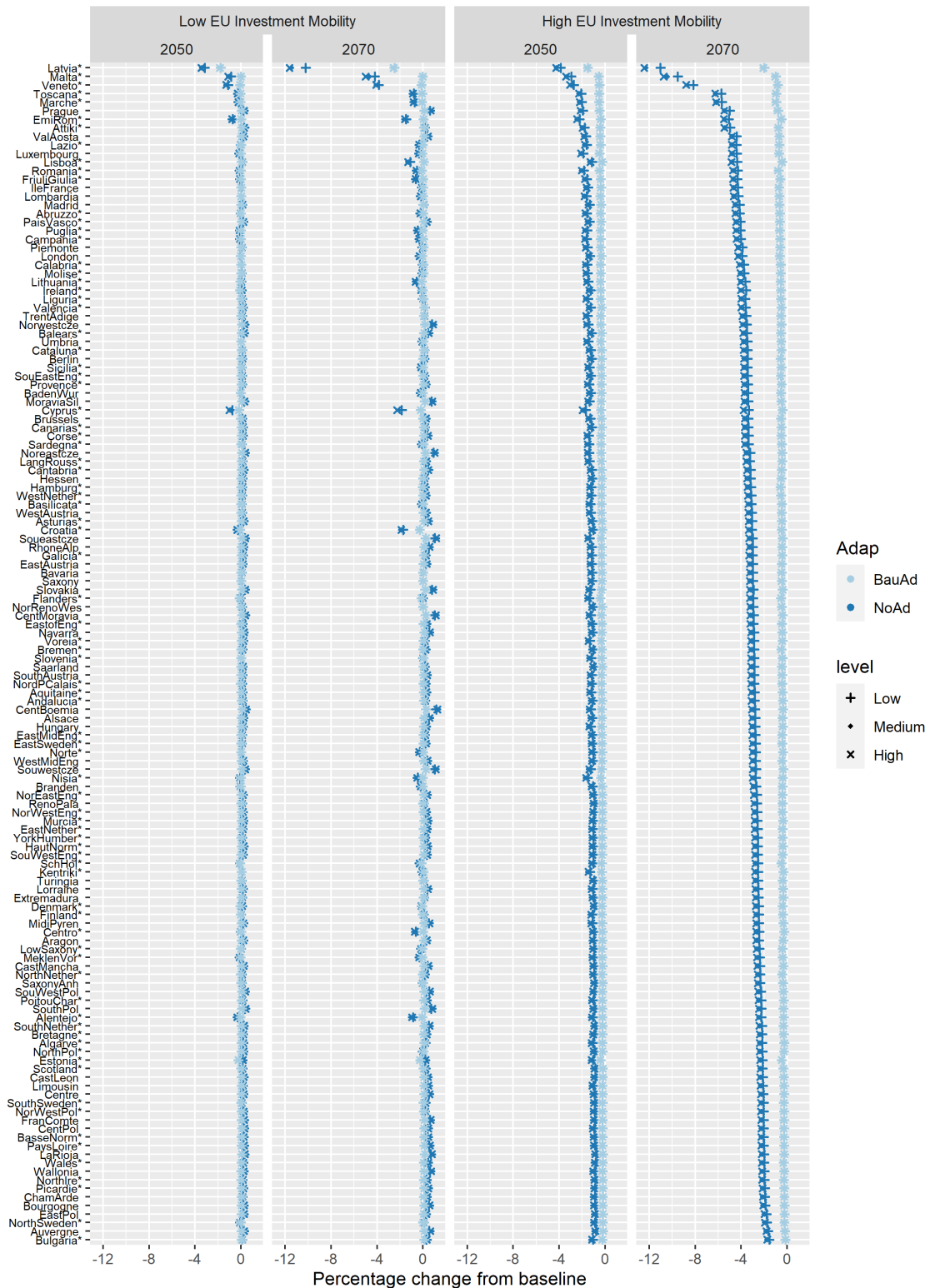
Figure 15. Climate change impacts on sea-level rise in the EU: GDP effects by region, under no and business as usual adaptation, high, medium and low impact case, investment mobility, for 2050 and 2070. SSP2-RCP6.0 scenario combination. Values are percentage changes from the baseline.

2.2.5 Riverine floods

i. Impact modelling

Data for the macroeconomic assessment of climate change impacts on river floods have been originated in COACCH D2.3 (Lincke et al. 2019).
These have been computed by the GLOFRIS model (Ward et al., 2020; Ward et al., 2017; Winsemius et al., 2016) that reports information on:

- Expected annual damages (EAD) in million USD PPP 2005 determined for three macro-areas: industrial, commercial, and residential;
- Population exposed to floods.

Both have been assessed for all the 9 SSP-RCP scenario combinations examined by the COACCH project. Climate forcing in each climate scenario has been derived by an ensemble of 5 different global circulation models (NorESM1-M, GFDL-ESM2M, HadGEM2-ES, IPSL-CM5A-LR, and MIROC-ESM-CHEM). The cross-model variability enabled the computation of a maximum, minimum and medium level of damage for each scenario combination.

As in the case of sea level rise, all values from GLOFRIS, expressed in US\$ PPP were converted to US\$ MER and the EAD data of the spatially resolved GLOFRIS model were aggregated to match the ICES regions. Then we calculated the ratio of each monetary value to the corresponding GDP for each SSP. Finally, those ratios were applied to the ICES GDP database to compute the corresponding values to be included as input for the CGE simulations.

River flood impacts have been then implemented into the ICES CGE model in terms of:

- Loss of labour productivity using the exposed population to compute the percent fraction of total labour lost in a year. The methodology applied for the assessment is the same used in the sea-level rise assessment and assumes that people affected by a flood event are unable to work for 2 weeks per year.
- Loss of capital stock by macro-sector. The fraction of capital lost is given by the ratio between EAD and the value of sectoral capital stock by region following the correspondence detailed in Table 2.

The matching between the 3 macro areas of economic activity of GLOFRIS and the 24 sectors of ICES is reported in Table 2.

Table 2. ICES-GLOFRIS sectoral correspondence

ICES sector mapping	GLOFRIS impact mapping
Oth_Crops	Industrial
Veg_Fruits	Industrial
Livestock	Industrial
Timber	Industrial
Fishery	
Coal	Industrial
Oil	Industrial
Gas	Industrial
Oil_Pcts	Industrial
TnD	Commercial
Nuclear	Commercial
FossilsEly	Commercial
Wind	Commercial
Hydro	Commercial
OthersEly	Commercial
Solar	Commercial
Heavy_ind	Industrial
Construction	Industrial
Light_ind	Industrial
Trp_Road	Commercial
Trp_Water	Commercial
Trp_Air	Commercial
Services	Commercial + Residential
PubServ	Commercial

ii.   Simulation results

Impacts from riverine flood transmit macro-economic consequences mainly through effects on the capital stock. Therefore, similarly to sea-level rise, assumptions on investment mobility are particularly important for the final economic result. Low investment mobility tends to reduce the spreading of impacts across regions and the magnitude of negative impacts.

In 2070 in the EU, under high investment mobility, the GDP impacts induced by river flooding are concentrated around -2.5%. An outlier is East Sweden that in the high impact case denotes losses around 10% (Figure 16). Losses are widespread, but higher in central north western and central south western EU. Northern Italian regions like Veneto, Marche and Tuscany and Campania in the Italian South, but also Hungary are particularly exposed.

In East Sweden, Veneto, Tuscany, Marche and Hungary the magnitude of impacts on capital stocks are higher in industrial activities and services. In the Hamburg area industry suffer higher impacts than commerce in relative terms leading to potential GDP losses of up to 4.5% in aggregate in the high investment mobility case.

In the low and medium impact case and especially before 2050 GDP losses from river floods do not imply significant differences from the current climate baseline case.

When investment is less mobile across regions, losses follow a similar geographical pattern, but are smaller in magnitude. Impacts are larger in the SSP3 fragmented world and negative in all the EU area with a median loss of roughly 1.2% of regional GDP in the high impact case. In the other scenario combinations, gains can be experienced in those regions not directly affected by floods. This is the consequence of a redistribution of production and demand.
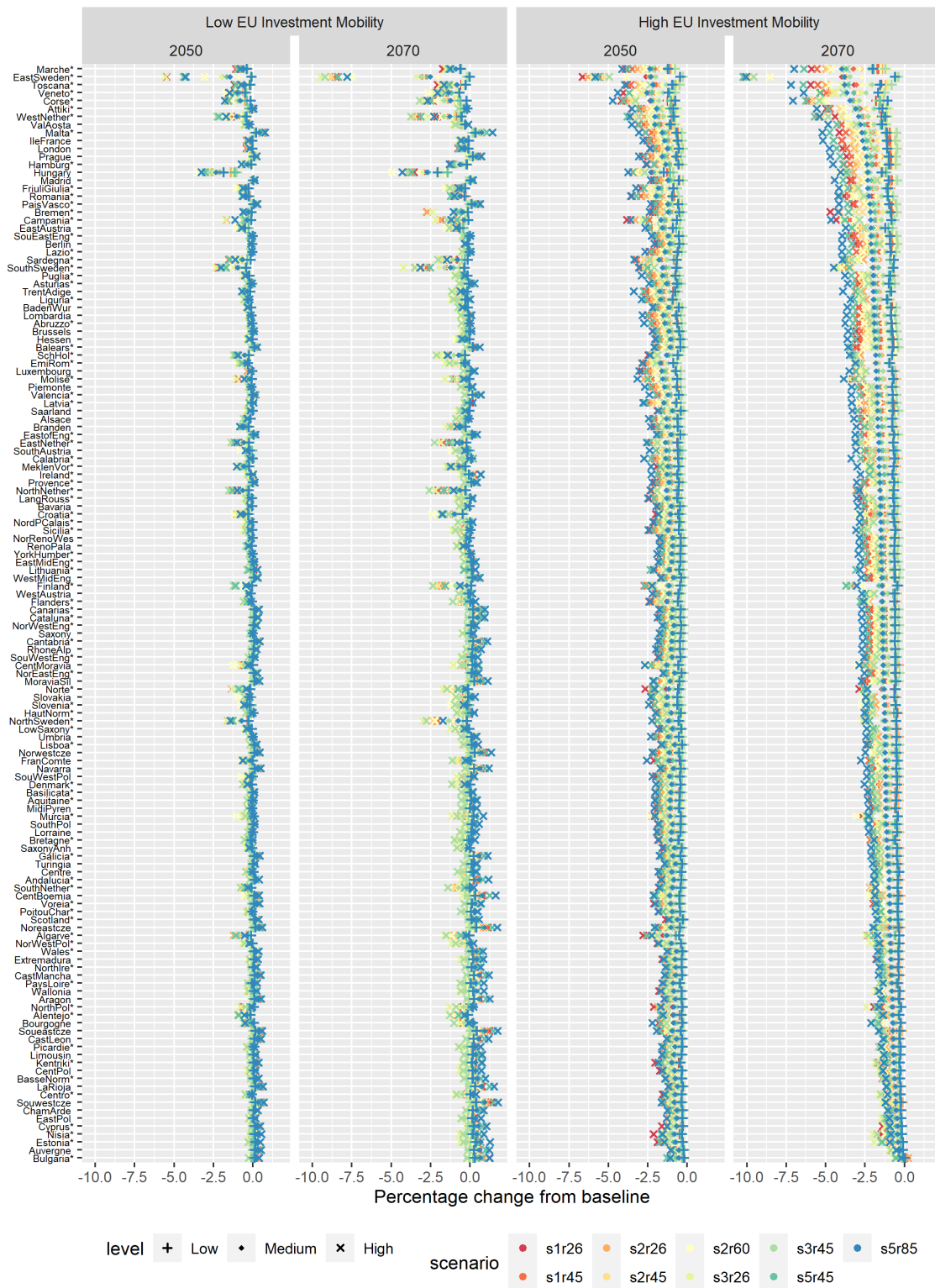
Figure 16 Climate change impacts on riverine flood in the EU: GDP effects by region, scenario combination, climate sensitivity, investment mobility for 2050 and 2070. Values are percentage changes from the baseline.

Low EU Investment Mobility
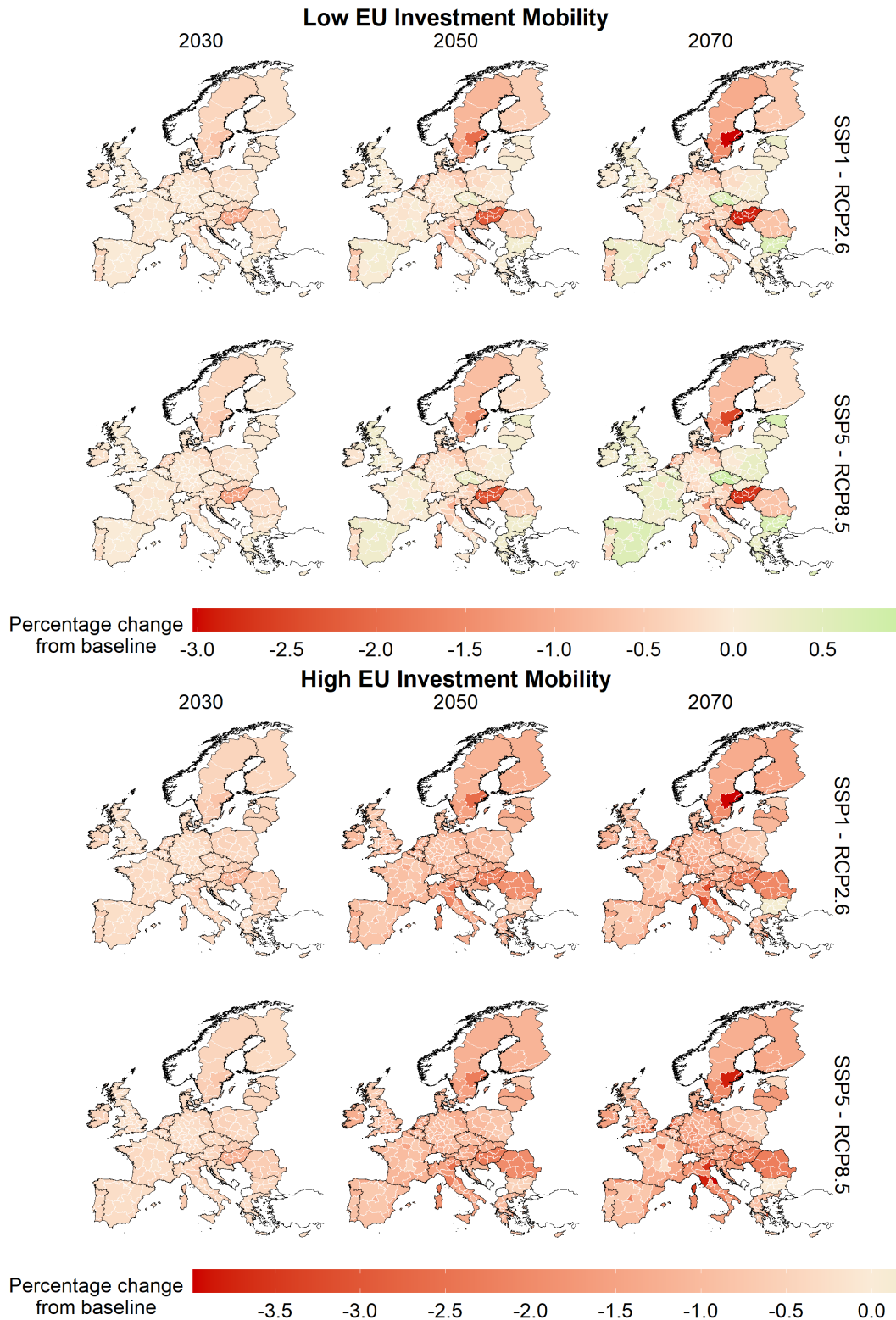
Figure 17 Climate change impacts on riverine floods: GDP effects by region in 2030, 2050 and 2070 in the MEDIUM impact case. SSP1-RCP2 and SSP5-RCP8.5 comparison. Low interregional investment mobility upper panel, high interregional investment mobility lower panel. Values are percentage changes from the baseline.

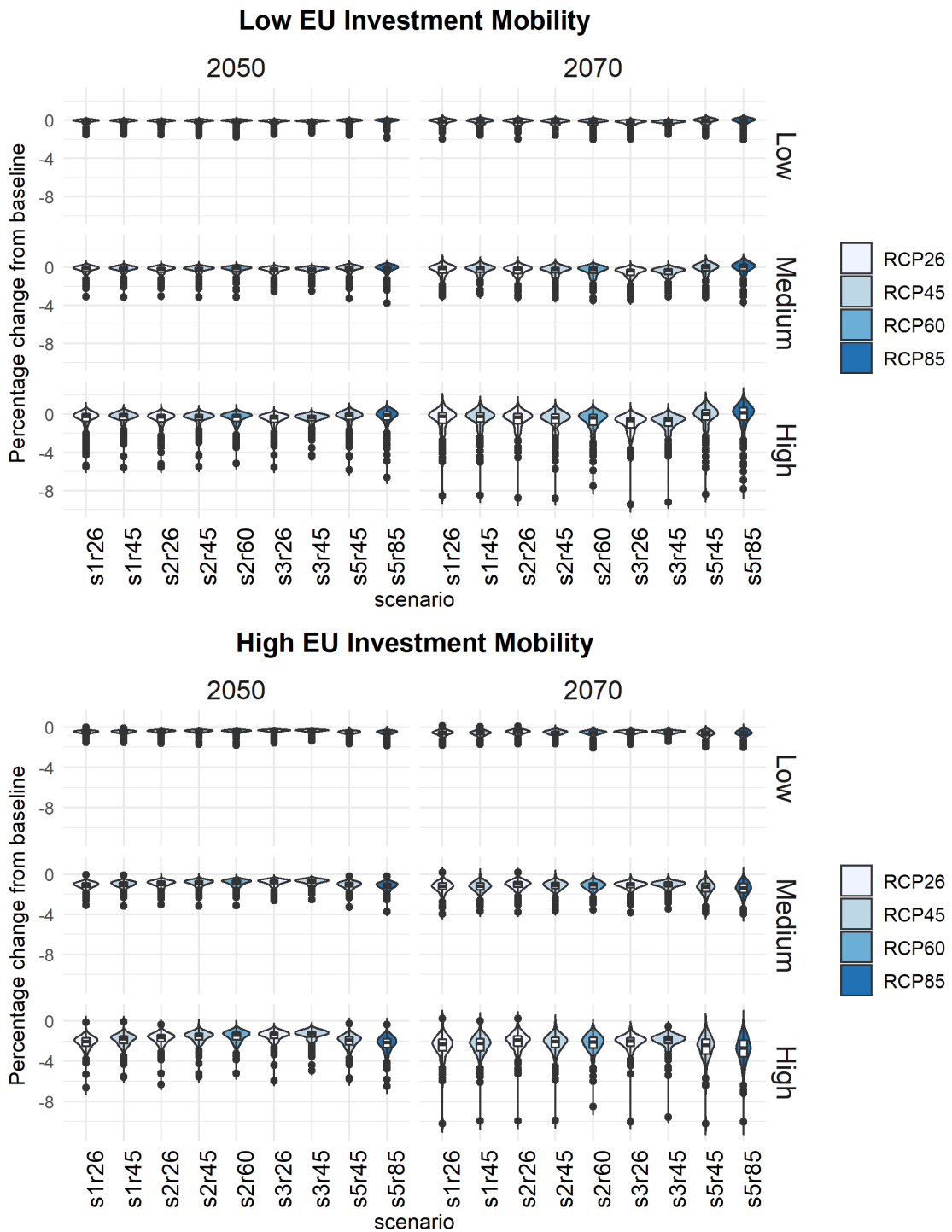**Figure 18 Climate change impacts on riverine flood: distribution of GDP impacts across all regions of the ICES model in 2050 and 2070, all scenario combinations; low, medium and high impact cases. Low interregional investment mobility upper panel, high interregional investment mobility lower panel. Values are percentage changes from the baseline.**

2.2.6 Transport

i. Impact modelling

Data for the macroeconomic assessment of climate change impacts on the transportation sector have been originated in COACCH D2.3 (Lincke et al., 2019).
There, the OSDaMage model (van Ginkel et al, 2020) has been applied to compute direct infrastructural expected annual damage (EAD) to road assets in the former EU-28, with the exclusion of Malta and Cyprus (Lincke et al., 2019). The data is available for RCP 4.5 and RCP 8.5. To extend the data for the remaining RCPs in order to use it for all COACCH SSP-RCP combinations, we computed the values for RCP 2.6 as the average between the baseline (corresponding to 2003 levels) and RCP 4.5, while for RCP 6.0 as the average between RCP 4.5 and RCP 8.5.

Impacts have been computed for all 9 combinations of SSPs and RCPs scenarios examined by the COACCH project. In addition, using 11 combinations of GCM-RCM models it has been possible to define for each combination a high, low, and medium level of potential damage. Direct impacts have been implemented in the ICES model as a uniform shock on the productivity of the labour and capital production factors used by the road transportation sector. To compute those shocks, we used the EAD as percentage of GDP to each region using data from the OSDaMage model and applied that percentage to the GDP values in ICES to obtain a consistent EAD. Finally, we computed the loss of productivity by dividing the EAD by the value of the output for the transport sector in each ICES region.

ii. Simulation results

Eventually, even though stock losses can be relevant in absolute terms and in a local context (see COACCH D2.3 (Lincke et al. 2019) and COACCH D3.4 (Botzen et al. 2020)), the direct economic costs of climate change impacts on road transportation infrastructure are a small percent of the total value of the capital assets of the sector. Furthermore, the use of EAD as input data for the macroeconomic assessment averages over a long period of time a loss that, in fact, is expected to occur in one moment in time. In doing so, EAD partly misrepresents the harmful and extreme-event nature of disruption in road transportation network. Both factors mentioned, contribute to associate a low impact on regional GDP to climate change impacts on road infrastructure. This outcome was already highlighted in Lincke et al. (2019) that emphasized the marginal share of damages to transport infrastructure in the total direct cost of floods. The macroeconomic assessment confirms and magnifies the result. Therefore, also different assumptions on investment mobility, even though the impact considered affects the capital assets of the sector, play a minor role in the final determination of economic losses. Indeed, regional GDP losses peak to a maximum of roughly 3% in southern Sweden and 2.5% in Saxony Anhalt in 2070 in the SSP5-RCP8.5 scenario combination under an assumption of high impact and high investment

mobility; the large majority of EU regions experiences a loss lower than 1% or regional product (Figure 19). In the medium impact case regional GDP losses are considerably smaller. They anyway replicate the same regional patterns with central and northern EU more severely hit (Figure 20). It also emerges that in the medium and low impact cases, losses are rather uniform across scenario combinations. Differences are more appreciable in the high impact case.
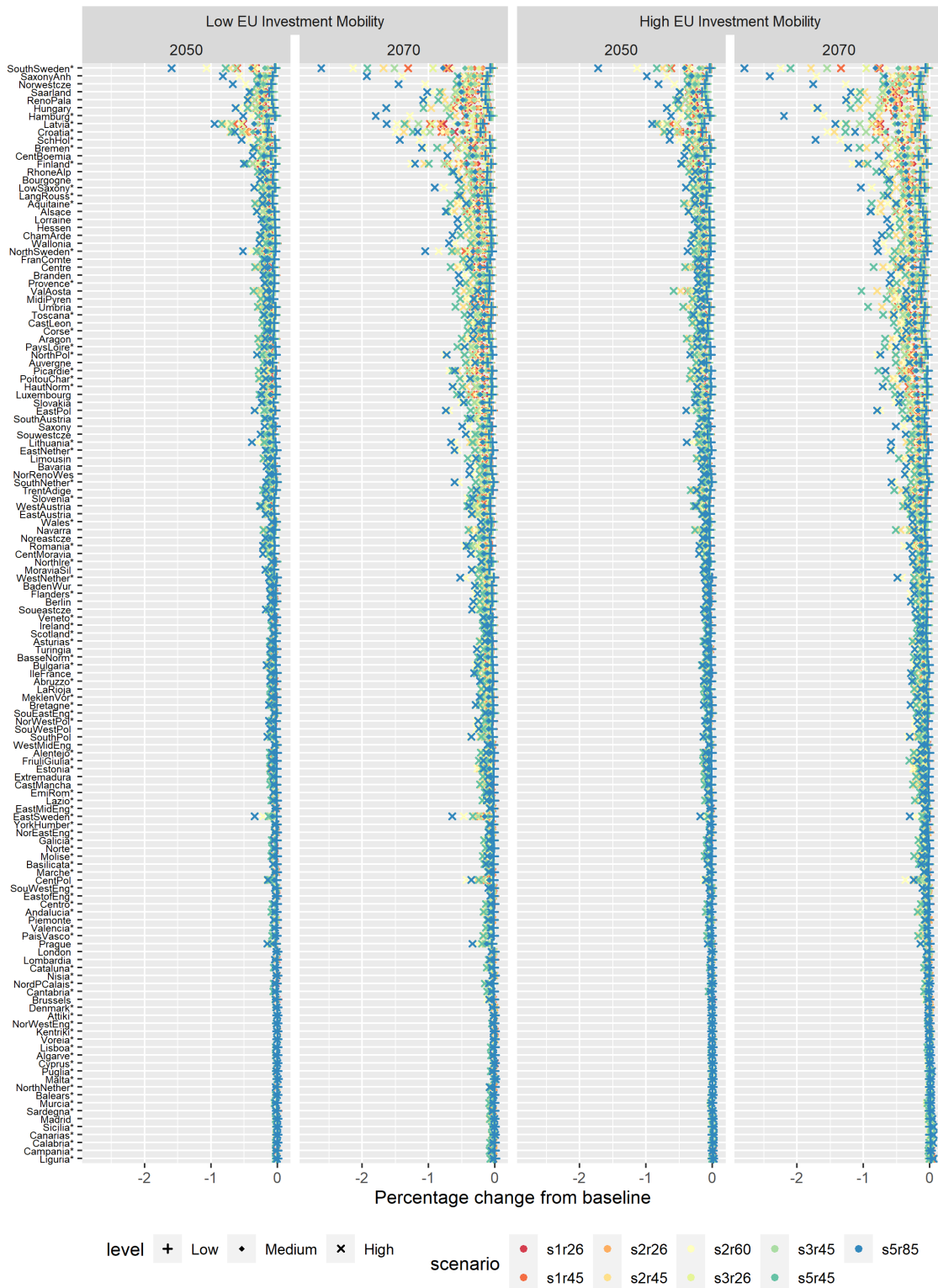
Figure 19 Climate change impacts on road transportation in the EU: GDP effects by region, scenario combination, climate sensitivity, investment mobility for 2050 and 2070. Values are percentage changes from the baseline.
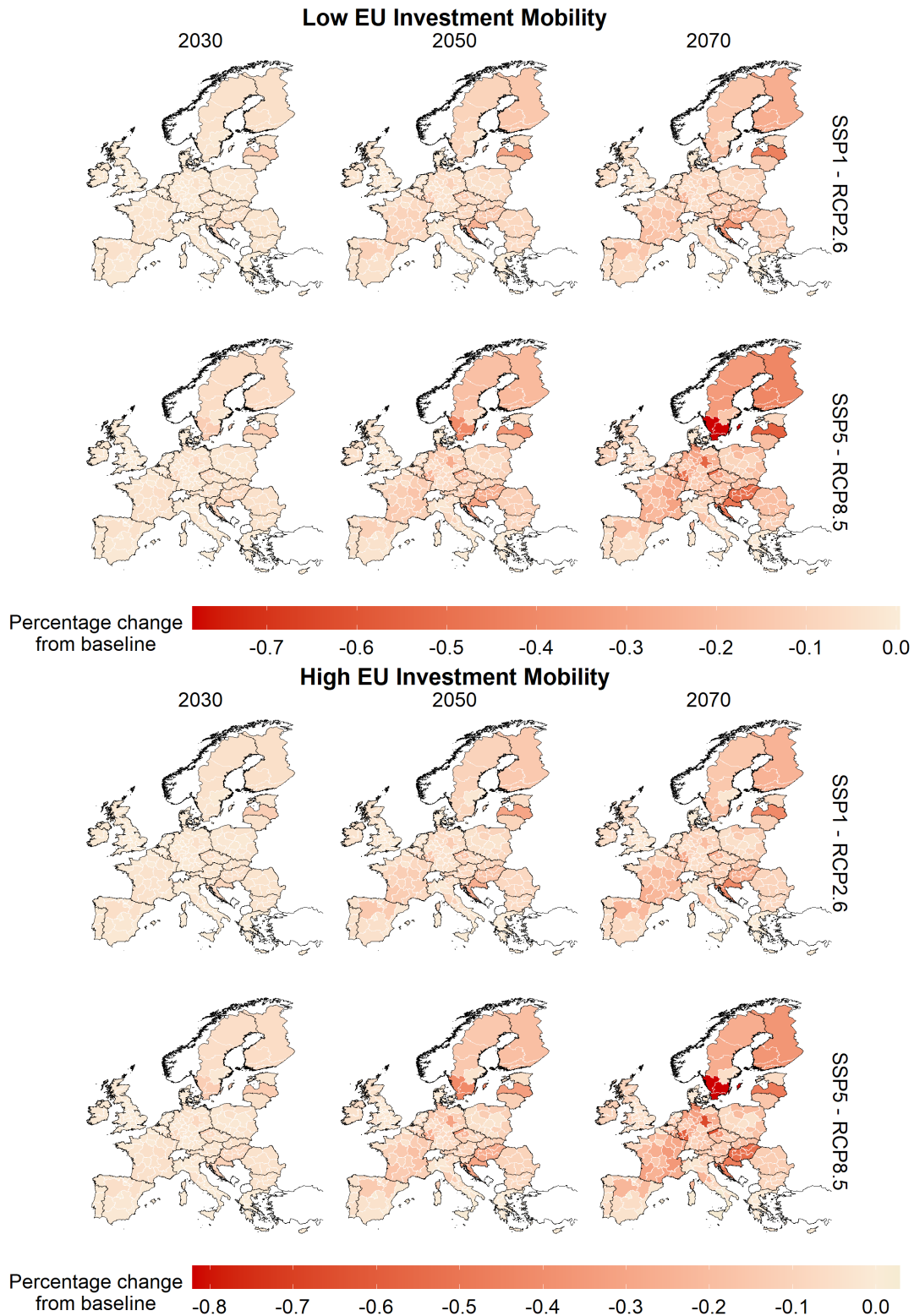
Figure 20 Climate change impacts on transportation: GDP impacts by region in 2030, 2050 and 2070. Medium impact case. SSP1-RCP2.6 and SSP5-RCP8.5 comparison. Low interregional investment mobility upper panel, high interregional investment mobility lower panel. Values are percentage changes from the baseline.
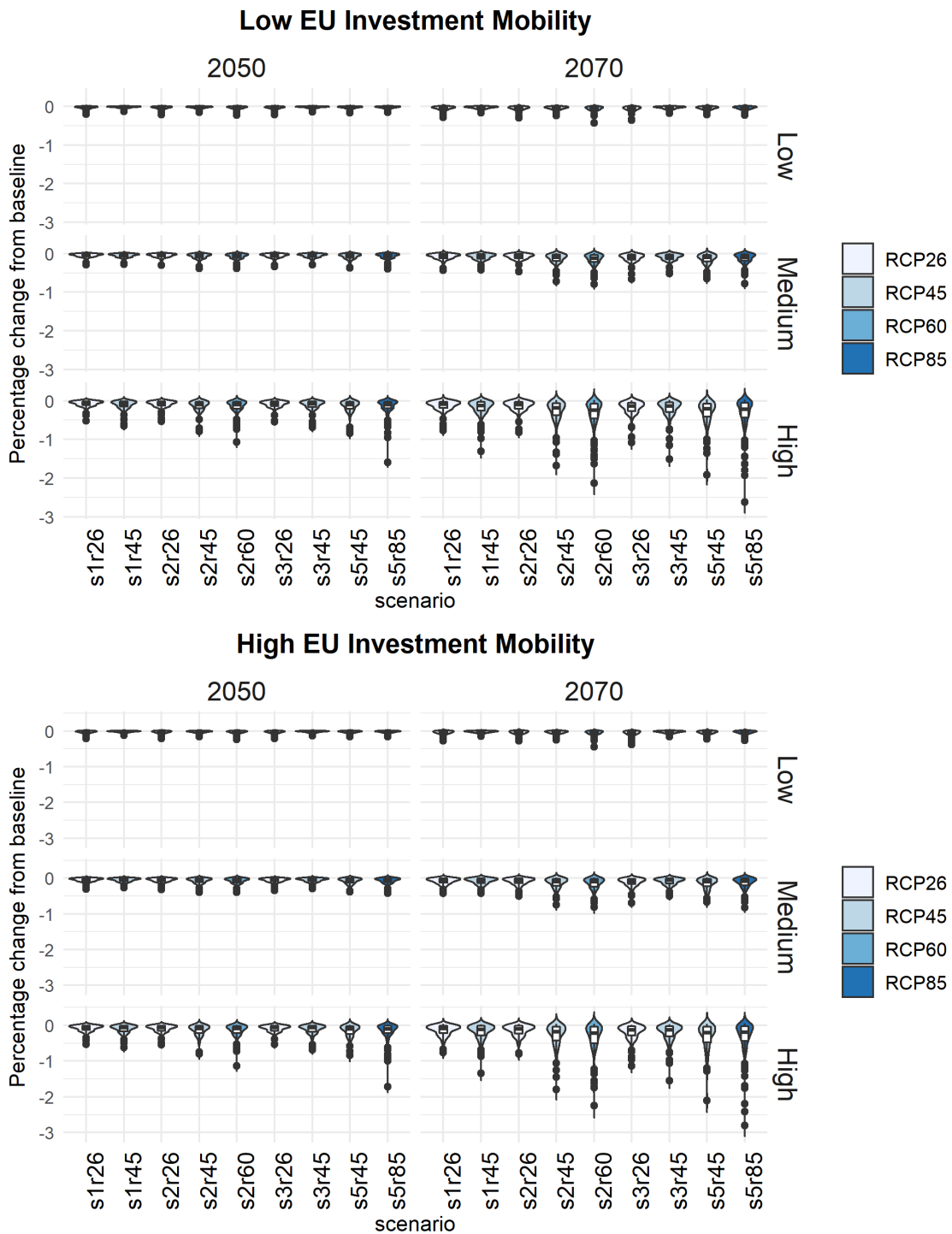
Figure 21 Climate change impacts on road transportation network: distribution of GDP impacts across all regions of the ICES model in 2050 and 2070, all scenario combinations; low, medium and high impact on transport network cases. Low interregional investment mobility upper panel, high interregional investment mobility lower panel. Values are percentage changes from the baseline.

2.2.7 Energy supply

i. Impact modelling

Input data for the macro-economic assessment of climate change impacts on wind power and hydropower supply have been computed in COACCH D2.4 (Schleypen et al., 2019).

The relation between wind energy supply and climate change has been estimated running a panel regression with location (NUTS-2) and multiple time (year, month, and hour) fixed-effects. The econometric analysis links wind power supply data available at the hourly level for the 1986-2015 period at the country-level along with various levels of sub-national aggregation (NUTS-1 and NUTS-2) from the EMHIRES database (Gonzalez Aparicio et al., 2016) and climate variables. Econometric estimates based on historical data are then used for projecting wind energy supply under the warming scenarios of all RCPs considered in COACCH using ensemble-mean temperature projections from different regional climate models (KNMI-RACMO22E, IPSL-CM5A-MR, MPI-ESM-LR, and CNRM-CM5).

At the end of this process we are able to derive a medium impact on the wind power generation (Gwh) in the period 2015-2070 for all RCPs and for the European regions detailed in ICES. Changes in wind energy supply are implemented in the ICES economic model as a proportional and uniform change in the productivity of the capital and labour factors of production used by the regional wind-power sectors.

Similarly, the relation between climate change and hydropower generation has been econometrically estimated merging data on electricity generation by energy source from the Global Energy & CO2 Data (Enerdata 2018) with high-resolution climatic data from the Global Land Data Assimilation System (GLDAS v2.1) dataset (Rodell et al. 2004) for 1971 – 2016.

Impacts of future climate change at the sub-national level have been computed combining the econometric estimates with various warming scenarios under RCP4.5 and RCP8.5 simulated using five different climate regional models (CCSM4, GFDL-CM3, INM-CM4, IPSL-CM5A-MR, and MIROC5).

Impacts under RCP6.0 have been obtained interpolating data from RCP4.5 and 8.5 using temperatures as a scaling factor. Impacts under RCP2.6 are set equal to zero given that the interpolation process originated extremely small numbers.

Direct impacts on hydropower supply are implemented into the ICES CGE model as a change in the productivity of the capital and labour factors of production used by the regional hydro-power sectors.

ii. Simulation results

Following climate change impacts on wind and hydropower supply, GDP falls moderately all over the EU regions, reaching a maximum decline in the Madrid region of roughly 0.6% in 2070 in the SSP2-RCP6.0 scenario combination and high interregional investment mobility (Figure 22). GDP impacts are very similar, although slightly smaller under the assumption of a lower mobility of investment. Considering RCP8.5, the scenario with the strongest climate signal, losses are concentrated in those

EU areas like northern EU countries or alpine regions where hydro power, and renewables in general, are more intensively produced and used (Figure 23). Interestingly, it can be also noted that negative GDP impacts in many regions can be larger in more moderate climate change scenarios, like RCP 4.5 or even 2.6 when associated to a SSP2 and SSP1 social development paths. This effect is driven by the fact that in SSP2 and SSP1 scenarios, higher use of renewable energy is foreseen compared for instance to a fossil energy based SSP5. Therefore, adverse impacts on these energy sources, when occurring, are more damaging. This specific case highlights the important role of the macro-economic context in impact determination that can be as influential as the climatic stressors.
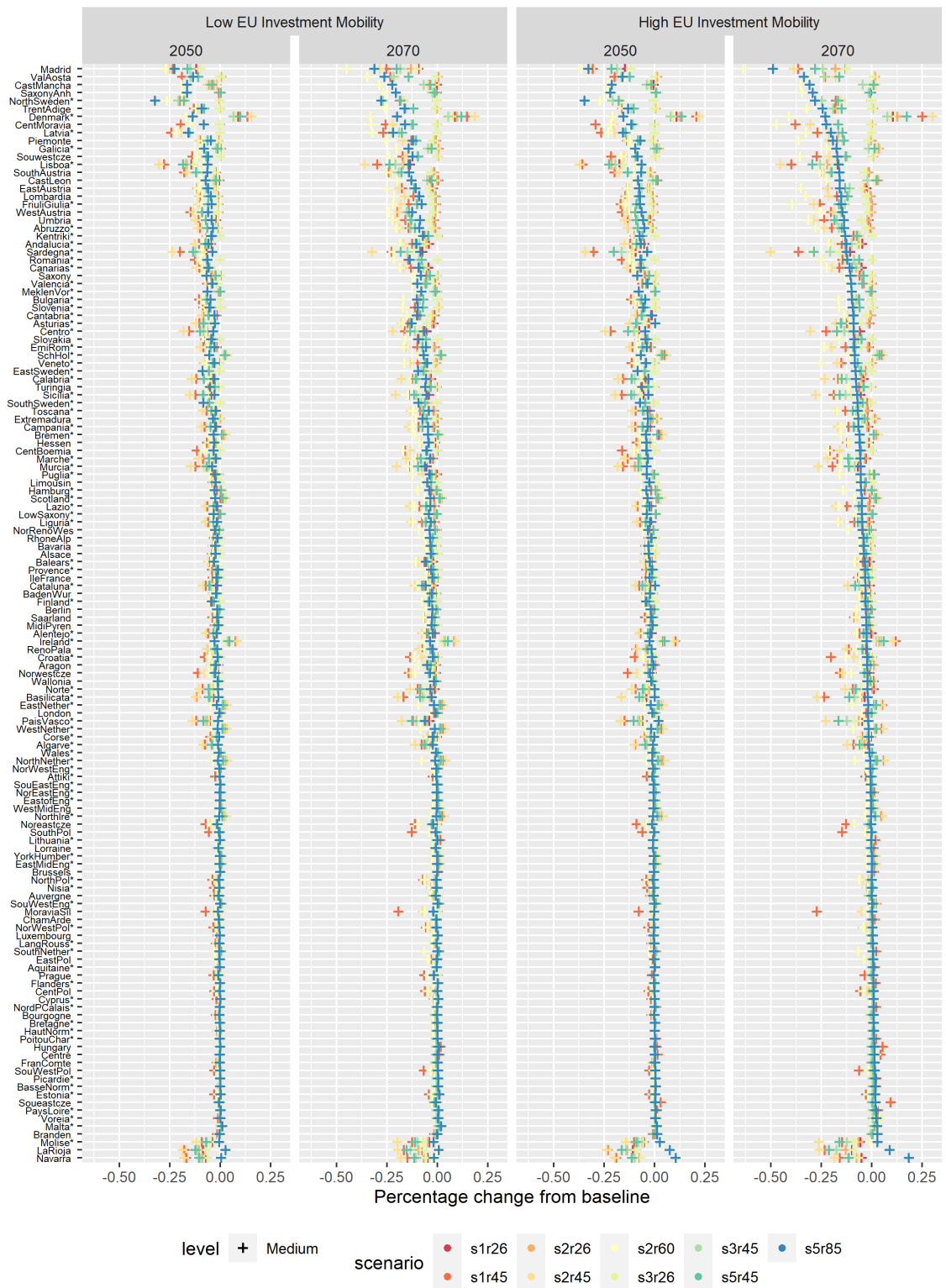
Figure 22 Climate change impacts on energy supply. GDP impacts by region, scenario combination, investment mobility in 2050 and 2070. Values are percentage changes from the baseline.
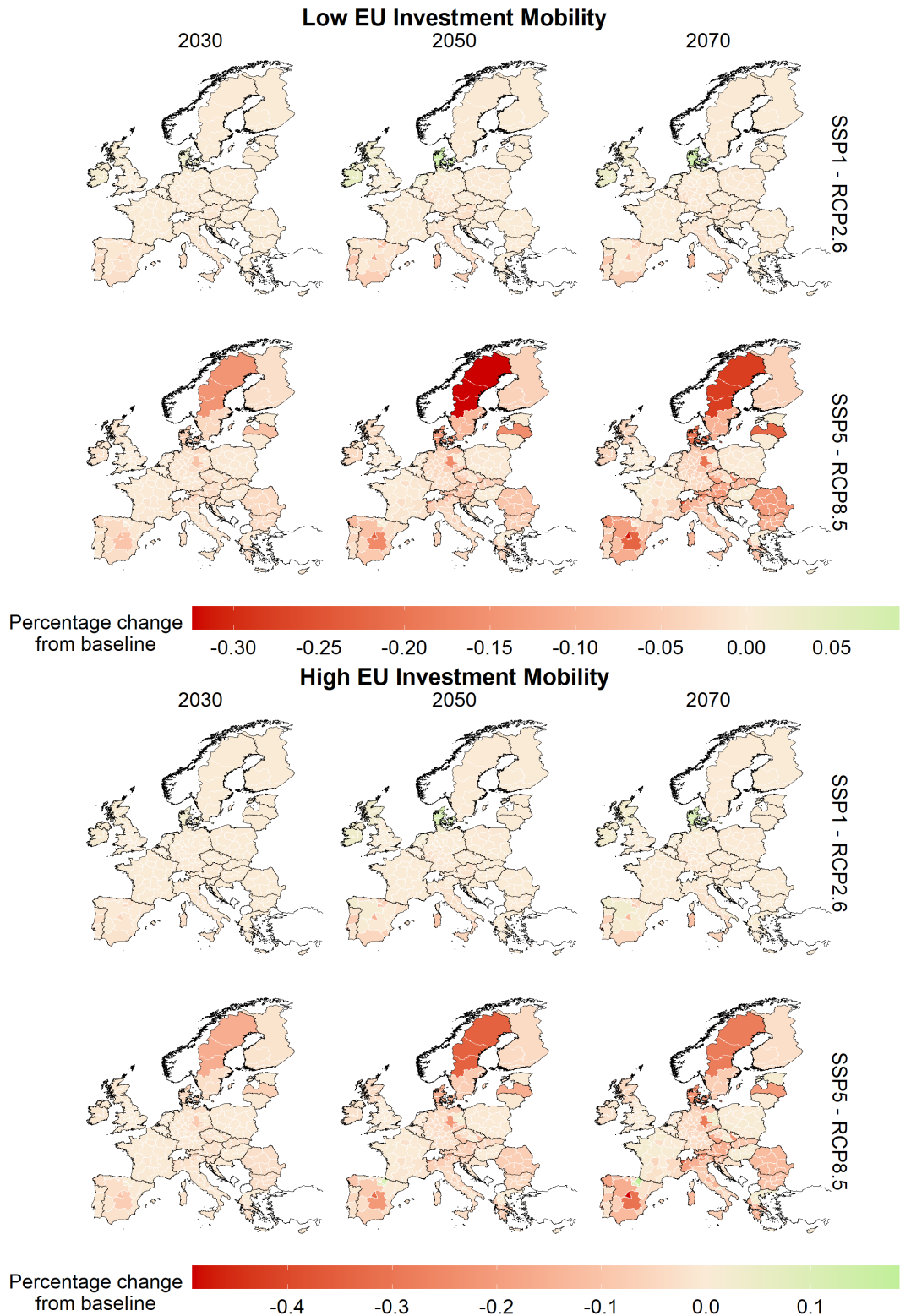
Figure 23. Climate change impacts on energy supply: GDP impacts by region in years 2030, 2050 and 2070. Medium impact case. SSP1-RCP2.6 and SSP5-RCP8.5 comparison. Low interregional investment mobility upper panel, high interregional investment mobility lower panel. Values are percentage change from the baseline.

Figure 24 summarizes the results of all the energy supply simulations. It confirms that, especially when moving towards the end of the century, and impacts are more evident, magnitude of economic losses can be in fact influenced more by the social economic scenario than the climate change one.

Figure 24. Climate change impacts on energy supply: distribution of GDP impacts across all regions of the ICES model in 2050 and 2070, by scenar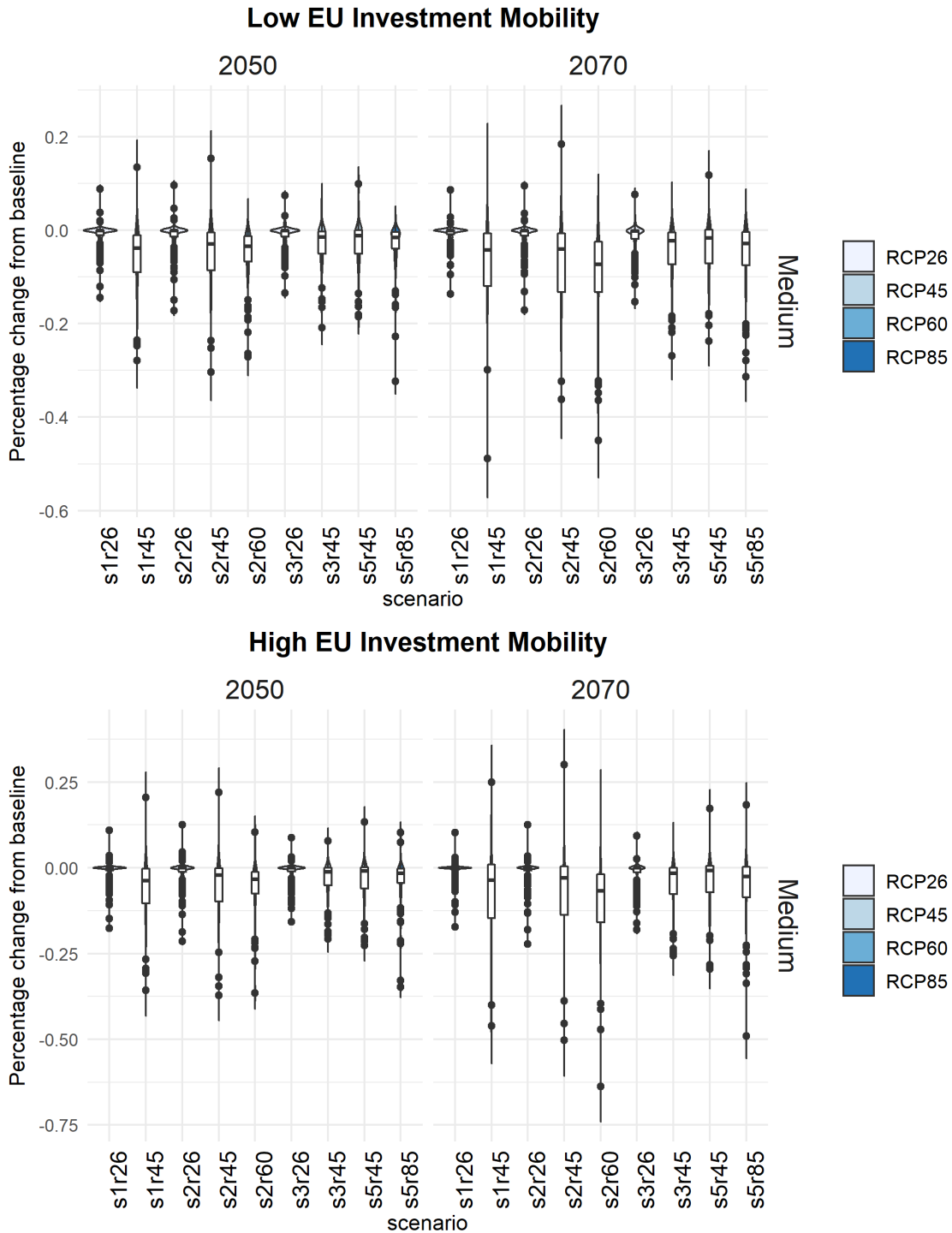io combinations; medium impact case. Low interregional investment mobility upper panel, high interregional investment mobility lower panel. Values are percentage changes from the baseline.

2.2.8 Energy demand

i. Impact modelling

Input data for the macro-economic assessment of climate change impacts on energy demand have been computed in COACCH D2.4 (Schleypen et., 2019).

The starting points are the econometric estimates of demand to temperature elasticity from De Cian and Sue Wing (2017). The study determines elasticity for electricity, petroleum products, and natural gas demand for four different uses (agriculture, industry, services and residential).

Future trends in regional energy demand are obtained combining these elasticities with high-resolution ensemble-mean temperature projections from four Regional Climate Models (RCMs): KNMI RACMO22E, IPSL-CM5A-MR, MPI-ESM-LR, and CNRM-CM5. In the ICES model this translates in implementing 12 different impacts i.e. the number of energy carriers times the number of economic activities. This has been done for each SSP-RCPs scenario combination examined by the COACCH project.

To implement changes in energy demand in the agriculture, industry, and services sectors we acted on the energy efficiency in those sectors. Accordingly, to increase (decrease) energy demand we imposed a lower (higher) efficiency in the use of energy in the sector. This is functional to push the sector to increase (decrease) energy use as desired.

A different procedure has been used in the case of the residential sector. In fact, this does not exist in the ICES model. It has been approximated by the representative regional household that is a component of the final demand. Energy demand shifts are obtained imposing exogenous shocks to household energy expenditure while keeping fixed the household budget constraint. This implies a re-adjustment of household consumption across all consumption items.

ii. Simulation results

GDP consequences of climate induced shifts on energy demand demonstrate a low sensitivity to investment mobility. They can be relevant either under high or low interregional investment mobility. According to the projections from the econometric estimates (Schleypen et al. 2019) the industrial, agricultural, and commercial activities are expected to increase substantively their electricity demand, the industrial sector also natural gas demand, especially in RCP8.5. These trends, induced primarily by cooling needs, represent an increase in the production costs for firms particularly felt in Southern European regions (Spain, Italy Greece, but also in Romania and Bulgaria). In 2070, in RCPs 8.5, 6.0 but also 4.5, these cost increases could induce macroeconomic losses larger than 1% of GDP in some regions of southern EU with a peak of -8% in Cyprus (Figure 25 and Figure 26) with possible losses in the order of 2% of GDP already in 2030. Increases in electricity demand, along with declines in oil and gas demand are foreseen for the residential sector. In this case the macroeconomic effects are more difficult to track as they trigger mostly a re-composition of households' demand across the different items they are consuming. Therefore, economic effects are more re-distributional and one can often compensate another.
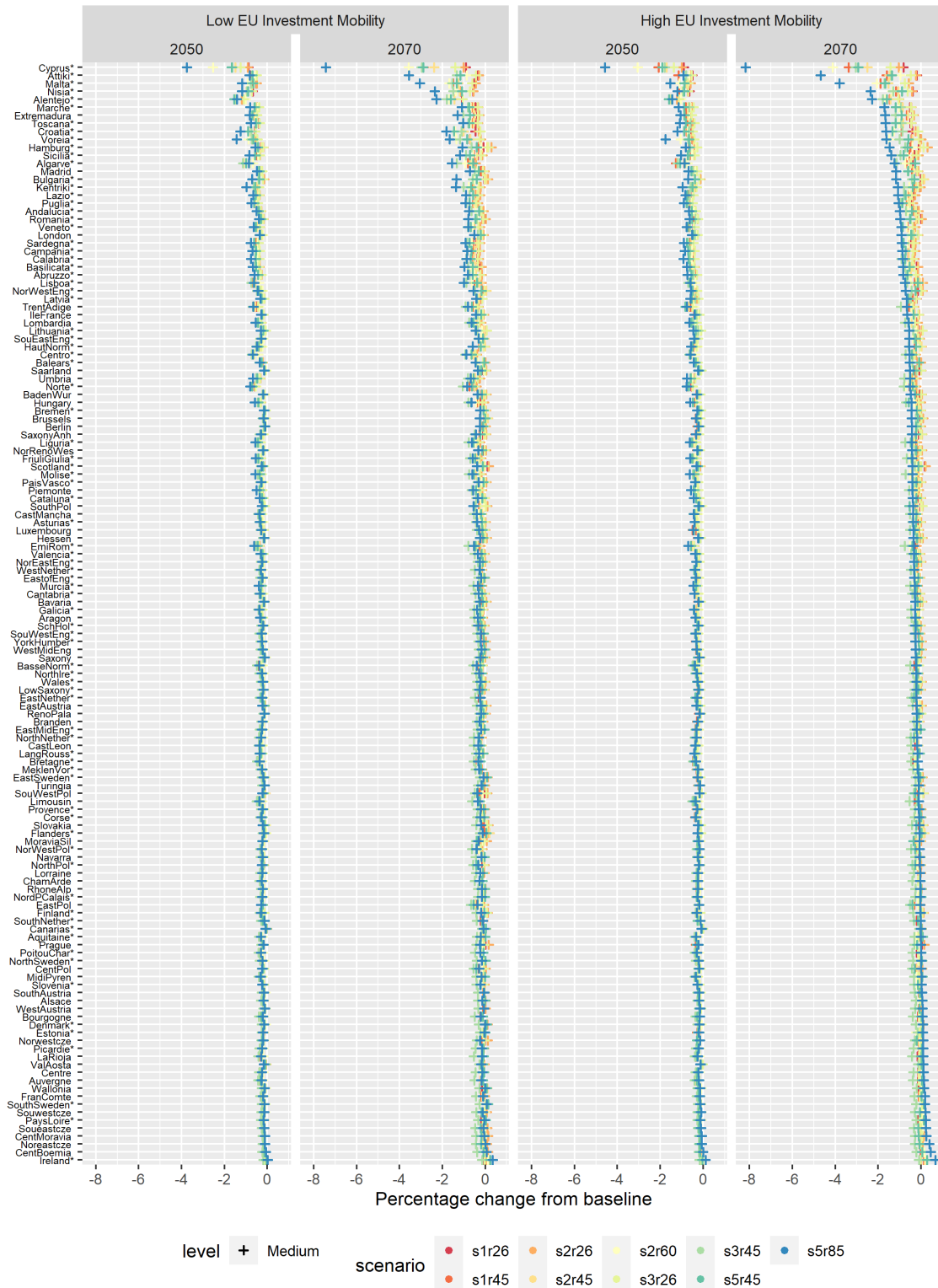
Figure 25 Climate change impacts on energy demand in the EU: GDP effects by region, scenario combination, investment mobility for 2050 and 2070. Values are percentage changes from the baseline.

Figure 26 Climate change impacts on energy demand: GDP impacts by region in years 2030, 2050 and 2070. Medium impact case. SSP1-RCP2.6 and SSP5-RCP8.5 comparison. Low interregional investment mobility upper panel, high interregional investment mobility lower panel. Values are percentage change from the baseline.

Figure 27 finally shows that in the case of energy demand the climate scenario tends to dominate the social economic scenario in the final determination of impacts.

Figure 27. Climate change impacts on energy demand: distribution of GDP effects across all regions of the ICES model in 2050 and 2070; medium impact case. Low interregional investment mobility upper panel, low interregional investment mobility lower panel. Values are percentage changes from the baseline.

2.2.9 Labour productivity

i. Impact modelling

In COACCH D2.4 (Schleypen et al., 2019) data on climate change impacts on labour productivity are estimated for all RCPs applying a fixed-effects panel regression method linking sectoral value added per working population to temperature, controlled for by including both the linear and its squared-term. Historical climatic data comes from the Global Land Assimilation System (GLDAS v2.1). Once the coefficients have been estimated, they are combined with future climate projections to obtain the final impacts. We opted to use data from four high-resolution Regional Climate Models (RCM): KNMI RACMO22E, IPSL-CM5A-MR, MPI-ESM-LR, and CNRM-CM5.

In the ICES macroeconomic model, labour productivity impacts are implemented directly as changes in the productivity of the labour production factor in the agricultural and industrial sectors. Econometric estimates foresee a decline in industrial productivity by 4.8% and in agricultural productivity by 6% in RCP8.5 by 2070 concentrated in Euro Mediterranean countries, and potential gains in Northern EU countries. Under RCP4.5, industrial productivity could decline by 2.6% by 2070 and agricultural productivity by 4.1%.

ii. Simulation results

Declines in labour productivity transmit through the overall economic activity eventually affecting the macroeconomic performance of the regions. The different degrees of investment mobility across regions play only a marginal role in determining GDP losses. These match quite well the profile of productivity losses. The highest are experienced under SSP5-RCP8.5 in 2070 (Figure 28 and Figure 29): southern and central-eastern European regions are hit more adversely showing potential GDP contractions in the order of 1.5-2%. Cooler areas like northern-Europe, but also Austria, or Italian Alpine regions, can gain roughly a 1% improvement in the economic performance. Note that GDP changes are considerably lower, and less differentiated, than the initial impacts on labor productivity. This is a direct consequence of the smoothing action played by market mechanisms: on the one hand, in the production function the less productive labor input is substituted, to the extent possible, with other production factors; on the other hand, the demand partly readjusts towards the consumption of less labor-intensive goods and services becoming cheaper in relative terms. The SSP1-RCP2.6 scenario combination shows the lowest losses with all the EU regions experiencing a GDP contraction of 0.5% or lower. Figure 30 finally demonstrates that, in the case of labour productivity, the temperature, i.e. the climate change scenario, exerts a larger importance than the social economic scenario in the determination of the final impacts. Still, the SSP3 scenario, featuring lower "flexibility"

in the energy production process and in trade mechanisms, tends to highlight, everything else equal, higher GDP losses than other SSPs.
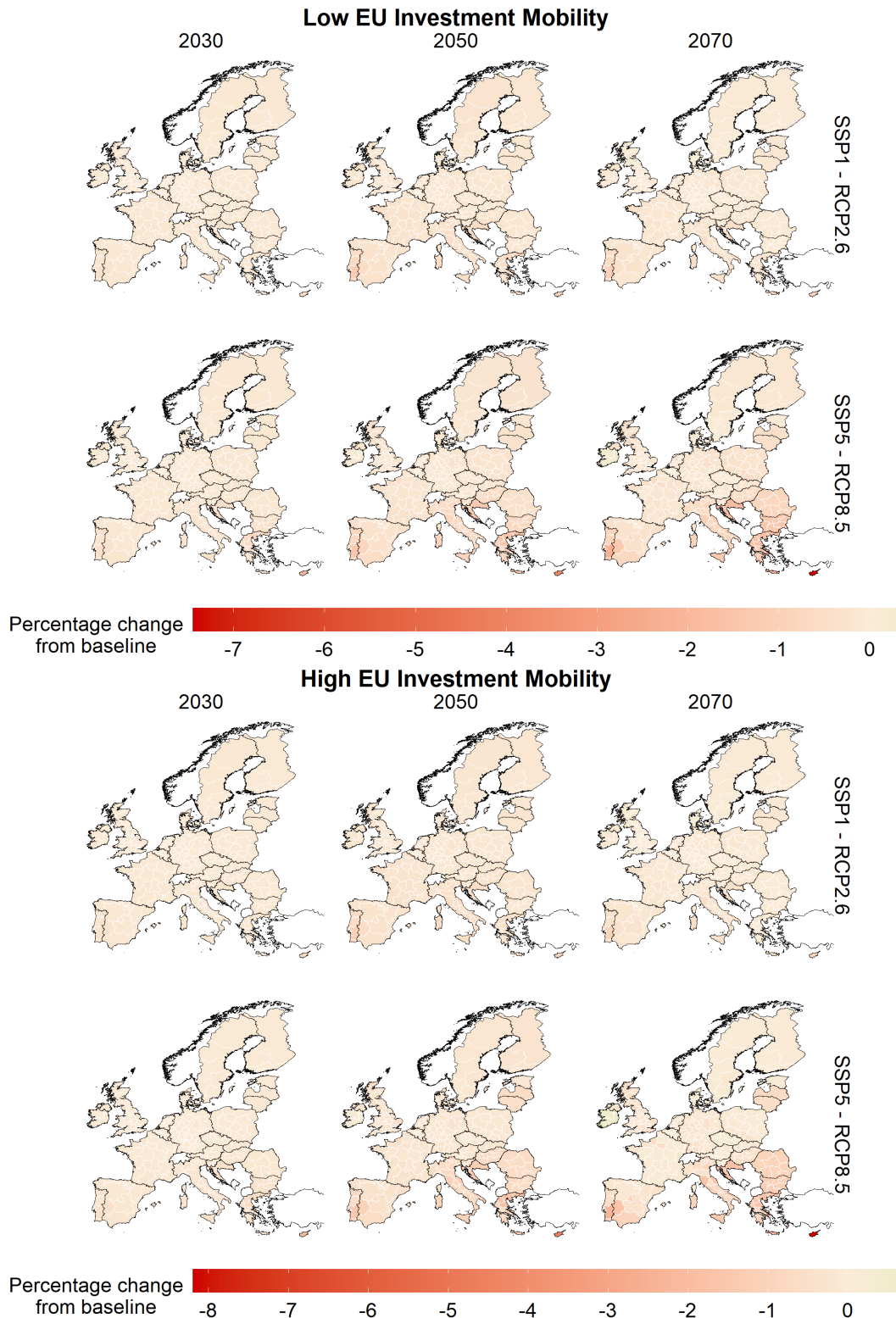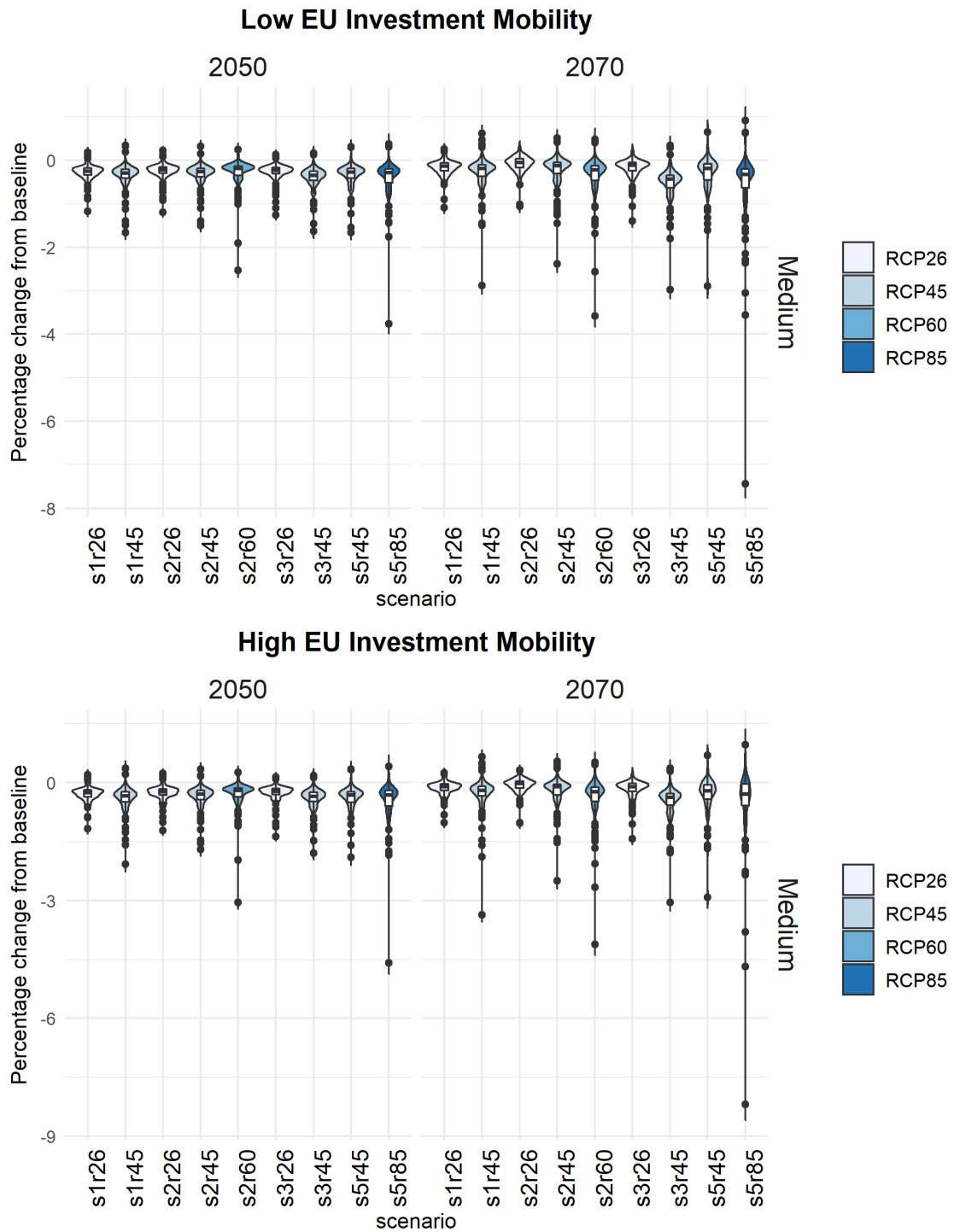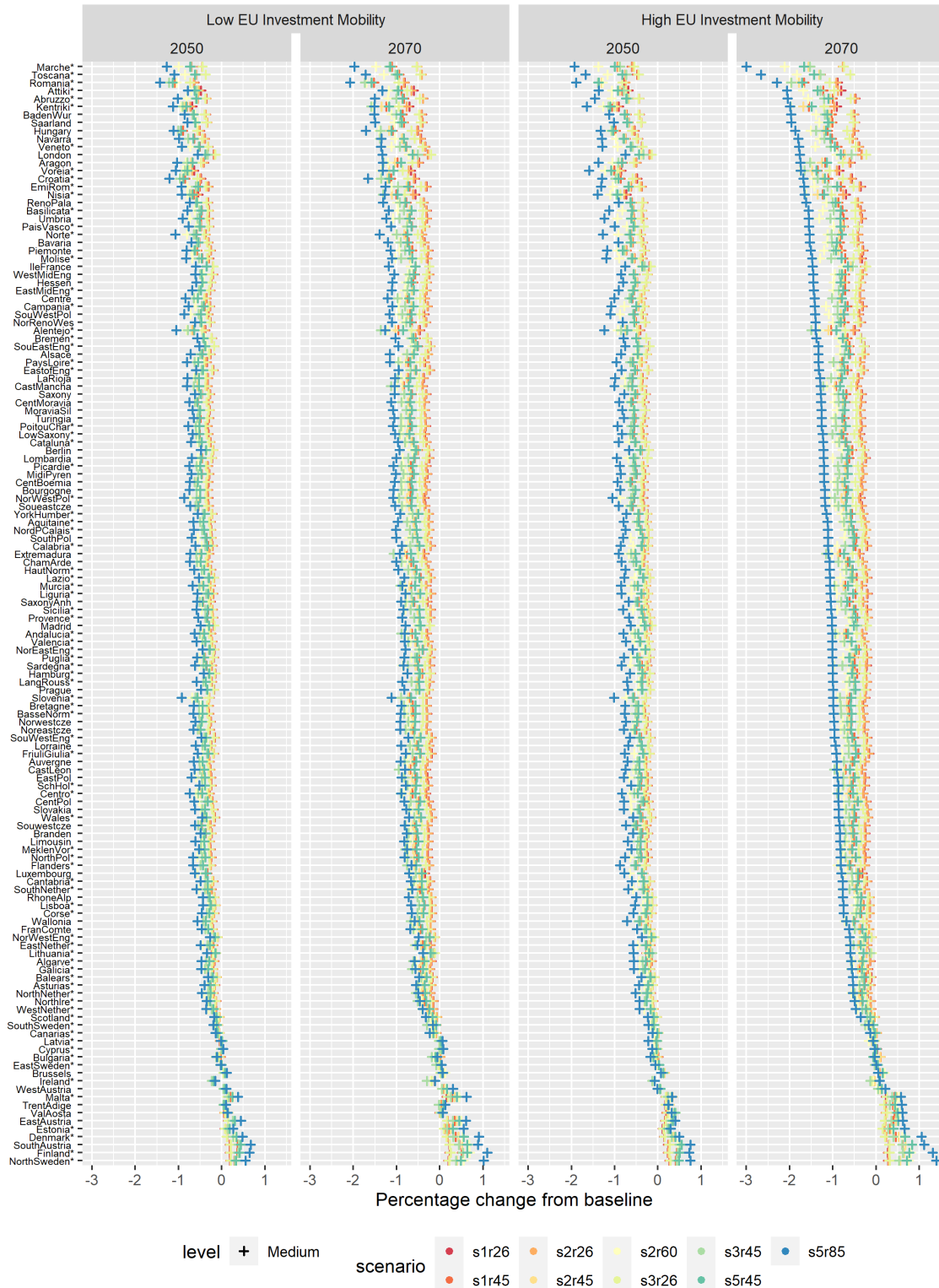

Figure 28 Climate change impacts on labour productivity in the EU: GDP effects by region, scenario combination, investment mobility in 2050 and 2070. Values are percentage change from the baseline.
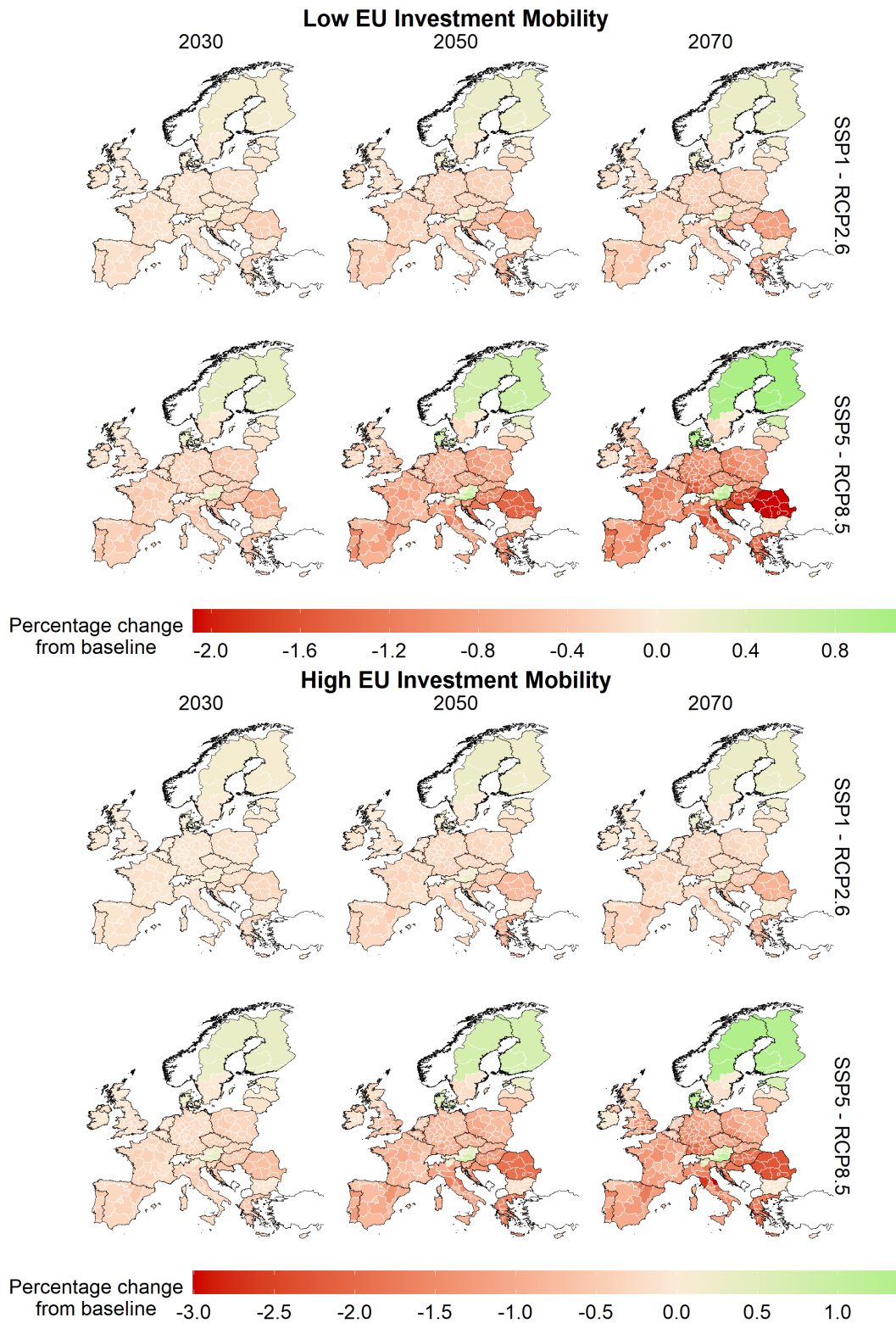
Figure 29 Climate change impacts on labour productivity: GDP impacts by region in years 2030, 2050 and 2070. Medium impact case. SSP1-RCP2.6 and SSP5-RCP8.5 comparison. Low interregional investment mobility upper panel, low interregional investment mobility lower panel. Values are percentage change from the baseline.

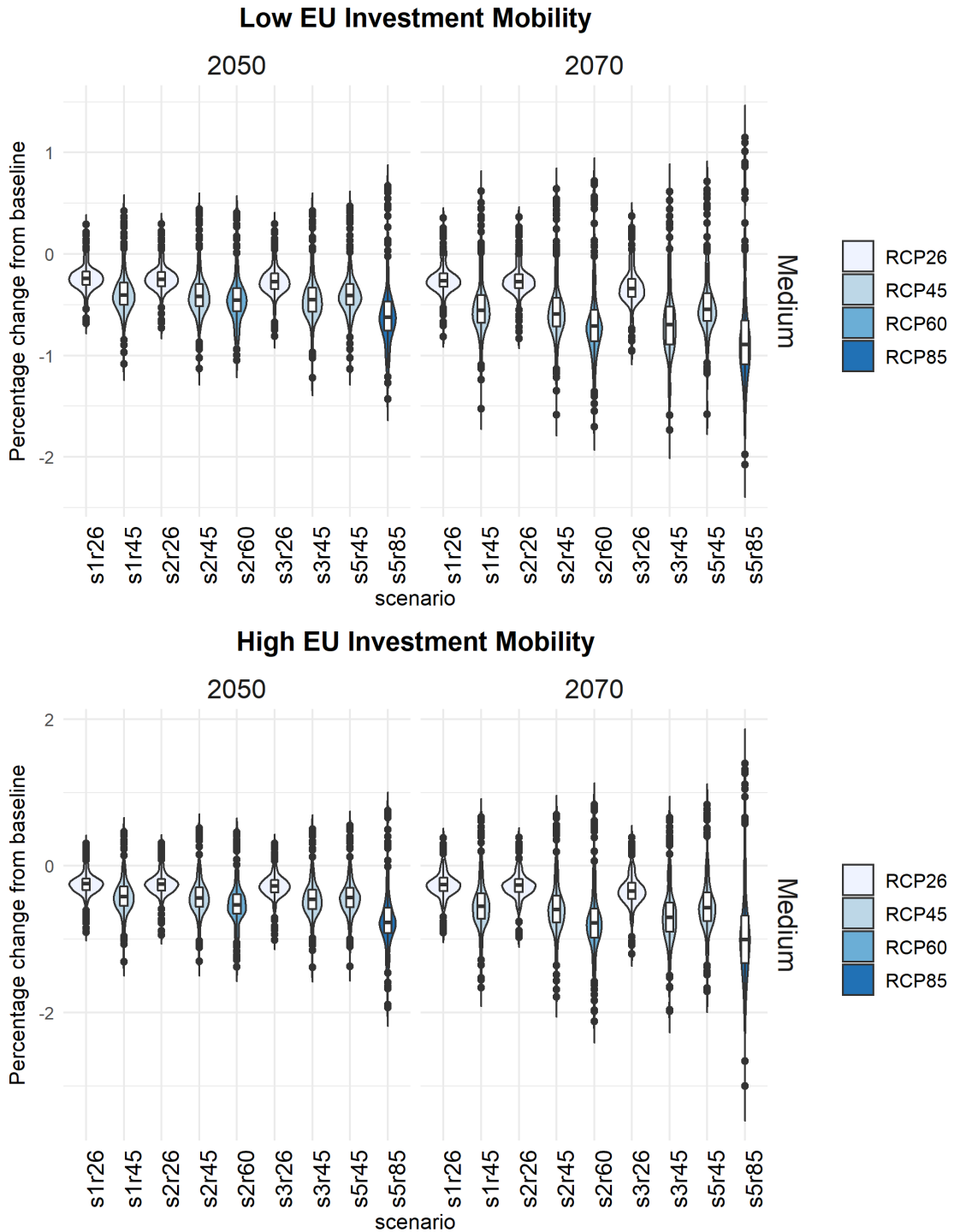**Figure 30. Climate change impacts on labour productivity: distribution of GDP effects across all regions of the ICES model in 2050 and 2070, by scenario combinations, medium impact case. Low interregional investment mobility upper panel, high interregional investment mobility lower panel. Values are percentage changes from the baseline.**

2.3 Compounded impact assessment

This section of the macroeconomic estimates implements jointly all the sectoral impacts of the previous sections. It highlights the compounded effect of all the impacts on regional GDP[2].

2.3.1 Simulation results

As a first representation of the full range of results Figure 31 shows all the regional GDP impacts across all years, regions, climate, social economic scenarios (including different assumptions on interregional investment mobility), and impact ranges. The "joint" effect of climate change implies a median GDP loss of 2.2%. It is important to stress that this analysis does not consider important non-market impacts including on health and on biodiversity and ecosystem services. It also does not include the potential impacts of climate or socio-economic tipping points – discussed in COACCH WP3. These would all be expected to increase GDP losses, and introduce much stronger impacts for high-warming scenarios. The figure also shows that the focus "just" on the median losses can be highly misleading. There are indeed strong regionally differentiated patterns and one fourth of EU regions can experience a loss that is larger than 5% of its GDP.
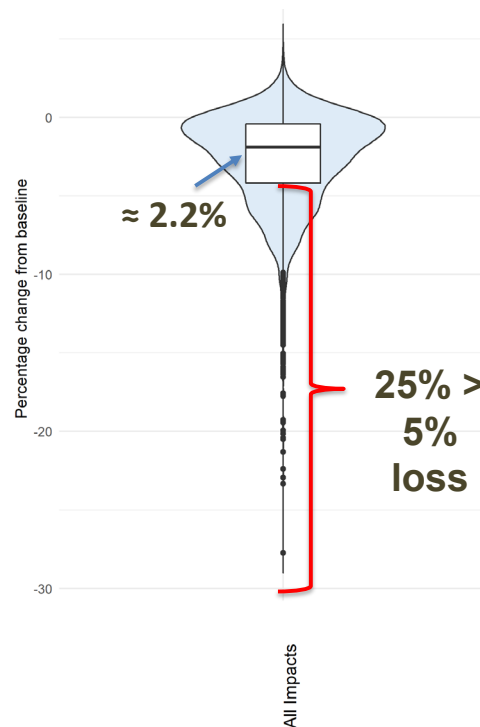
Figure 31. GDP losses in EU regions: all years, all impacts, all scenario combinations. Values are % change from the baseline.

---

[2] For completeness Appendix 1 reports a comparison of direct versus higher order costs.

Turning to the more detailed regional picture (Figure 32), in most EU regions climate change impacts can become non negligible already by mid-century. As expected, this is more evident in the "high impact case" with high investment mobility and in scenarios with the stronger climate signal: RCP6.0 and RCP8.5. Losses can be larger than 1-2% of regional GDP. Nonetheless, this result, even though partly moderated, is confirmed in the "low" and "medium impact" cases and with low investment mobility. Here, losses larger than 0.5% of regional GDP are common in 2050. The "high impact case" also highlights the higher economic vulnerability of regions, mostly located in southern and eastern European countries where the loss is close or larger than 5%. In Latvia the loss can potentially exceed 10% (see COACCH D3.4 (Botzen et al., 2020) for further discussion on extreme economic losses and social economic tipping points). Until 2050 macro-economic effects are quite similar across the SSP-RCP combinations. The ampler difference in the results indeed originates more by the choice of the impact forcing data, whether they are taken from the low, medium, or high impact case, or by the assumptions on investment mobility than by the different SSP-RCP combination (Figure 33).

In 2070 GDP impacts and their variability increase. There is an evident difference across the low and high investment mobility cases. Although losses prevail in both specifications, and the geographical distribution of macroeconomic effects is robust across set ups, in the former, losses are smaller, and more regions may gain under a lower climate signal (either from lower warming scenarios or lower climate sensitivity). The divergence is almost entirely due to the behaviour of two impacts: primarily sea-level rise and partly riverine floods. These two impacts affect the regional capital assets. Investment reactions to capital return are thus one of the main drivers of systemic macroeconomic effects. Accordingly, the way in which investment mobility is modelled can play a large role. In the specific case, sea-level rise losses are considerably smaller and less widespread under low investment mobility. Given that sea-level rise costs are also among the larger sources of economic losses, this explains the width of the difference.

The following dynamics can be further described:

- The low impact case highlights potential gains in agriculture, forestry, and fisheries in many EU regions. At the same time, negative impacts from other drivers are small. This eventually originates the possibility of net GDP gains in regions generally located in the central and northern EU, but also in some southern European countries where the local economic activity is particularly oriented to these sectors. Gains are however moderate (mostly lower than 1% of GDP) with just the exception of Bulgaria close to 5% of regional GDP in SSP1-RCP2.6. On average, over the sample of EU regions, losses prevail over gains (Figure 33). When present, losses are more widespread in southern EU regions, nonetheless they can affect northern areas mostly because of sea-level rise.
- Gains from agriculture, forestry and fishing that increase with climate change can originate, in some regions, lower net losses (or higher net gains) in a stronger climate signal scenario like RCP8.5 than in a more moderate one like RCP4.5.

- The main drivers of macroeconomic impacts from climate change are (Figure 35, Figure 36) sea-level rise (especially in the high investment mobility case), riverine floods and crop yield changes. Impacts on fishery and forestry (that in the majority of EU regions originate GDP gains), roughly comparable in magnitude with impacts on labour productivity, energy supply and demand (the latter inducing GDP losses), follow. Less relevant in terms of GDP effects (with some regional exceptions) are interruptions of road networks. On the one hand these can be good news as we demonstrated in sub section 2.2.4 that adaptation can deal cost-effectively with one of the most concerning of these climate change impact: sea level rise. On the other hand, less optimism is induced noting that positive GDP impacts in low and moderate warming scenarios, are due to investment mobility patterns or indirect trade effects for natural resource dependent sectors such as agriculture, forestry and fishing. Some caution needs to be taken because of the high uncertainty associated with these dynamics and sectors, and because there may be other constraints.

Figure 32: Compounded effect of climate change impacts on the EU GDP by region, scenario combination, investment mobility in 2050 and 2070. Values are percentage change from the baseline.
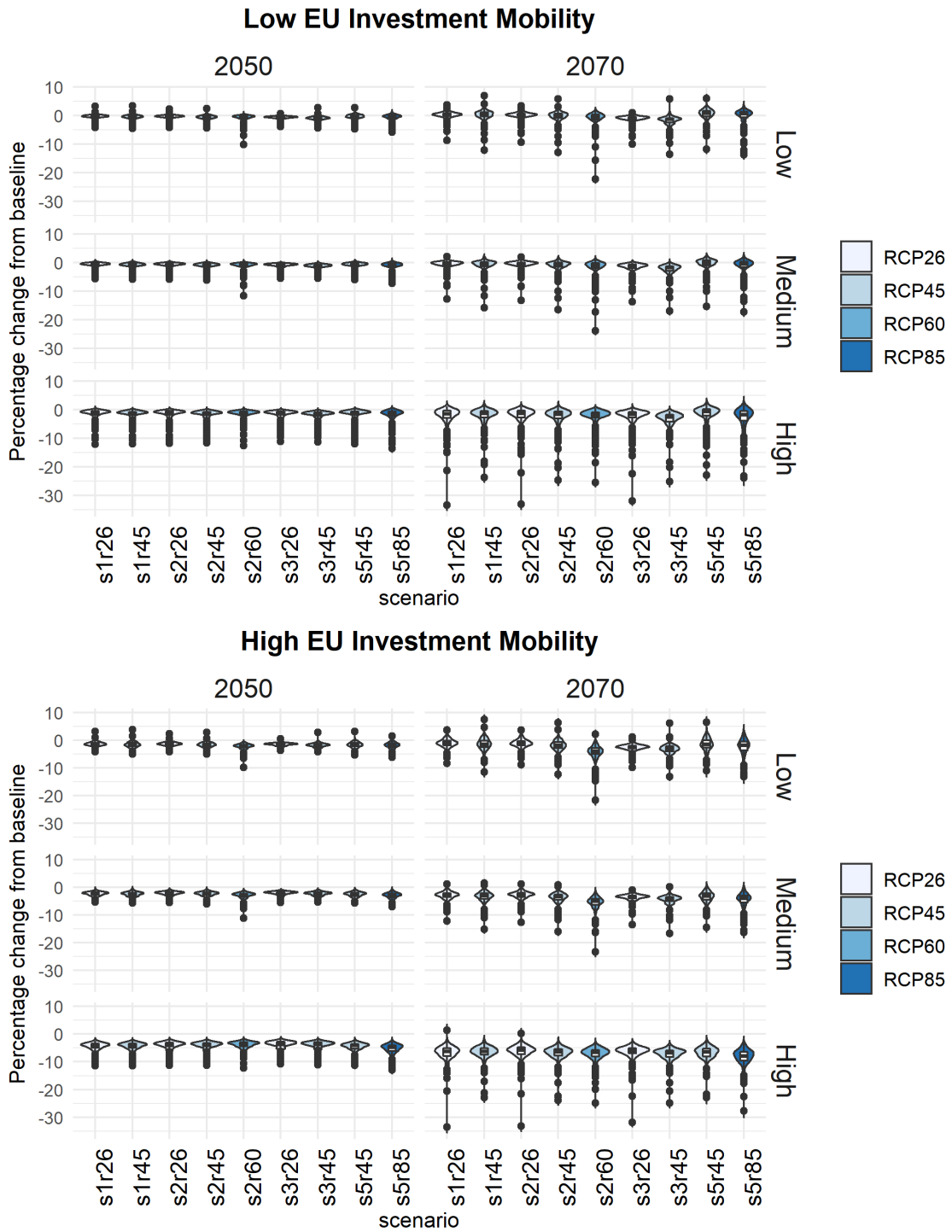
Figure 33 Distribution of compounded effect of climate change impacts on GDP across all regions of the ICES model in 2050 and 2070, all scenario combinations; Low, medium, high impact case, low interregional investment mobility upper panel, high interregional investment mobility lower panel. Values are percentage changes from the baseline.
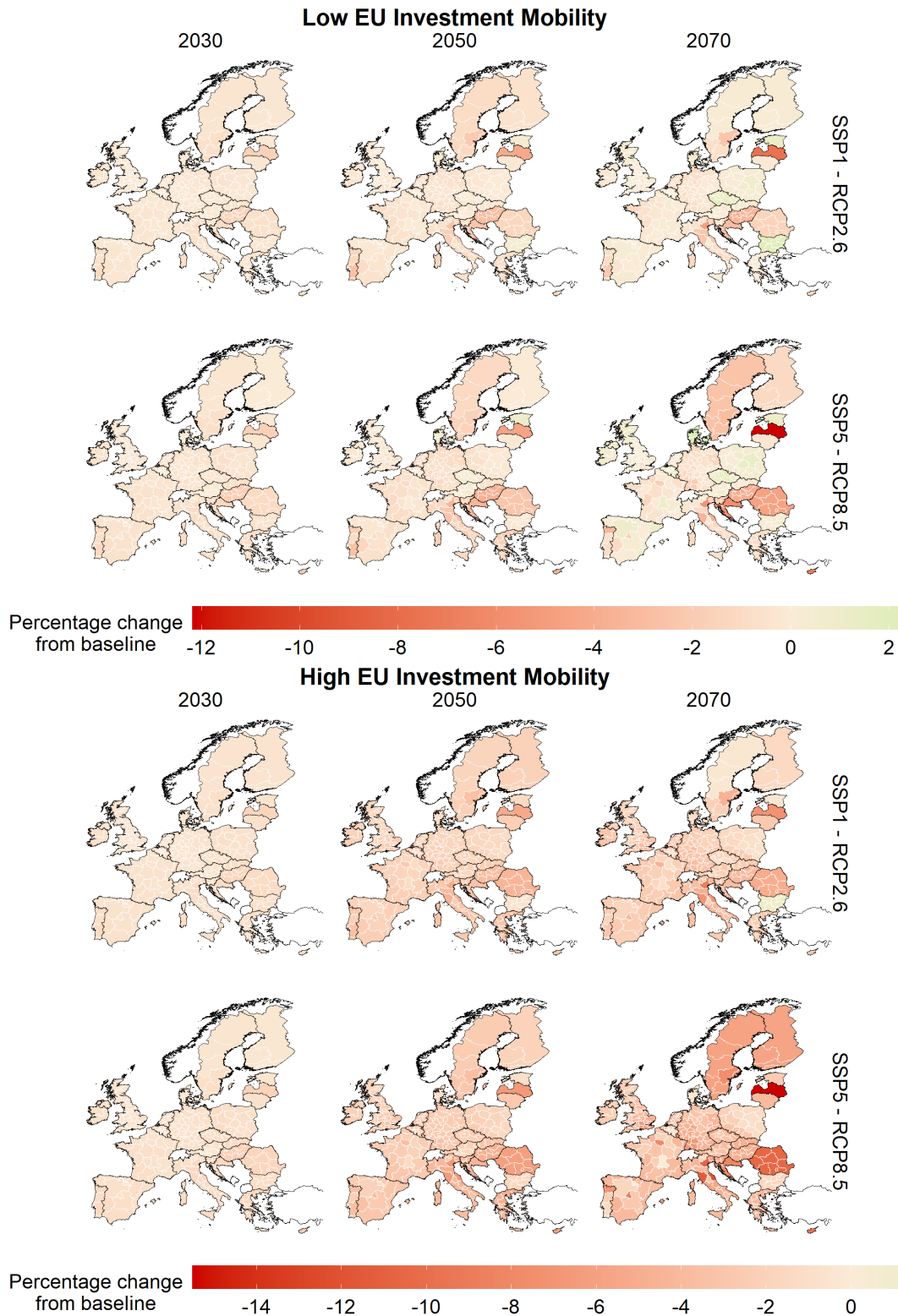
Figure 34 Compounded climate change impacts on EU GDP impacts by region in years 2030, 2050 and 2070. Medium impact case. SSP1-RCP2.6 and SSP5-RCP8.5 comparison. Low interregional investment mobility upper panel, high interregional investment mobility lower panel. Values are percentage change from the baseline.

Figure 35: Decomposition of compounded effect of climate change impacts on the EU GDP by region in 2070, LOW EU Investment Mobility, HIGH impact case. SSP1-RCP2.6 left, SSP2-RCP6.0 center, SSP5-RCP8.5 right. Dots are the total net effect, they may slightly differ from the sum of individual impacts as they take into account the impact interaction. Values are percentage changes from the baseline.
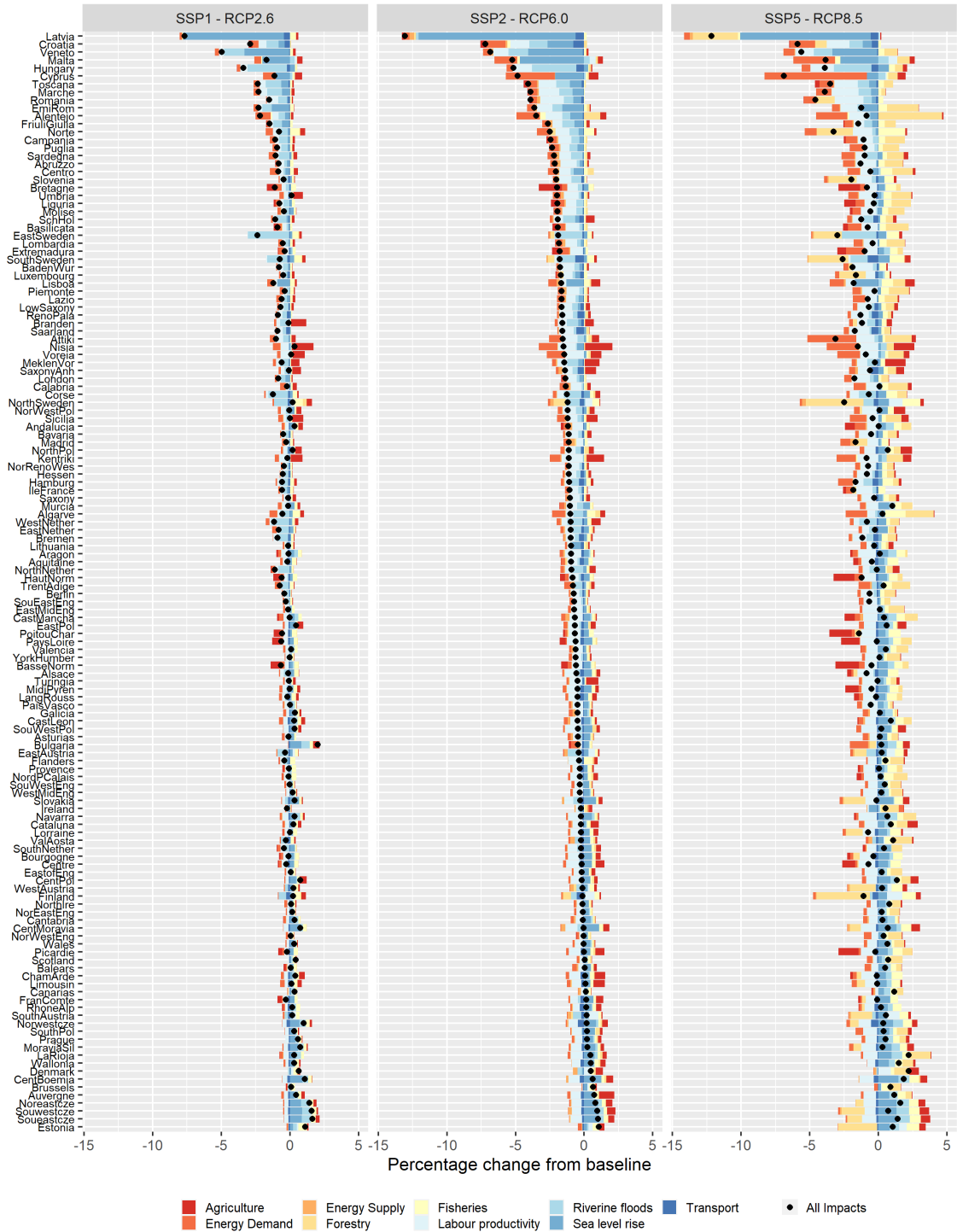
Figure 36 Decomposition of compounded effect of climate change impacts on the EU GDP by region in 2070, LOW EU Investment Mobility, MEDIUM impact case. SSP1-RCP2.6 left, SSP2-RCP6.0 center, SSP5-RCP8.5 right. Dots are the total net effect, they may slightly differ from the sum of individual impacts as they take into account the impact interaction. Values are percentage changes from the baseline.
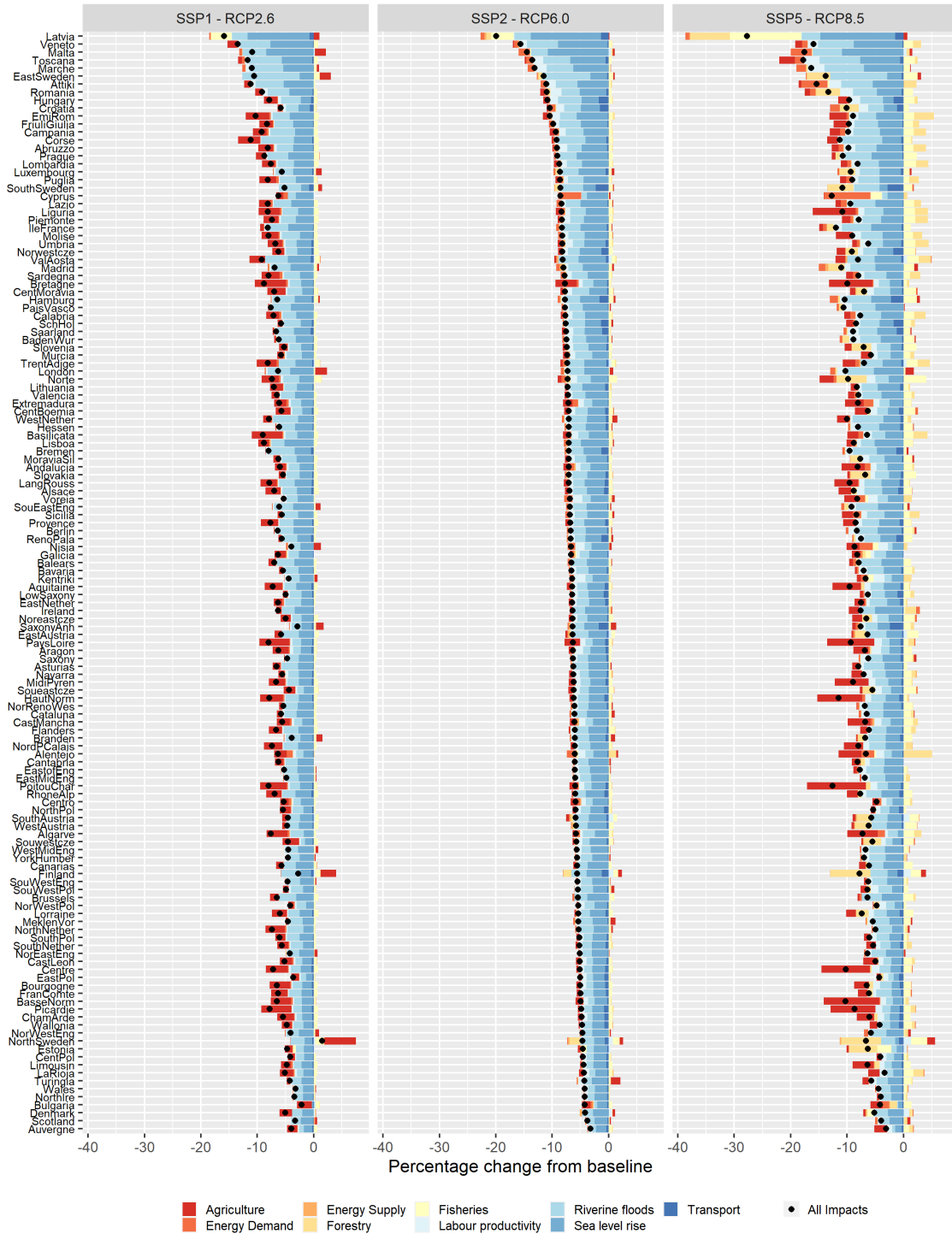
Figure 37: Decomposition of compounded effect of climate change impacts on the EU GDP by region in 2070, HIGH EU Investment Mobility, HIGH impact case. SSP1-RCP2.6 left, SSP2-RCP6.0 center, SSP5-RCP8.5 right. Dots are the total net effect, they may slightly differ from the sum of individual impacts as they take into account the impact interaction. Values are percentage changes from the baseline.

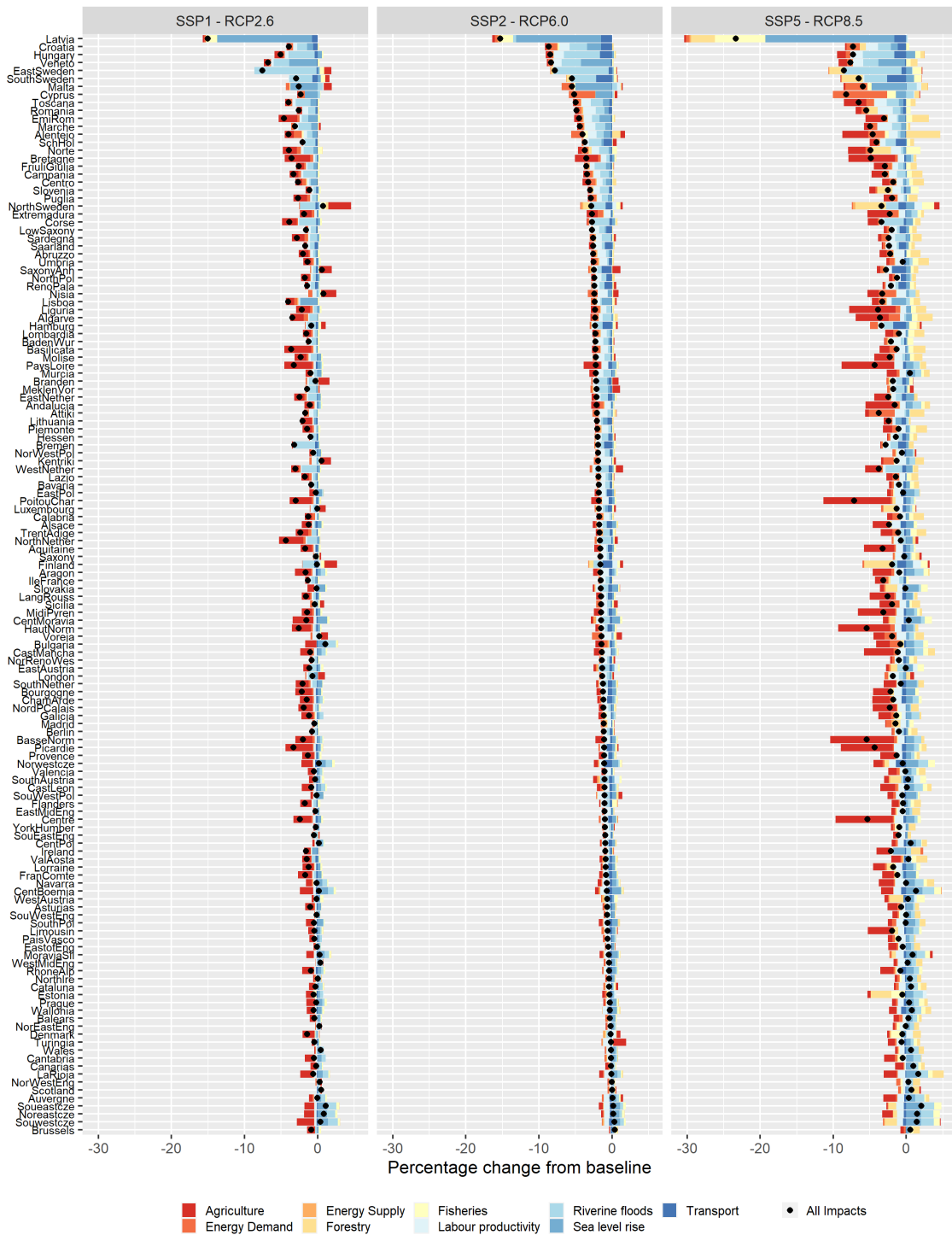**Figure 38 Decomposition of compounded effect of climate change impacts on the EU GDP by region in 2070, HIGH EU Investment Mobility, MEDIUM impact case. SSP1-RCP2.6 left, SSP2-RCP6.0 center, SSP5-RCP8.5 right. Dots are the total net effect, they may slightly differ from the sum of individual impacts as they take into account the impact interaction. Values are percentage changes from the baseline.**
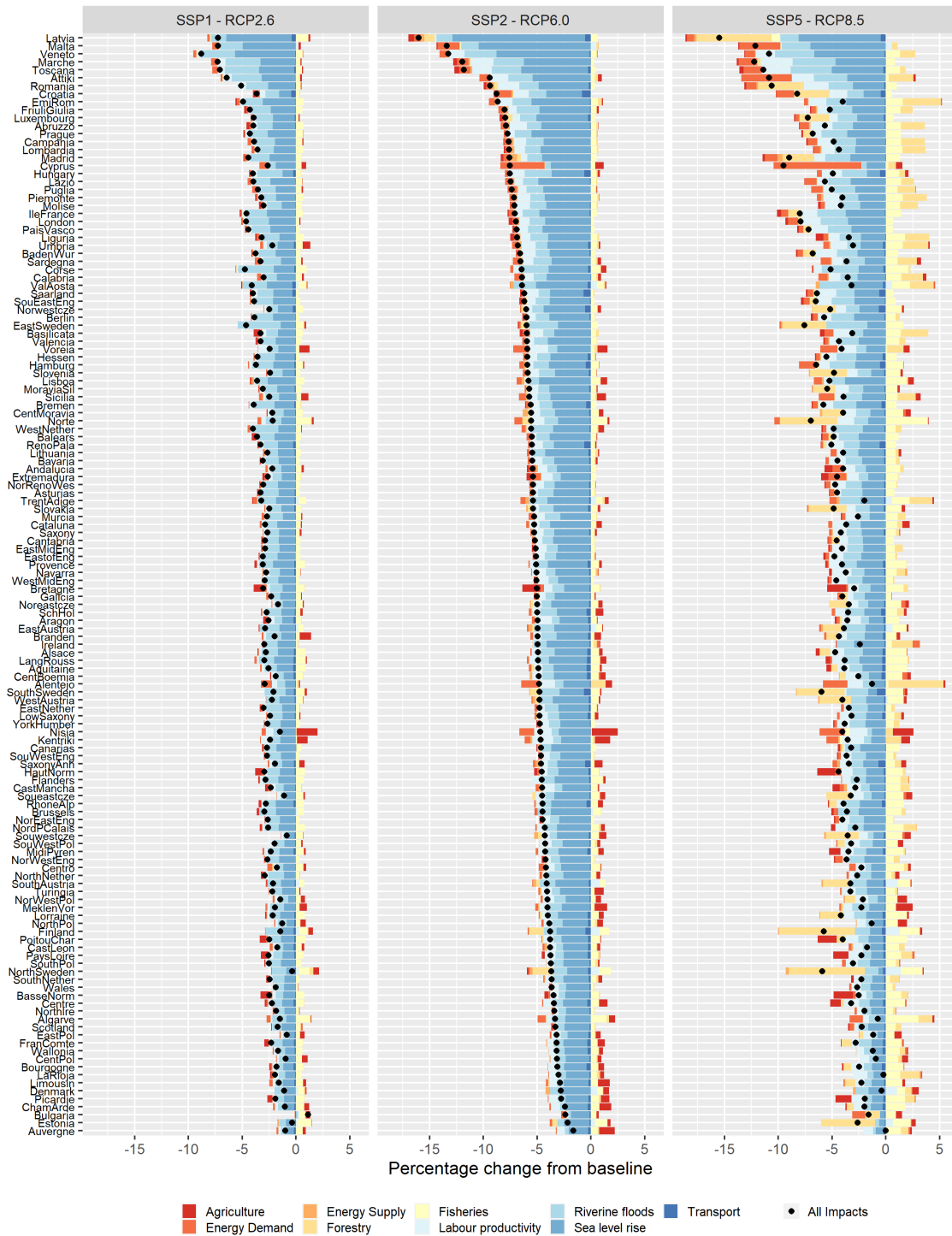
2.3.2 Uncertainty analysis

With the huge amount of data generated and their multidimensionality, it is important to understand, analyze, and transparently communicate the role of the different sources of uncertainty characterizing our investigation.

Macroeconomic results, or their variability, are influenced by four uncertainty sources: the social economic scenarios (SSPs), the climate change scenarios (RCPs), the "impact model/climate sensitivity", that is whether input for the economic assessment derive from the low, medium, high impact case, and, finally, by the assumption on interregional investment mobility, high or low.

The contribution of each factor is firstly disentangled with the analysis of variance (ANOVA) and then by a principal component analysis (PCA). Both have been conducted over the full period and then the two sub-periods 2020-2045 and 2046-2070 to highlight possible differences as times passes.

ANOVA:

Over the full period, the ANOVA coefficients (Table 3) highlight that:
- Compared to RCP2.6, all the other three RCPs contribute to higher damages.[3]
- Compared to SSP2, SSP1 and SSP3 results in higher damages, interestingly SSP5 is associated with lower damages.
- Compared to the low impact case, high and medium impact cases imply higher damages.
- Compared to high investment mobility, low investment mobility implies lower damages.

Table 3: Anova (full 2020-2070)		
	Coef.	P>t
RCP4.5	0.275	0.000
RCP6.0	0.495	0.000
RCP8.5	0.761	0.000
SSP1	0.025	0.002
SSP3	0.151	0.000
SSP5	-0.031	0.002
Level - High	1.240	0.000
Level - Medium	0.445	0.000
Low Inv. Mobility	-1.466	0.000

The magnitude of the ANOVA coefficients also provides an information of the role of the different uncertainty sources in determining the macroeconomic results. The larger are associated with investment mobility, closely followed by "impact model sensitivity", then by the climate scenarios and finally by the social economic scenarios. This analysis conveys important messages. It stresses the possibility to experience high economic losses also in low climate change scenarios. Uncertainty associated with the impact models, which in our case often coincides with climate sensitivity, is indeed a

---

[3] More precisely: the group mean of economic losses in RCP4.5, RCP6.0, RCP8.5 is statistically significantly different and larger than that in RCP2.6.

larger driver of economic losses than climate scenarios themselves. This is a further incentive to implement aggressive mitigation policy as any fraction of degree avoided can make a large difference. Furthermore, an important impact smoother seems to be associated with investment mobility. However, these impact reduction opportunities are far from certain given the difficulty to represent or predict many of the associated dynamics.

The ANOVA replicated in the two subsamples 2020-2045 and 2046-2070, confirms the analysis over the full sample with some minor, but interesting differences (Table 4). Firstly, uncertainty clearly increases as time passes (coefficients are increasing). Uncertainty from climate sensitivity and investment mobility still dominates, but in relative terms it increases less than that of the RCPs. SSP3, initially brings lower damages than SSP2, but then consolidates as an economic losses' amplifier. We recall that in SSP3, to represent a "fragmented world", international trade is more difficult. SSP5 leads to higher damages in the 2020-2040 period but lower damages thereafter compared to SSP2.

Table 4: Anova sub periods 2020-2045 (left), 2046-2070 (right)

	Coef.	P>t			Coef.	P>t
RCP4.5	0.091	0.000		RCP45	0.495	0.000
RCP6.0	0.095	0.000		RCP60	0.976	0.000
RCP8.5	0.283	0.000		RCP85	1.334	0.000
SSP1	0.057	0.000		SSP1	-0.013	0.263
SSP3	-0.025	0.000		SSP3	0.363	0.000
SSP5	0.021	0.002		SSP5	-0.094	0.000
Level – High	0.515	0.000		Level – High	1.965	0.000
Level – Medium	0.189	0.000		Level - Medium	0.694	0.000
Low Inv. Mobility	-0.618	0.000		Low Inv. Mobility	-2.483	0.000

Principal Components Analysis

When there are complex interactions across variables, like, in our case, between macro-economic impacts, climatic and social drivers, the Principal Components Analysis (PCA) can offer an efficient method to compact and highlight the underlying relations. The PCA aims to create a new set of uncorrelated variables, that are a linear combination of the initial variables, and explain as much of the initial variation as possible.

Thus, the perspective offered by PCA is different, even though connected, to that the ANOVA. The variables that we test in their ability to determine variance in macroeconomic outcomes are: the nine combinations of SSPs-RCPs, the three determinations of impacts from impact models sensitivity, and the two settings for investment mobility. The relationships between socioeconomic, climatic, impact, investment mobility scenarios and climate damages in the full sample are shown in Table 5 below. Only components with factor loadings > 0.3 were retained (Lu and Marlow, 1999).

Table 5: PCA Eigenvalues of the correlation matrix (2020-2070)

Variable	PC1 (SSP5-RCP8.5)	PC2(SSP3-RCP4.5)	PC3(High-mobility)
Eigenvalue	2.31	1.58	1.50
Variance (%)	39.4	26.7	18.3
Cumulative variance (%)	39.4	66.1	84.4

In the full sample, the highest correlation coefficients obtained between the principal components and individual variables indicate that climate damages were 84.4% determined by three elements. The first principal component (PC1) is the combination of SSP5-RCP8.5 (39.4%), the second one (PC2) is the combination of SSP3-RCP4.5 (26.7%), while the third component (PC3) is influenced by high investment mobility (18.3%).

Interestingly, when scenarios are considered as SSP-RCP combinations, their relative importance increases considerably with respect to the other components. In particular, SSP5-RCP8.5 that represents somehow the "worst case" for climatic conditions and SSP3-RCP4.5 that represents the more rigid economic system, are the major explanatory/drivers of variance in macroeconomic losses. Investment mobility still plays an important role but ranks third. This enriches the information from ANOVA. It points out the importance of avoiding both: i) a SSP5-RCP8.5 future that is a major "contributor" of the volatility of economic performances, and, ii) SSP3-RCP4.5 with an economic system where flexibility (or adaptive capacity) is low.

Table 6. PCA Eigenvalues of the correlation matrix (2020 – 2045 top, 2046-2070 bottom)

Variable	PC1 (SSP5-RCP8.5)	PC2(SSP3-RCP2.6)	PC3(High-mobility)
Eigenvalue	2.25	1.58	1.143
Variance (%)	27.9	21.8	12.1
Cumulative variance (%)	27.9	49.7	61.8

Variable	PC1 (SSP5-RCP8.5)	PC2(SSP3-RCP4.5)	PC3(High-mobility)
Eigenvalue	2.52	1.599	1.150
Variance (%)	43.2	32.5	15.4
Cumulative variance (%)	43.2	75.7	91.1

PCA for the sub-periods 2020-2045 and 2046-2070 are reported in Table 6. Results are robust along the two sub-periods and with the full sample PCA, with just one difference. In the first half of the century, climate signals are less differentiated and more mixed. This explains why in 2020-2045, in the second component (PC2), RCP2.6 substitutes RCP4.5.

Appendix 1
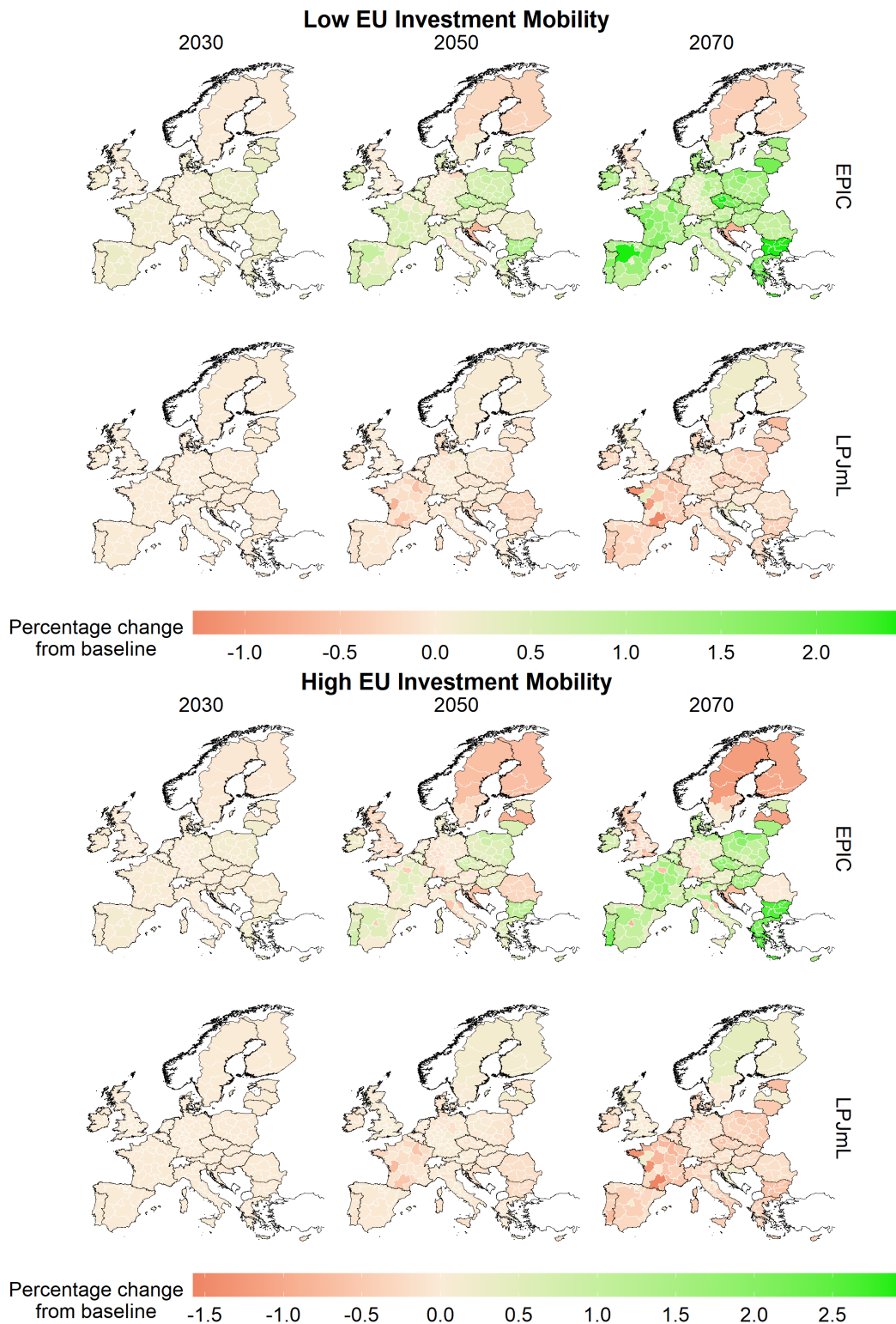
Figure 39. Climate change impacts on agriculture: GDP effects by region in 2030, 2050 and 2070 in the LOW impact-on-yield case, SSP2-RCP4.5 scenario combination. EPIC and LPJmL models' comparison. Low interregional investment mobility upper panel, high interregional investment mobility lower panel. Values are percentage changes from the baseline.
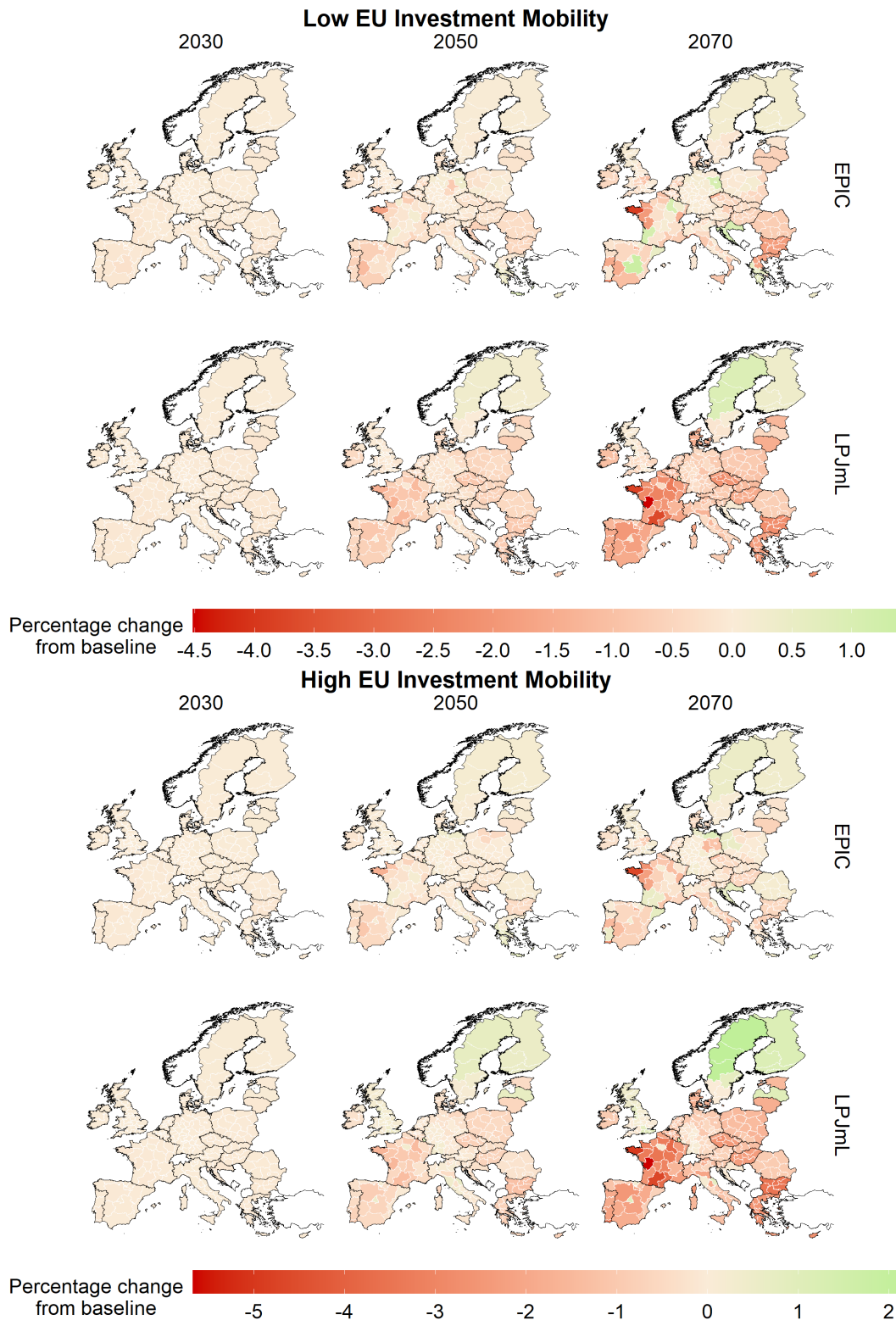
Figure 40. Climate change impacts on agriculture: GDP effects by region in 2030, 2050 and 2070 in the HIGH impact-on-yield case, SSP2-RCP4.5 scenario combination. EPIC and LPJmL models' comparison. Low interregional investment mobility upper panel, high interregional investment mobility lower panel. Values are percentage changes from the baseline.
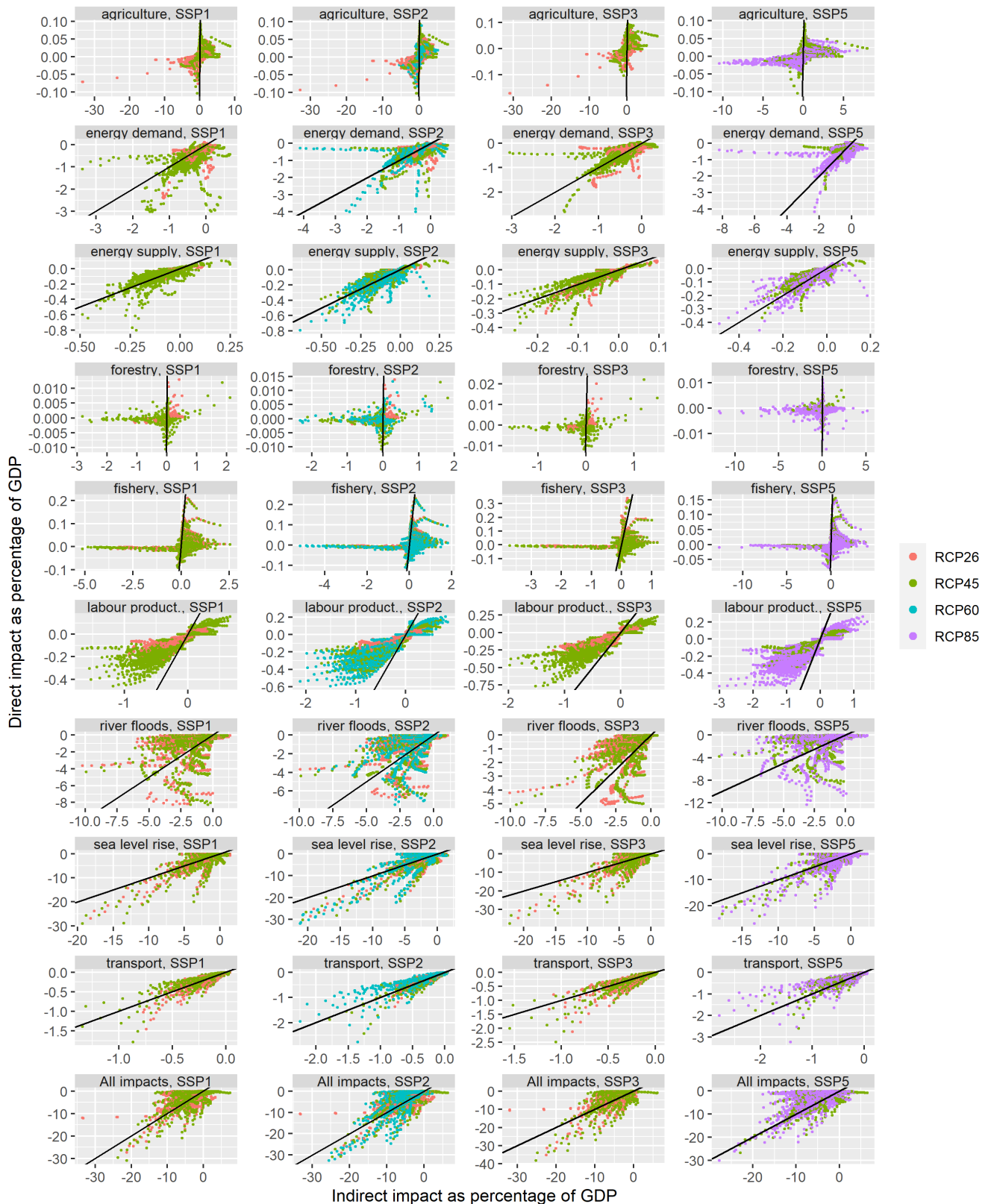
Figure 41. Comparison of direct vs indirect costs of climate change mpacts, both expressed in % of GDP.

3 Spatial analysis of climate change impacts

3.1 Downscaling macroeconomic impact at the 1x1 km grid level for the EU

3.1.1 Introduction

We propose an approach to downscale the GDP projections of the ICES model at the grid level. With downscaling, we refer to an information-guided disaggregation of data to a unit of reference of lower spatial resolution. Projections of variables relevant to climate change issues often come from top-down aggregated models that infer their future state starting from aggregate statistics. These statistics are usually gathered from national or international institutions, and therefore, are available predominantly at the national or regional level (Swan and Ugursal, 2009). Many policy applications could need a level of disaggregation at an even finer spatial resolution. This is especially necessary for the evaluation of climate impacts, which are characterized by a relevant spatial heterogeneity linked to both on the scenario and the type of impacts. The spatial levels could span from provinces (such as the NUTS 3 European classification) to Local Administrative Units (municipalities). Moreover, to prevent distorting effects posed by administrative boundaries, downscaling methods are often applied a homogenous partition of space, hence the analyses at the grid level to varying degrees of resolution.

In this work, we employ downscaling techniques to obtain a geographically explicit dataset of the ICES scenarios at the 1x1 km grid level for Europe, starting from regional data. Following the most recent literature, we base our methodology on each grid's level of current and projected total population and urban area (Murakami and Yamagata, 2019).

In the next Sections, first, we provide some context by summarising the literature on related topics. We then illustrate our methodological approach, as well as the description and the sources of the data used. To conclude, we describe the resulting datasets and propose this approach as a valid starting point for more complex analyses on the spatial distribution of climate impacts.

3.1.2 Review of the literature

Following an increasing availability of projection studies and geo-referenced data, downscaling applications are becoming more common and endowed with statistical methods of increasing complexity.

We first consider works that downscale GDP and GDP projections. First seminal work is the one by Gaffin et al., (2004), that proposes a linear downscaling of global population and GDP until 2100 for the SRES (Special Report on Emissions Scenarios) data A1, A2, B1, and B2. As limitations, the authors report implausible high growth rates, a discontinuity of the projection algorithm, and an assumption of independence between Population and GDP levels. Van Vuuren et al. (2007) apply an external-input

based downscaling for population and a convergence-based downscaling for GDP and emissions by the IPCC- SRES scenarios to the grid level of 0.25 degrees (approximately 27.75 KM). However, the algorithm is applied independently of per capita income levels. Moreover, this work does not consider additional potentially related variables like infrastructure, education, or urbanization. Grübler et al., (2007) work on total GDP from 1990 to 2010, obtained from the SRES scenarios A2, B1, B2, to obtain a 0.5-degree grid estimate. They employ a 2-step approach: a first estimation of the mathematical equation for GDP growth and income (GDP per capita) and then an optimization procedure to reconcile regional deviations from the country's total. They report as limitations the availability of starting data, inconsistencies in available data, and a lack of addressing uncertainty. Taking the global population as a starting point, Fujimori et al. (2017) downscales its levels with a rank-size rule and distributes GDP and emissions accordingly.

Kummu and Guillaume (2018) propose a global downscaling of subnational-level administrative data guided by the Hyde population dataset (Klein Goldewijk et al., 2011). In addition to GDP and GDP per capita in PPPs, they also downscale the Human Development Index in a 5-arc minutes resolution (9.3 × 9.3 km grid cells at the equator) for the years from 1990 to 2015. Finally, Murakami and Yamagata (2019) downscale the GDP and population scenarios developed by the SSP pathways to a 0.5-degree grid (approximately 50 Km near the equator). They apply a 4-step approach based on the Global Rural-Urban Mapping (GRUMP) project's city population value. In a first step, the approach estimates the population growth of a sample of the GRUMP cities population with a two-stage least squares spatial econometric model. They then define urban and rural potentials per grid based on the grid distance from the collection of cities and project urban and rural areas according to these potentials. Finally, they apply a dasymetric mapping approach to downscale rural and urban population and GDP by defining a set of models based on auxiliary variables, from which they select the most suitable combination through an ensemble learning approach. The latter therefore considers spatial and socioeconomic interactions, accounting for road networks, land cover, and allows a better differentiation for urban and non-urban areas, as well as allowing urban expansion/shrinkage (therefore avoiding an overly homogenous downscaling).

For the scope of this work, even if not directly tailored to a GDP application, it is valuable to consider also articles that provide downscaling methodologies for population levels. Indeed, our review of the literature reveals a closed link between exercises looking at the downscaling of GDP levels or growth rates, and the ones on population, as the two variables are intuitively intertwined.

Bengtsson et al., (2007) propose a trend-extrapolation to downscale the population in the timeframe 1990-2100 from SRES scenarios, accounting for the separation of urban and rural areas in 0.5 degrees grids. They highlight as limitations the heterogeneous definitions of urban populations by each country, and that they adopt a constant urbanization ratio. Hachadoorian et al., (2011) also adopt a trend-extrapolation, and compared it to an age-cohorts method in order to downscale the global population of 1995, and projected to 2025.

Referring to more specific demographic data is sometimes advocated, although their availability is often questioned (Yamagata et al., 2015). For instance, while not strictly a downscaling, Raftery et al., (2012) propose a Bayesian hierarchical model estimated via Markov chain Monte Carlo to project Countries population, based on fertility data. This shows how we can expect additional refinements of old works and methodologies based on the availability of new and better data.

Asadoorian (2008) simulates population and emissions up to 2100 by employing a conditional beta distribution with parameters calibrated on macroeconomic variables. Nam and Reilly (2013) downscale population density from the NASA SEDAC (Socioeconomic Data and Application Center) for the years 1990-2015, to a 0.25-degree grid with a rank-size rule-based approach to estimate city size.

Some works are focused on a single country. Jones and O'Neil (2013) look at the population in the US for the SRES A2 and B2 within a population potentials model, introducing free parameters to be calibrated. This includes varying scales of spatial analysis, urban and rural separation, and avoids grid's edge-effects and limiting habitable land area issues. Also for the US population, but for the years 2030 and 2050, McKee et al., (2015) apply a locally adaptive spatial interpolation technique and dasymetric modelling. This latter work, however, does not address climate change, land cover change, and migration. Fang and Jawitz (2018) work at a lower resolution of a 1 km pixel, applying a power-law scaling to estimate past urban areas. They test five models to distribute the US population from Census data, with the most complex including urban-rural divide, inhabitable land, topographic suitability, and socioeconomic desirability. This approach is particularly sensitive to the availability of census data.

Jones and O'Neil also proposed an analysis at the global level (Jones and O'Neil, 2016) where they adopt a parametrized downscaled gravity approach for urban and non-urban areas in order to downscale the population from all five SSPs. They report that gravity-based approaches might develop population figures also in unrealistic areas.

Yamagata et al., (2015) apply a model ensemble approach comparing different downscaling methods such as constant-share, share of growth, log-linear trend extrapolation methods, time series methods (ARIMA) for the Japanese Population projections, in order to estimate residential electricity.

Finally, to conclude this non-exhaustive list, we highlight a final strand of the literature: a downscaling tailored for regional or specific contexts. For instance, Merkens et al. (2016) and Reimann et al., (2018), use a comparable methodology to downscale and assess SSP scenarios for coastal areas (the former on a global scale, and the latter for the Mediterranean area). These works embed a higher difficulty due to finding proper data to categorize relevant factors (e.g. migration propensity to coastal areas) but show an interesting potential for the field of climate impacts evaluation.

3.1.3 Methodology

We follow Murakami and Yamagata, (2019) approach of downscaling GDP based on Urban Areas and Population at the grid level, each conditioned by the contribution of

auxiliary variables[4]. However, we depart from their approach rather significantly in two main directions.

The first is that they found their work on the projection of urban potentials, which are in turn based on the projection of a sample of the greatest cities' population from the Global-Rural Urban mapping dataset. The main reason to depart here is that our starting grid dataset is endowed with population figures already downscaled for the years 2006 and 2011. We therefore condition the growth of each grid g urban (or artificial) area directly on the evolution of the grid total population. This information allows us to discount the contribution of inhabited rural areas to the distribution of GDP levels to each grid[5].

The second main deviation is that instead of averaging through ensemble learning the contribution to urban areas by the different auxiliary variables, we include them directly in an econometric model. The resulting projections of urban areas are therefore conditioned to each grid's cell effects by the auxiliary variables as fixed effects.

To project grid-level urban areas, we need to condition the projections to one primary time-varying variable that we design as population per grid. Having a starting value, for 2011, we define a projection of population per grid through a simple downscaling procedure known as a "share of growth method" (Yamagata et al., 2015). This method links the growth of a lower scale unit (in our case the grid g) to the one at an upper (and available) level (in our case the country C) at times $T, t, t - \tau$:

$$P_{T,g} = \left(P_{T,C} - P_{t,C}\right)\frac{\left(P_{t,g} - P_{t-\tau,g}\right)}{\left(P_{t,C} - P_{t-\tau,C}\right)} + P_{t,g}$$

To apply this method, we consider the Countries total population growth rates available from the SSP scenarios, which are in turn employed in ICES. We define four main urban area trajectories based on the different population projections at the country level, which corresponds to SSP1, SSP2, SSP3 and SSP5.

Notice that the share of growth method requires three points in time to iterate the formula, whether our starting dataset has only two. We obtain therefore the first downscaling at the grid level for the year 2015 with a more straightforward method known as a "constant share of growth", where the growth rate is equally shared across region's grids. Once the 2015 value is computed as third point for our grids, and the actual population levels from Eurostat data are derived for 2015 and 2011[6], we also obtain the rest of the years' population through the SSP growth rates. We projected then each grid g population for each of the selected SSP scenarios.

---

[4] We attempt first a direct replication of their methodology. However, restricting the sample of their starting data to the European Union did not provide realistic coefficients and urban area projections. We then deviate from their approach also to obtain a finer resolution for our final grid.

[5] We plan to investigate also this direction in future applications with the aim of categorizing climate impacts with specific effects on different crops

[6] To have comparable population levels we adapt the Eurostat data by removing some NUTS2 value which are missing in ICES, such as French dominions and Portugal's islands of Madeira and Azores.

The second step in our approach is to model Urban Area (UA) per grid g in our starting year $t = 2011$, $UA_{g,t}$ based on Population $P_{g,t}$ and a matrix of k auxiliary variables $X_{g,k}$.

To account for the nested structure of the dataset, where each grid is part of groupings of increasing size (Country, and NUTS levels classification), we employ a linear mixed model (West et al., 2014). We declare our model as:

$$UA_{g,2011} = \alpha_g + \beta_1 P_{g,t} + \beta_k X_{g,k} + Z_{g,qj} u_{qj} + \varepsilon$$

Where, in addition to UA and P, we consider k auxiliary variables $X_{g,k}$ as fixed effects, which in our best model includes: the log of the distance from the nearest coast, the log of the distance from the nearest border, the log of the distance from the closest Functional Urban Area centroid, the grid road density, the grid land percentage rescaled to 0-1, and the ratio of the grid population levels of 2011 and 2006. We further assume that the location of grid g affects the urbanized area but in non-systematic ways. For this purpose, we assume country-specific (C) and region-specific (R) random effects u.

Table 3 Best linear mixed model estimation results

Dependent variable: Urban Area 2012		
Variables	*Coefficients*	*P-value*
Pop 2011	0.041***	(0.00003)
Distance to coasts	-0.001***	(0.00004)
Distance to border	-0.003***	(0.0001)
Distance to FUA	-0.001***	(0.0001)
Distance to the airport	-0.006***	(0.0001)
Ratio Pop 2011/2006	-0.068***	(0.0001)
Road Density	0.00003***	(0.00000)
Land Percentage	0.005***	(0.0003)
Constant	0.091***	(0.004)
Observations	4,436,642	
Marginal R^2	0.5250447	
Conditional R^2	0.6087025	
Note: *p**p***p<0.01		

The model is fitted with Restricted Maximum likelihood with the *lme4* package of software R (Bates et al., 2018). Prior to fitting, we partially address a non-normal distribution of the data by log-transforming the variables for Urban Area and Population.

The results are shown in Table 3. We predict the values of the model given our best model population coefficient, and proceed to project the Urban Area for each grid by taking the difference of the prediction by the two models over the simplifying assumption that the time-invariant exogenous variables will cancel out their effects over time:

$$\widehat{UA}_{g,T} = \widehat{UA}_{g,t} + \hat{\beta}\tilde{P}_{g,T} - \hat{\beta}\tilde{P}_{g,t}$$

Iterating this procedure by using the known time $t = 2011$ as a starting value, and the end time T as a projected year reference allows us to project Urban Area per grid until 2070 by a five years interval.

To avoid unrealistic results, we bound these projections to a set of assumptions. The first is that the projected urban area cannot be higher than the land percentage of the grid, which provides a maximum value of the buildable area. Notice that this assumption implies that an expansion of the urban area would overcome any rural or natural area. The second assumption is that we take urbanization as irreversible, meaning that if the prediction by our model sets a decrease in urban area we fix its level as the $T - 5$ one. This fits our CLC data-based definition of urban area, as actually a collection of artificial areas which could fit different purposes (such as activities and services) aside from population dwellings. The last condition is that we condition the evolution of urban areas to the last year of the data from which we calculate our urban area per grid, which is, at the time of writing, 2018.

The GDP projections from ICES are downscaled by aggregating the model's regions R projected urban area for a given year, and distributing the GDP level according to the grid share over the whole region:

$$GDP_{g,t} = \frac{\widehat{UA}_{g,t}}{\widehat{UA}_{R,t}} GDP_{R,t}$$

3.1.4 Data

In Table 4 we describe the data used to model the projection of population and urban area at the grid level.

Table 4 Description and source of the variables

Variable	Description	Source
Urban area (2000, 2006, 2012, 2018)	Area in square meters per grid, summed over the CLC codes "1", "Artificial Surfaces", which include Urban fabric, Industrial, commercial and transport units, Mine dump and construction sites, and other artificial non-agricultural areas.	CORINE Land cover data
Grid	Grid for the European area at the 1 KM resolution.	
Population per grid (2006, 2011)	Population values by grid	GEOSTAT1 and GEOSTAT 2006 initiative of the European Commission
Land Percentage	Share of land per grid (compared to water and other non-classified areas).	
Country ID and NUTS classification (0,1,2,3 levels)	Code for the administrative location of the grid, in NUTS 2016 classification.	
Border distance	Distance in meters from the closest national border. Distances are always defined from the centroid of the grid cell	
Airport distance	Own elaboration of the distance from the grid's closest airport. The airports are collected from the point dataset "airports 2013"	European Commission GISCO, "Transport networks"
FUA distance	Own elaboration of the distance from the closest Functional Urban Area (as per the 2018 definition) centroid	European Commission GISCO, "Urban Audit"
Road Density	Meters of Roads for square meter retrieved from the Global Roads Inventory Project (GRIP) dataset, and paired to the closest grid cell	Global Roads Inventory Project, GLOBIO (Meijer et al., 2018)
GDP projections	Projections by the ICES model at the regional level for the selected scenarios	ICES
Population SSP trends	Country level total population growth rates for the selected SSP scenarios	IIA

3.1.5   Results

The downscaling exercise results in a collection of .csv datasets storing the GDP levels for each projected scenario. ICES developed nine baseline scenarios, each with three different levels of climate impacts, totaling 36 datasets of downscaled GDP time series. The classification of the datasets follows the regional-level GDP projections, reporting the scenario combining the selected SSP (Shared Socioeconomic Pathway) and RCP (Representative Concentration Pathway) both in the baseline and in the climate impacts (low, medium, or high) versions. To provide an example, the dataset "GDP_ds_base_s1r26" refers to the downscaled GDP for the base scenario s1r26, which combines SSP1 and RCP2.6. "GDP_ds_impacts_s2r45h" refers to the downscaled GDP for the impact scenario "High" for the s2r45, combining SSP 2 and RCP 4.5.

Each dataset includes a grid level identifier, which is left unmodified from the European Commission Geostat initiative. Each grid is then classified with the ICES model reference region, labelled as "Final_ID". Notice that ICES regions are not directly comparable with the NUTS 2 classification of 2016, as they are based on the 2013 classification. Moreover, in ICES a couple of regions are aggregated (Trento-Bolzano and Andalucia). Finally, the GDP time series is labelled as "GDP_scenario_Year", ordered from the starting year 2015 to the final year 2070.

The collection of datasets includes a geo-referenced file, "GDP_geo.gpkg", which includes only the grid identifiers, as well as the topological representation of the GDP datasets. It can be used to generate maps and other visualizations of the data quickly. An example is provided in Figure 42 to Figure 48 where we map some GDP percentage and absolute variations comparing different years and baseline and impacts.
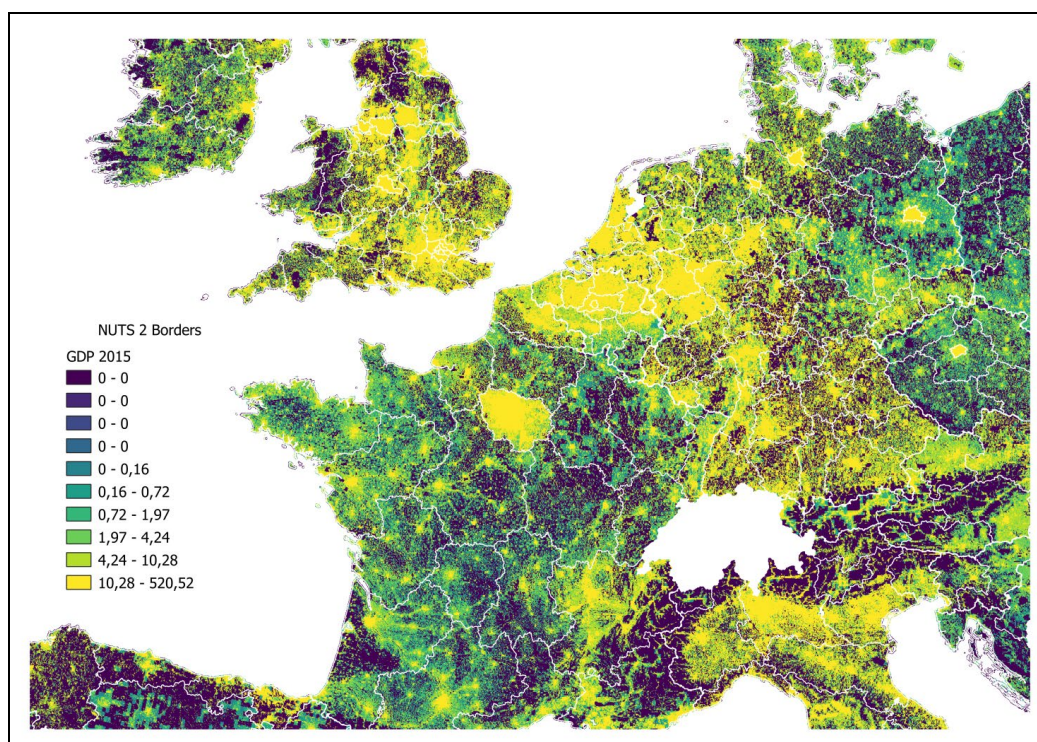

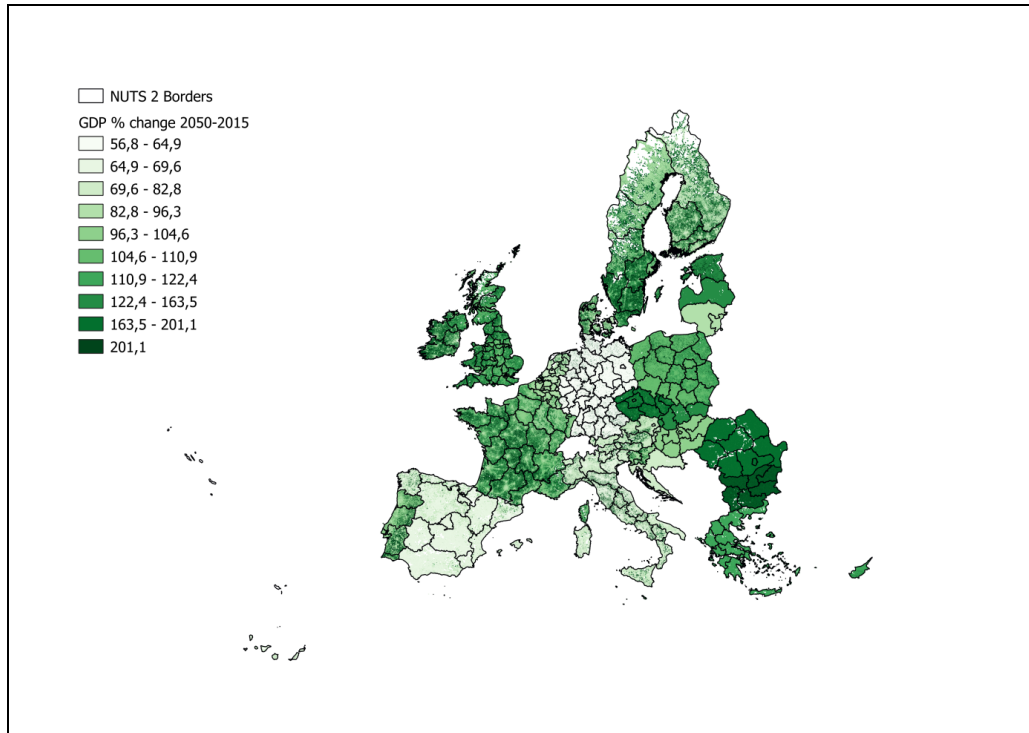**Figure 42: Magnified GDP levels in 2015, scenario S1R26 (million 2007 USD)**

Figure 43: Percentage change in GDP levels from 2015 to 2050 in the scenario S1R26
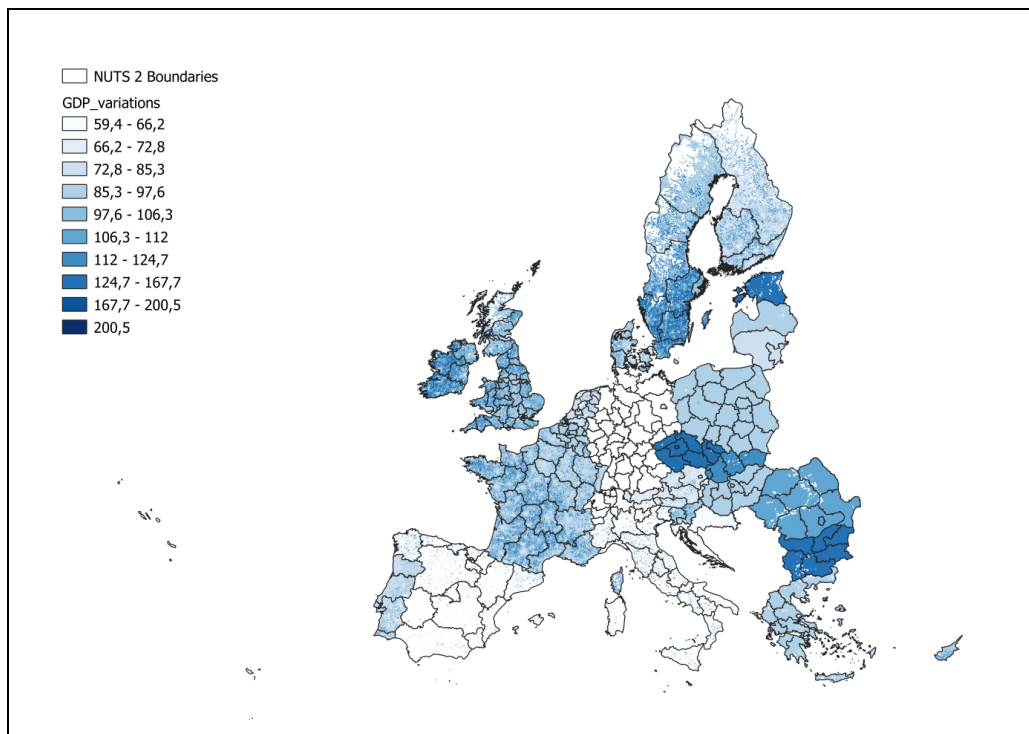
Figure 44: Percentage change in GDP levels from 2015 to 2050 in the scenario S2R60
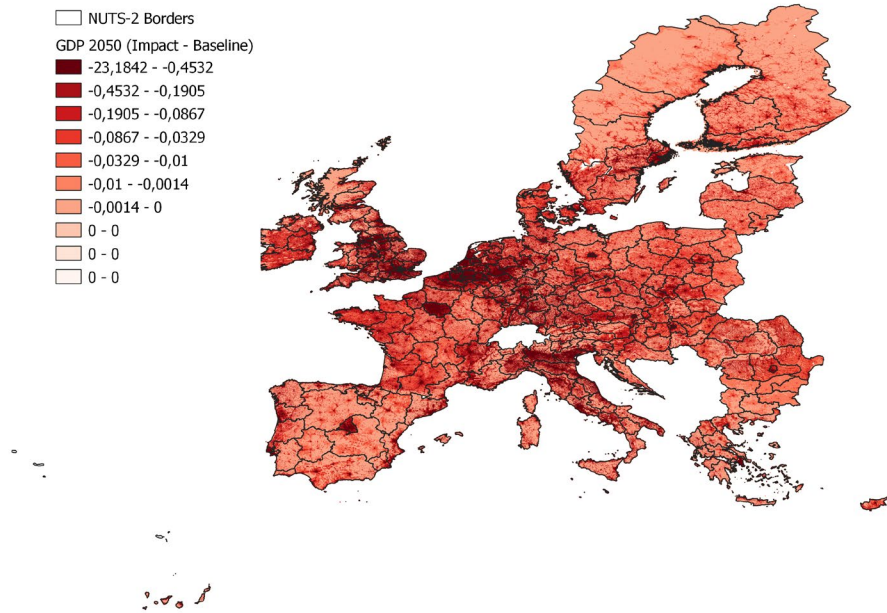
Figure 45: Delta of GDP levels in 2050 comparing the baseline and medium impact scenario of S1R26 – High EU Investment mobility (million 2007 USD)
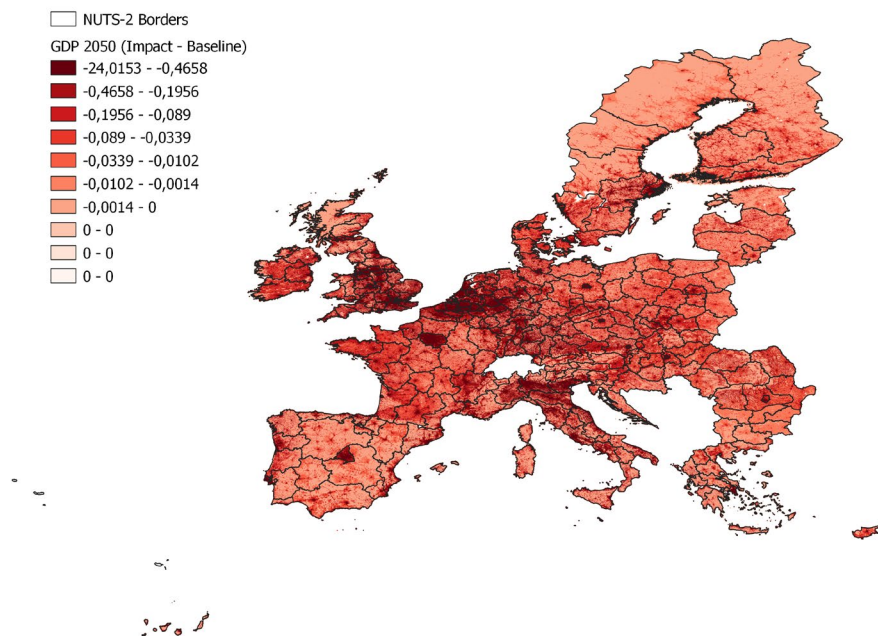
Figure 46: Delta of GDP levels in 2050 comparing the baseline and medium impact scenario of S1R26 – Low EU Investment mobility (million 2007 USD)

Figure 47: Delta of GDP levels in 2050 comparing the baseline and the medium impact scenario of S2R60 – High EU Investment mobility (million 2007 USD)

Figure 48: Delta of GDP levels in 2050 comparing the baseline and the medium impact scenario of S2R60 – Low EU Investment mobility (million 2007 USD)

3.1.6   Concluding Remarks

This exercise resulted in a more precise distribution of the GDP levels and their changes over time and across different climate impacts.

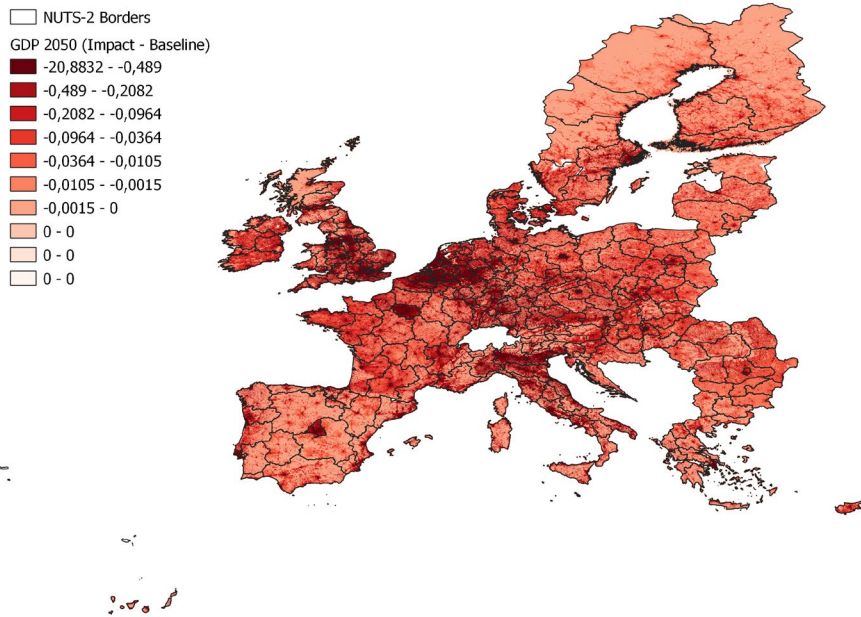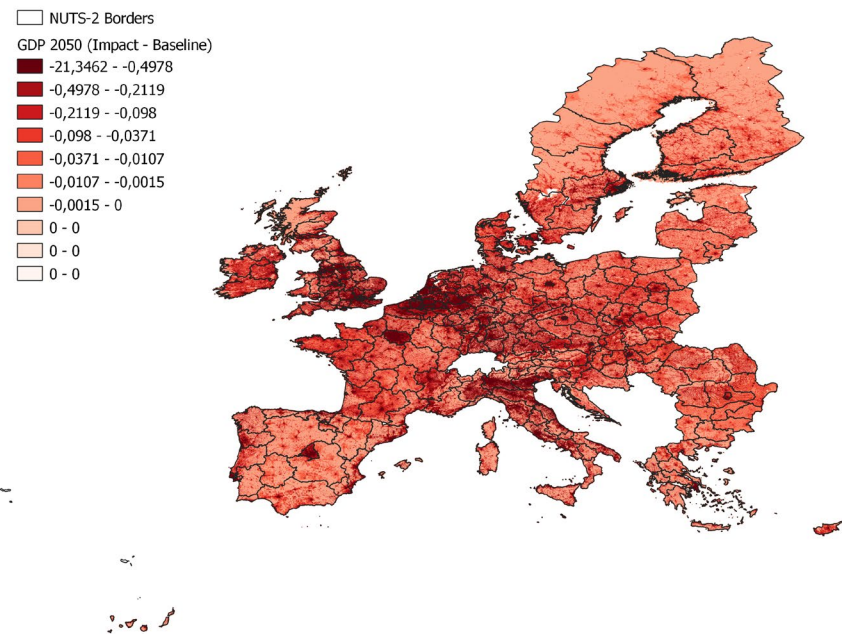Due to the focus on the urban area variable, the final distribution of the GDP levels follows closely that of cities and other population centres. However, having based our projections of the artificial area on the grids' total population should mitigate the omission of rural areas. Moreover, given that urban area is a rather inelastic variable, the GDP distribution in space is rather stable across scenarios, the main variations due to the impacts and the change in population levels.

As a caveat, additional refinements to the econometric model should be tested, as well as some robustness checks and validation procedures. For instance, it would be interesting to retake the analysis with a generalized linear method and with other distributions that could better fit the data, although, given the fine spatial resolution of 1 Km, the computational burden is relevant. Moreover, more involved random effects and additional time-varying variables could help in obtaining more precise results.

Besides the visualization of the climate impacts, this exercise could act as a solid base to develop more complex methods that can be useful to represent a significant spatial change in the GDP distribution due to the climate impacts.

A promising example regards the differentiation of climate shocks: if a shock could be categorized appropriately concerning its impact on a variable that can be included in this method, then also the spatial distribution will change within the given region in the same scenario. Our methodology allows this inclusion of shocks effects through different channels that could then be modelled as parameters affecting the within-region distribution.

Indeed, many of the already considered variables would be affected by climate shocks: for instance, climate shocks affecting coasts could be amplified in the grids located near the ocean. Another interesting extension is to add the CLC classification of rural areas. Disaggregating then the classification of CLC rural and artificial area to more detailed levels could permit to classify the shocks to different crops and economic activities.

To conclude, downscaling the projections of GDP changes due to different scenarios and climate impacts is a relevant exercise, as it laid the base towards a properly spatial understanding of what is to come at resolutions far lower than the ones employed by climate assessment models. This information could be very relevant to the policymaker, as the latter could therefore apply its finite resources in a far more precise and efficient effort to prevent and contrast the effects of climate change.

4   Distributional implications of climate change for the EU

4.1   Introduction

Several studies have looked into the distributional impacts of climate change. Dell et al. (2012) have investigated the impacts of poor and non-poor countries[7]. Results have shown that economic growth in poorer countries are negatively affected by increasing temperatures, whereas results for non-poor countries are not robust. Mendelssohn et al. (2006) have looked into future impacts of climate change in countries grouped by income quartile (with GDP per capita as the benchmark). Their results showed that, in terms of impacts as a share of GDP, the lowest income quartile has a larger estimated damage, and the damage declines as income quartiles increase. Two hypotheses were presented and tested: (1) could the damage be due to severity of climate change for poor countries? The answer was: not really. Even with the same magnitude of changes, the future distribution of impacts shows the same. (2) Could the impact be due to poorer countries located in lower altitudes that already experience higher temperatures? The answer was: Yes, but it's not the only reason. Mendelsohn et al. speculate that this could be due to the share of climate-sensitive sectors being higher in poorer countries, and generally to lower technology. Park et al. (2018) looks more closely into household level exposure bias, and found that 37 of the 51 countries analyzed have a positive Poverty Exposure Bias, indicating that more of the poorest quintile are exposed to extreme temperatures that the country average. Using Ordinary Least Squares, majority of the countries with negative relationship between temperature in the hottest month and wealth percentile of households are tropical countries with already hot average climate. For countries with average temperatures below 20°C, the opposite relationship is seen. Furthermore, there is a clear negative relationship between occupational exposure and household wealth within 47 countries included in the analysis.

This chapter contributes to the current scientific knowledge by investigating the distributional impacts of climate change in the EU at the NUTS2 level using, not only current climates, but also multiple variables relating to human development, with corresponding projections under the Shared Socioeconomic Pathways (SSPs). The analysis takes the perspective of adaptive capacity, represented by human development indicators, as a factor in changing the magnitude of impacts in the future, and considers in-country disparities at the NUTS2 level.

---

[7] Poor countries defined as having below-median PPP-adjusted per-capita GDP in the first year the country enters the dataset.

4.2 Data

Two impact datasets are sourced from the outputs of the H2020 COACCH project: (1) impacts to agriculture of which impacts to crops can be separately analyzed, and (2) impacts to the gross domestic product (GDP). Historical data of human development indicators are sourced from the Eurostat (ESTAT), while the projections are sourced from the ICES model (CMCC) and SSP2 (Lutz et al., 2018). Agricultural impacts taken as 30-year averages around the 10-year time-step (e.g. for 2020 2005-2035), are projected by the biophysical model EPIC. GDP losses are projected with the CGE model ICES, which include nine climate impacts from the same H2020 project: Agriculture, Forestry, Fisheries, Sea level rise, Riverine floods, Transport, Energy demand, Energy supply and Labour productivity, as described in the first part of this deliverable. Population density is computed by dividing the total population by the total land area in square kilometers (as of 2016 from ESTAT). Table 5 presents the details of each indicator.

Table 5: Indicator description

General category	*Specific indicators*	*Spatial resolution*	*Unit*	*Source*
H2020 COACCH Impacts	Impacts to crops	NUTS 2, NUTS 0	Gross value-added, constant prices	IIASA
	Impacts to total agriculture	NUTS 2, NUTS 0	Gross value-added, constant prices	IIASA
	Impacts to GDP	NUTS 2, NUTS 0	Percent change	CMCC
Income	Gross value-added by sector	NUTS 2, NUTS 0	Gross value-added, constant prices	ESTAT
	GDP per capita	NUTS 2, NUTS 0	Million Euros per person	ESTAT
	Population by sex	NUTS 2, NUTS 0	Persons	ESTAT
Education	Percent of population (15-64) by educational attainment	NUTS 2, NUTS 0	Percent	ESTAT
Health	Life expectancy at birth by sex	NUTS 2, NUTS 0	Years	ESTAT
SSP2 projections	GDP PPP (constant 2005 USD)[1,2] GDP MER[3]	NUTS 2[3], NUTS 0[1]	Billion USD	ICES model, OECD
	Population by sex	NUTS 2[3], NUTS 0[2]	Persons	ICES model, Lutz et al. (2018)
	Percent of population (15-64) by educational attainment and sex [3]	NUTS 0	Percent	Lutz et al. (2018)
	Life expectancy at birth by sex[3]	NUTS 0	Years	Lutz et al. (2018)
Climate Indicators	Mean annual temperature (historical)	NUTS 2	degrees Celsius	

[1] *Source: OECD;* [2]*Source: Wittgenstein Centre, Human Capital Data Explorer with data from Lutz, Goujon, KC, Stonawski, and Stilianakis (Eds.) (2018);* [3] *GDP and Population projections from the ICES model, consistent with the SSPs (https://tntcat.iiasa.ac.at/SspDb/dsd?Action=htmlpage&page=10).*

4.3   Methodology

Unlike existing global studies (Mendelsohn, 2006; Tol et al., 2003) wherein a clear trend can be seen between the per capita income of countries and climate impacts, the results for the EU countries is less clear.

The methodology of this research, therefore, extends the method in Mendelsohn et al. (2006), such that more indicators are considered in determining the distribution of economic impacts, using a model-based cluster analysis. The parameters considered in the analysis are selected, based on the results of existing publications such as income and initial levels of temperature, as well as the components of the Human Development Index (HDI)[8] to include possible determinants of adaptive capacity. The components referring to development consider initial levels, as well as projected levels as specified in the SSPs.

4.3.1   Gaussian finite mixture modelling

A probability density function defined by a finite mixture model specified the distribution of observations in $x = \{x_1, x_2, \ldots, x_n\}$. In a Gaussian mixture model, this distribution takes the form

$$f(x_i; \psi) = \sum_{k=1}^{G} \pi_k f_k(x_i; \theta_k), \text{ where } f_k(x_i; \theta_k) \sim \mathcal{N}(\mu_k; \Sigma_k)$$

ψ contains the parameters of the mixture model, f_k is the kth component density for observation x_i with parameter vector θ_k, π_k are the mixing weights, and G is the number of mixture components. The component density is normally distributed around a mean vector, μ_k, and other geometric characteristics determined by the covariance, Σ_k. In this study, a multivariate parameterization of covariance matrices is implemented, thus allowing the volume, shape, and orientation of the covariances to be either equal or variable across groups. The optimal number of components, G, and the covariance parameterization is determined by using the Bayesian Information Criterion (BIC) for all models considered. Assuming that G is obtained and fixed, a maximum likelihood estimator (MLE) of the finite mixture model is calculated using the expectation-maximization (EM) algorithm. Each component of the finite mixture density is associated to a cluster.

In order to have a 1 x N matrix for each of the variables in the cluster analysis, the following aggregations have been done as shown in Table 6:

---

[8] Health, education, standard of living. Other forms of HDI include adjustments for income and gender inequality, which are treated as separate indicators in this analysis.

Table 6: Data aggregation

Variable	Temporal aggregation	Scenario filters	Other filters
Historical data on temperature, income, education, health, population density	Average from 2010-2015	None	none
Projections of temperature, income, education[1], health[2], population density	The difference of the 30-year average for temperature, and 10-year average for income, education, and health to the historical data	SSP2, with growth rates for the country applied to all NUTS 2 regions.	none
COACCH impact - Agriculture and Crops	Impact at 2050	SSP2, RCP 2.6	With CO2 fertilization, constant prices, mean impact
COACCH impact - GDP	Impact at 2050	SSP2, RCP 2.6	Mean impact

[1] *Population projection by education for 5-year time steps on a NUTS 0 level. The variable has been transformed to reflect the share of the change in population over 15 years old in each of the education levels (Level 0-2: no education, incomplete primary, primary, lower secondary; Level 3-4: upper secondary, short post-secondary, post-secondary; and Level 5-8: bachelor, master and higher) relative to the change in total population. Base year is 2015. For this analysis, we only consider the change in population of education level 5-8.* [2] *Life expectancy represents the number of years a newborn is expected to live. The variable has been transformed to reflect the change in number of expected life years in the future relative to 2015.*

The aggregation results in a cross-sectional dataset by NUTS2 region. The values are standardized to reflect comparable variations across variables before they are subjected to the model-based clustering method.

4.3.2 Cluster analysis relevant for the distributional impacts of climate change

We perform a correlation analysis on all the variables before clustering to gain an insight on pairs of variables (Figure 49). Then, we perform the model-based clustering for two purposes: first, to have a systematic grouping of NUTS2 regions based on a multivariate set of components; and second, to be able to compare the mean values across clusters to find any emerging patterns between future climate change impacts and the other socioeconomic variables at present and in the future.

4.4 Results

4.4.1 Correlation

The results of the correlation analysis show that there is a strong negative correlation between GDP impact and current temperature, such warmer NUTS2 regions are expected to have lower (climate change-adjusted) GDP in 2050. A higher projected GDP impact in 2050, referring to the estimated change in GDP relative to a no climate change scenario, is also positively correlated a higher share of the population having tertiary education presently and in the future, higher life expectancy, and a lower population density.
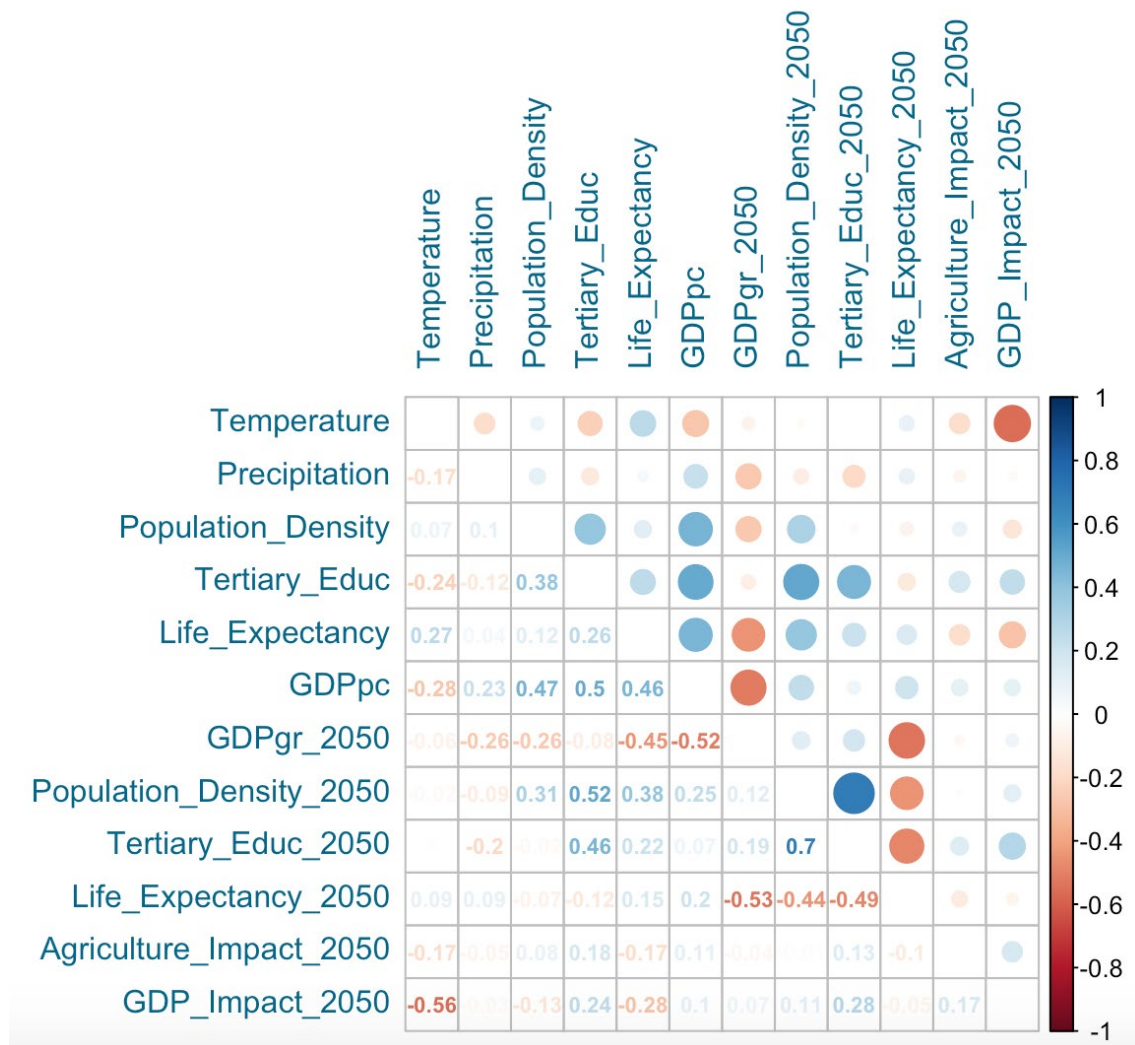

Figure 49: Correlation analysis for main data indicators

4.4.2 Cluster Analysis

The results of the model selection using BIC refer to an optimal of nine clusters, and a covariance parameterization that suggests an ellipsoidal distribution with equal volume, equal shape, and a variable orientation (EEV). The orientation of clusters is also defined, supporting the use of the model-based clustering (Figure 50)
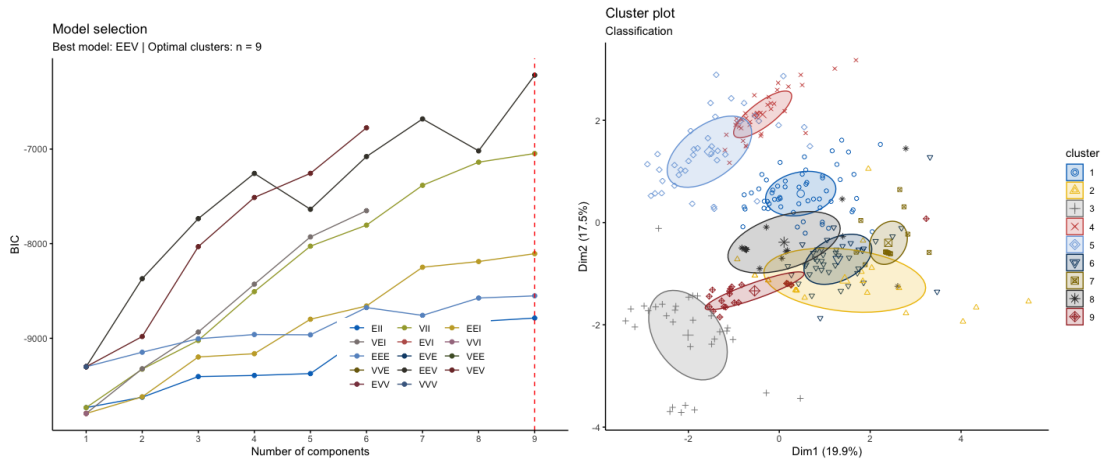
Figure 50
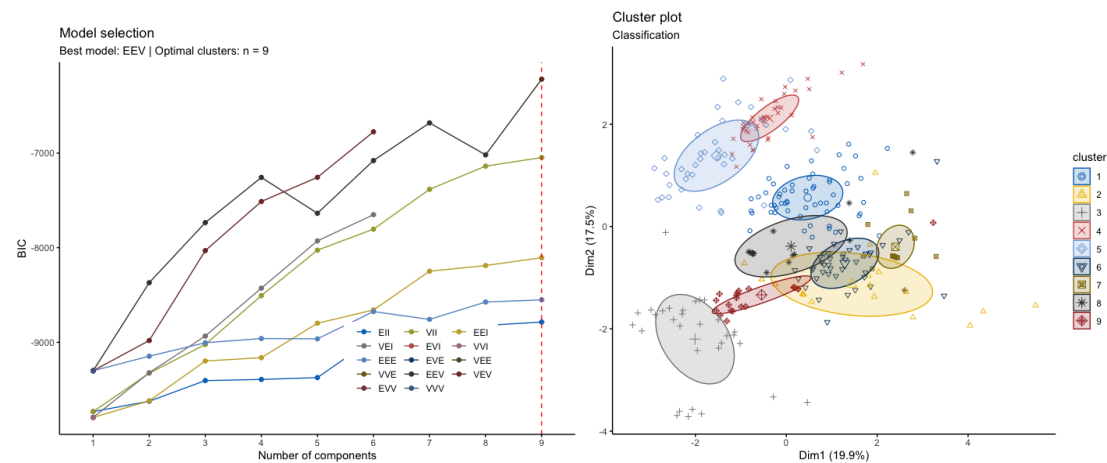
Figure 50: Results of the model-based cluster analysis showing the optimal number of clusters using the BIC as the criterion, and a graphical representation of data points grouped into the optimal number of clusters, where a Principal Component Analysis (PCA) is performed to represent the group of variables to two dimensions ('Dim1' and 'Dim 2').

Figure 51 below presents the mean parameter values of the standardized deviation from the sample mean for each of the variables.

Figure 51: Mean parameter values in each cluster by variable.

Projected GDP impact in 2050

The results suggest that regions with the largest projected GDP loss in 2050 are present in **Cluster 5**, and are the same regions with the warmest climate, the lowest share of the population with tertiary education, relatively low current population density and G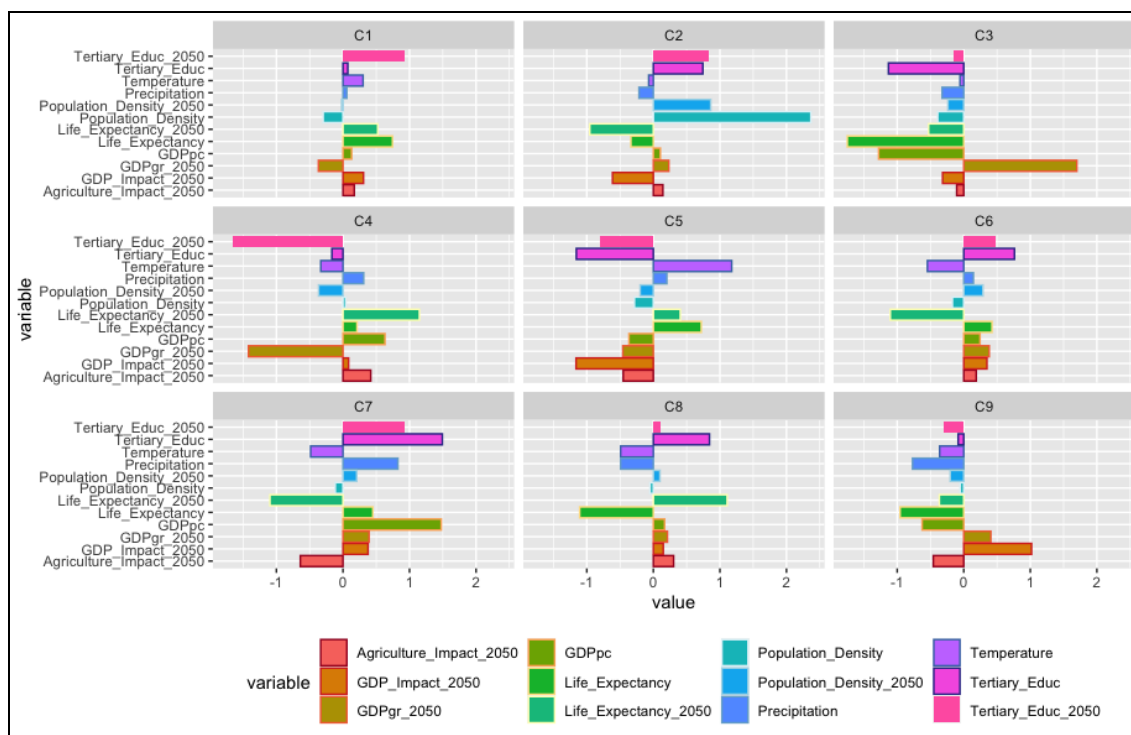DP per capita, and above average life expectancy among the EU-27 + UK countries. In terms of future changes in socioeconomic indicators under SSP2, the same group of NUTS2 regions also show one of the lowest projected shares of the population with tertiary education in 2050. Belonging to this cluster are regions in Spain, Italy, and Portugal.

The highest mean GDP gainers are NUTS2 regions grouped under **Cluster 9**, which show an above average projected GDP growth, relatively cool climate with the lowest precipitation. The same cluster also shows values below the mean for all other socioeconomic variables, both current and in the future particularly life expectancy.

Other cluster characteristics

Cluster 1 *(high future education, high life expectancy)* is expected to experience moderate gains in GDP with climate change and Agriculture due to climate change. Regions belonging to this cluster have relatively warmer climates, below average population density, a large improvement in the share of the population having tertiary education in 2050, and high life expectancy, currently and in the future.

Cluster 2 *(highest population density, high education, low life expectancy)* show relatively greater losses in GDP and above average increases in agricultural production due to climate change. Regions in this cluster experience moderate climates and slightly below average precipitation compared to other clusters. The regions also have the highest population density, currently and in the future, and a relatively large share of population having tertiary education currently and low life expectancy in the future.

Cluster 3 *(low socioeconomic characteristics, high GDP without CC)* is characterized by the lowest life expectancy, current GDP per capita, and among the smallest share of the population with tertiary education. The regions belonging to this cluster have below-average population density, relatively dry, yet cool climate. Despite the highest projection of GDP in 2050, GDP impacts due to climate change are expected to be greater than the sample average.

Cluster 4 *(lowest future education, high future life expectancy, lowest GDP without CC)* is characterized by the highest life expectancy in the future, but has the lowest share of the population having tertiary education and projected GDP growth in the future. Regions in this cluster experience below average climate, above average precipitation, and relatively higher GDP per capita; and are expected to have above average increases in GDP and agriculture due to climate change.

Cluster 6 *(low temperature, high education, low future life expectancy)* include regions experiencing cooler climates, above average life expectancy, a relatively large share of the population with tertiary education, and GDP per capita in the EU. The regions in this cluster are expected to have above-average GDP with climate change and higher projected agricultural production relative to the rest of the EU in 2050.

Cluster 7 *(highest education, highest GDP per capita, low temperature, high precipitation, low future life expectancy)* is characterized by the highest share of the population having tertiary education, and the highest GDP per capita in the EU. Regions belonging to this cluster also show a combination of the highest amount of precipitation and a cool climate; a moderately low population density. In terms of impacts, the regions in this cluster show a higher increase in GDP with climate change compared to other clusters, but a larger negative agricultural impact due to climate change.

Cluster 8 *(low temperature and precipitation, low life expectancy but high improvement in the future, high current education)* represent regions that have a relatively cooler and dry climate compared to the rest of the EU. The regions in this cluster is expected to have a relatively higher GDP and agriculture production due to climate change in 2050 compared to the rest of the EU. In terms of socioeconomic characteristics, regions in this cluster have a high share of the population with tertiary education, higher than average GDP per capita, average population density, and among the lowest life expectancy, however is projected to have large improvements in life expectancy in 2050.

4.5 Conclusions and recommendations for further study

This study aimed at systematically investigating the distributional impacts of climate change in the context of current values of temperature and human development indicators, as well as changes in these indicators in the future. The pairwise correlation suggest that NUTS 2 regions with warmer climates tend to have lower projected GDP due to climate change. An improvement in health and higher education relates to higher GDP in the future, despite climate change impacts. The correlation to development indicators is, however, weak.

In analyzing all the components together, the results show that, while we see relatively low values of education and per capita income at present and in the future, and the warmest climate among the regions being associated with the largest losses in GDP due to climate change in a single cluster, we do not see a clear pattern in relation to the largest GDP gains due to climate change. The various combinations of levels of higher education, efforts to improve health, and population density, coupled with diverse climates, result in different levels of expected economic growth in the future, and consequently, the resilience of each to withstand climate change. The results suggest that initial levels of temperature may play a role in determining the GDP impacts due to climate change, however, it is not the only determinant.

Further study is needed to understand the dynamics between the development indicators and the possible impact of climate change to GDP, in order to get a grasp of the magnitude of contribution of each. The results presented here, while showing the importance of development as a means to reduce GDP impacts of climate change, correlate development components to estimated GDP impacts (mainly representing an income channel) which are highly influenced by the composition of the models from which the economic impacts are projected; and similarly, the projections of the socioeconomic variables are also determined by the model simulations.

Appendix 2

Cluster	Cluster members[9]
1	"AT11" "AT12" "AT21" "AT22" "AT31" "AT32" "AT33" "AT34" "BE22" "BE23" "BE24" "BE25" "BE31" "ES11" "ES12" "ES13" "ES21" "ES22" "ES23" "ES24" "ES41" "ES42" "ES43" "ES51" "ES52" "ES53" "ES61" "ES62" "FR21" "FR22" "FR23" "FR24" "FR25" "FR26" "FR41" "FR42" "FR43" "FR51" "FR52" "FR53" "FR61" "FR62" "FR63" "FR71" "FR72" "FR81" "FR82" "FR83" "NL11" "NL12" "NL13" "NL21" "NL22" "NL23" "NL34" "NL41" "NL42"
2	"ES30" "FI19" "FI1C" "FI1D" "FI20" "HU10" "RO32" "SI03" "UKD3" "UKD7" "UKG3" "UKI5" "UKI6" "UKI7"
3	"BG31" "BG32" "BG33" "BG34" "BG41" "BG42" "CZ02" "CZ03" "CZ04" "CZ05" "CZ06" "CZ07" "CZ08" "EE00" "HU21" "HU22" "HU23" "HU31" "HU32" "HU33" "LV00" "RO11" "RO12" "RO21" "RO22" "RO31" "RO41" "RO42" "SK02" "SK03" "SK04"
4	"DE11" "DE12" "DE13" "DE14" "DE21" "DE22" "DE23" "DE24" "DE25" "DE26" "DE27" "DE30" "DE40" "DE50" "DE60" "DE71" "DE72" "DE73" "DE80" "DE91" "DE92" "DE93" "DE94" "DEA1" "DEA2" "DEA3" "DEA4" "DEA5" "DEB1" "DEB2" "DEB3" "DEC0" "DED2" "DED4" "DED5" "DEE0" "DEF0" "DEG0"
5	"EL30" "EL41" "EL42" "EL43" "EL51" "EL52" "EL53" "EL54" "EL61" "EL62" "EL63" "EL64" "EL65" "ITC1" "ITC2" "ITC3" "ITC4" "ITF1" "ITF2" "ITF3" "ITF4" "ITF5" "ITF6" "ITG1" "ITG2" "ITH1" "ITH2" "ITH3" "ITH4" "ITH5" "ITI1" "ITI2" "ITI3" "ITI4" "PT11" "PT15" "PT16" "PT17" "PT18"
6	"DK01" "DK02" "DK03" "DK04" "DK05" "IE01" "LU00" "SE11" "SE12" "SE21" "SE22" "SE23" "SE31" "SE32" "SE33" "UKC1" "UKC2" "UKD1" "UKD4" "UKD6" "UKE1" "UKE2" "UKE3" "UKE4" "UKF1" "UKF2" "UKF3" "UKG1" "UKG2" "UKH1" "UKH2" "UKH3" "UKJ1" "UKJ2" "UKJ3" "UKJ4" "UKK2" "UKK3" "UKK4" "UKL2" "UKM6" "UKN0"
7	"FI1B" "IE02" "NL31" "NL32" "NL33" "SI04" "UKK1" "UKM5"
8	"BE21" "BE32" "BE33" "BE34" "BE35" "CZ01" "FR10" "FR30" "LT00" "SK01"
9	"AT13" "PL11" "PL12" "PL21" "PL22" "PL31" "PL32" "PL33" "PL34" "PL41" "PL42" "PL43" "PL51" "PL52" "PL61" "PL62" "PL63"

---

[9] Clustering is only possible for complete entries and the following regions with missing data were taken out from the dataset: Missing agricultural impact: MT00, HR03, HR04, ES63, ES64, ES70, BE10, UKI3, UKI4; missing life expectancy data: UKM7, UKM8, UKM9; No climate data: UKL1; No agricultural impacts nor data on education: CY00.

References

Asadoorian, M. O. (2008). Simulating the spatial distribution of population and emissions to 2100. Environmental and Resource Economics, 39(3), 199-221.

Balkovič, J., van der Velde, M., Schmid, E., Skalský, R., Khabarov, N., Obersteiner, M., ... & Xiong, W. (2013). Pan-European crop modelling with EPIC: Implementation, up-scaling and regional crop yield validation. Agricultural Systems, 120, 61-75.

Bates, D., Maechler, M., Bolker, B., Walker, S., Christensen, R. H. B., Singmann, H., ... & Green, P. (2018). Package 'lme4'. Version, 1, 17

Bengtsson, M., Shen, Y., & Oki, T. (2006). A SRES-based gridded global population dataset for 1990–2100. Population and Environment, 28(2), 113-131.

Blanchard, J. L., Jennings, S., Holmes, R., Harle, J., Merino, G., Allen, J. I., ... & Barange, M. (2012). Potential consequences of climate change for primary production and fish production in large marine ecosystems. Philosophical Transactions of the Royal Society B: Biological Sciences, 367(1605), 2979-2989.

Boere, E., Valin, H., Bodirsky, B. Baier, F., Balkovic, J., Batka, M., Folberth, C., Karstens, K., Kindermann, G., Krasovskii, A., Leclere, D., Wang, X., Weindl, I., Havlik, P., Lotze-Campen, H. (2019). D2.2 Impacts on agriculture including forestry & fishery. Deliverable of the H2020 COACCH project.

Bondeau, A., Smith, P. C., Zaehle, S., Schaphoff, S., Lucht, W., Cramer, W., ... & Smith, B. (2007). Modelling the role of agriculture for the 20th century global terrestrial carbon balance. Global Change Biology, 13(3), 679-706.

Bosello, F., Eboli, F., Pierfederici, R. (2012b) Assessing the economic impacts of climate change. An updated CGE point of view, working papers 2012.02, Fondazione Eni Enrico Mattei.

Bosello, F., Nicholls, R.J., Richards, J., Roson, R., & Tol, R. (2012a) Economic impacts of climate change in Europe: sea-level rise. Climatic Change, 112:63–81.

Bosello, F., Roson, R., & Tol, R. (2007). Economy-wide Estimates of the Implications of Climate Change: Sea Level Rise. Environmental & Resource Economics, European Association of Environmental and Resource Economists, vol. 37(3), pages 549-571, July.

Bosello, F., Parrado, R.M., Standardi, G. (2019). ICES NUTS-2 model calibrated on the selected set of scenarios. Milestone 8 of the H2020 COACCH project.

Botzen, W., Ignjacevic, P., Kuik, O., Tesselaar, M., Tiggeloven, T., Bachner, G., Bednar-Friedl, B., Grossmann, W., Knittel, N., Steininger, K., Williges, K., Bosello, F., Dasgupta, S., Standardi, G., Parrado, R., Watkiss, P., Cimato, F., Hunt, A., Boere, E., Valin, H., Hinkel, J., Lincke, D., Costa, A.L., van Ginkel, K., de Groen, F., Haasnoot, M. and A. Jeuken (2020). D3.4 Social-economic Tipping Point Analysis. Deliverable of the H2020 COACCH project.

Burke, M., S. Hsiang, and E. Miguel. (2015). Global non-linear effect of temperature on economic production. Nature; 527,235–239, doi:10.1038/nature15725.

Cheung, William W. L., Gabriel Reygondeau, and Thomas L. Frölicher. 2016. 'Large Benefits to Marine Fisheries of Meeting the 1.5°C Global Warming Target'. Science 354 (6319): 1591–94.

De Cian, E. and Sue Wing, I.(2017). Global energy consumption in a warming climate. Environ Resource Econ. 1–46. https://doi.org/10.1007/s10640-017-0198-4.

Dellink, R., Lanzi, E., & Chateau, J. (2019). The Sectoral and Regional Economic Consequences of Climate Change to 2060. Environmental and Resource Economics, 72(2), 309–363. https://doi.org/10.1007/s10640-017-0197-5

Enerdata (2018). Available at: https://www.enerdata.net/research/energy-market-data-co2-emissions-database.html

ECORYS, (2012). Mapping resource prices: the past and the future. Avaialable at: https://ec.europa.eu/environment/enveco/resource_efficiency/pdf/studies/report_mapping_resource_prices.pdf

Fang, Y., & Jawitz, J. W. (2018). High-resolution reconstruction of the United States human population distribution, 1790 to 2010. Scientific data, 5, 180067.

Feyen L., Ciscar J.C., Gosling S., Ibarreta D., Soria A. (editors) (2020). Climate change impacts and adaptation in Europe. JRC PESETA IV final report. EUR 30180EN, Publications Office of the European Union, Luxembourg, ISBN 978-92-76-18123-1, doi:10.2760/171121, JRC119178.

Fujimori, S., Abe, M., Kinoshita, T., Hasegawa, T., Kawase, H., Kushida, K., ... & Tatebe, H. (2017). Downscaling global emissions and its implications derived from climate model experiments. PloS one, 12(1).

Gaffin, S. R., Rosenzweig, C., Xing, X., & Yetman, G. (2004). Downscaling and geo-spatial gridding of socioeconomic projections from the IPCC Special Report on Emissions Scenarios (SRES). Global Environmental Change, 14(2), 105-123.

Gonzalez Aparicio, I., Zucker, A., Careri, F., Monforti, F., Huld, T., Badger, J. (2016). EMHIRES dataset. Part I: Wind power generation European Meteorological

derived High-resolution RES generation time series for present and future scenarios; EUR 28171EN; 10.2790/831549.

Grübler, A., O'Neill, B., Riahi, K., Chirkov, V., Goujon, A., Kolp, P., ... & Slentoe, E. (2007). Regional, national, and spatially explicit scenarios of demographic and economic change based on SRES. Technological forecasting and social change, 74(7), 980-1029.

Hachadoorian, L., Gaffin, S. R., & Engelman, R. (2011). Projecting a gridded population of the world using ratio methods of trend extrapolation. In Human population (pp. 13-25). Springer, Berlin, Heidelberg.

Havlík, P., Schneider, U. A., Schmid, E., Böttcher, H., Fritz, S., Skalský, R., ... & Leduc, S. (2011). Global land-use implications of first and second generation biofuel targets. Energy policy, 39(10), 5690-5702.

Kindermann, G., M. Obersteiner, et al. (2008). Global cost estimates of reducing carbon emissions through avoided deforestation. Proceedings of the National Academy of Sciences of the United States of America 105(30): 10302-10307.

Jones, B., & O'Neill, B. C. (2013). Historically grounded spatial population projections for the continental United States. Environmental Research Letters, 8(4), 044021.

Jones, B., & O'Neill, B. C. (2016). Spatially explicit global population scenarios consistent with the Shared Socioeconomic Pathways. Environmental Research Letters, 11(8), 084003.

Klein Goldewijk, K., Beusen, A., Van Drecht, G., & De Vos, M. (2011). The HYDE 3.1 spatially explicit database of human-induced global land-use change over the past 12,000 years. Global Ecology and Biogeography, 20(1), 73-86.

Kummu, M., Taka, M., & Guillaume, J. H. (2018). Gridded global datasets for gross domestic product and Human Development Index over 1990–2015. Scientific data, 5, 180004.

Lincke, D., Hinkel, H., van Ginkel, K., Jeuken, A., Botzen, W., Tesselaar, M., Scoccimarro, E., Ignjacevic, P. (2019). D2.3 Impacts on infrastructure, built environment, and transport Deliverable of the H2020 COACCH project.

McKee, J. J., Rose, A. N., Bright, E. A., Huynh, T., & Bhaduri, B. L. (2015). Locally adaptive, spatially explicit projection of US population for 2030 and 2050. Proceedings of the National Academy of Sciences, 112(5), 1344-1349.

Meijer, J.R., Huijbegts, M.A.J., Schotten, C.G.J. and Schipper, A.M. (2018): Global patterns of current and future road infrastructure. Environmental Research Letters, 13-064006. Data is available at www.globio.info

Mendelsohn, R., Dinar, A., & Williams, L. (2006). The distributional impact of climate change on rich and poor countries. Environment and Development Economics, 11(2), 159-178. doi:10.1017/S1355770X05002755

Merkens, J. L., Reimann, L., Hinkel, J., & Vafeidis, A. T. (2016). Gridded population projections for the coastal zone under the Shared Socioeconomic Pathways. Global and Planetary Change, 145, 57-66.

Murakami, D., & Yamagata, Y. (2019). Estimation of gridded population and GDP scenarios with spatially explicit statistical downscaling. Sustainability, 11(7), 2106.

Murakami, D. and Yamagata, Y. (2016) Estimation of gridded population and GDP scenarios with spatially explicit statistical downscaling, ArXiv, 1610.09041, URL: https://arxiv.org/abs/1610.09041.

Nam, K. M., & Reilly, J. M. (2013). City size distribution as a function of socioeconomic conditions: an eclectic approach to downscaling global population. Urban Studies, 50(1), 208-225.

Newell, R.G., Prest, B.C. and Sexton, S.E. (2018). The GDP Temperature Relationship: Implications for Climate Change Damages. RFF Working Paper Series, WP 18-17 REV. Available at http://www.rff.org/research/publications/gdp-temperature-relationship-implicati ons- climate-change-damages

Nordhaus, W.D. (2011). Integrated Economic and Climate Modeling. Yale University Cowles Foundation for Research in Economics, Discussion Paper 1839.

Park, J., Bangalore, M., Hallegatte, S., & Sandhoefner, E. (2018). Households and heat stress: Estimating the distributional consequences of climate change. Environment and Development Economics, 23(3), 349-368. doi:10.1017/S1355770X1800013X

Parrado, R., Bosello, F., Delpiazzo, E., Hinkel, J., Lincke, D., & Brown, S. (2020). Fiscal effects and the potential implications on economic growth of sea-level rise impacts and coastal zone protection. Climatic Change, 1-20.

Raftery, A. E., Li, N., Ševčíková, H., Gerland, P., & Heilig, G. K. (2012). Bayesian probabilistic population projections for all countries. Proceedings of the National Academy of Sciences, 109(35), 13915-13921.

Reimann, L., Merkens, J. L., & Vafeidis, A. T. (2018). Regionalized Shared Socioeconomic Pathways: narratives and spatial population projections for the Mediterranean coastal zone. Regional environmental change, 18(1), 235-245.

Rodell M, HouserPR, JamborU, GottschalckJ, MitchellK, MengC-J, ArsenaultK, CosgroveB, RadakovichJ, BosilovichM, EntinJK, WalkerJP, Toll DL (2004) The Global Land Data Assimilation System.Bull AmerMeteorolSoc85:381-394, doi:10.1175/BAMS-85-3-381.

Schleypen, J.R., Dasgupta, S., Borsky, S., Jury, M., Ščasný, M., Bezhanishvili, L. (2019). D2.4 Impacts on Industry, Energy, Services, and Trade. Deliverable of the H2020 COACCH project.

Succra, L., Fop, M., Murphy, T. B., Raftery, A. E. (2016). mclust 5: Clustering, Classification and Density Estimation Using Gaussian Finite Mixture Models. The R Journal Vol. 8/1, Aug. URL: https://journal.r-project.org/archive/2016/RJ-2016-021/RJ-2016-021.pdf

Swan, L. G., & Ugursal, V. I. (2009). Modeling of end-use energy consumption in the residential sector: A review of modeling techniques. Renewable and sustainable energy reviews, 13(8), 1819-1835.

Tol, R.S.J., Downing, T.E., Kuik, O.J., Smith, J. B. (2003). Distributional Aspects of Climate Change Impacts. OECD Workshop on the Benefits of Climate Policy: Improving Information for Policy Makers.

van Ginkel, K. C. H., Dottori, F., Alfieri, L., Feyen, L., and Koks, E. E.: Direct flood risk assessment of the European road network: an object-based approach, Nat. Hazards Earth Syst. Sci. Discuss., https://doi.org/10.5194/nhess-2020-104, in review, 2020. https://nhess.copernicus.org/preprints/nhess-2020-104/

van Vuuren, D. P., Lucas, P. L., & Hilderink, H. (2007). Downscaling drivers of global environmental change: Enabling use of global SRES scenarios at the national and grid levels. Global environmental change, 17(1), 114-130

West, B. T., Welch, K. B., & Galecki, A. T. (2014). Linear mixed models: a practical guide using statistical software. CRC Press.

Ward, P.J., H.C. Winsemius, S. Kuzma, M.F.P. Bierkens, A. Bouwman, H. de Moel, A. Díaz Loaiza, et al. 2020. "Aqueduct Floods Methodology." Technical Note. Washington, D.C.: World Resources Institute. Available online at: www.wri.org/publication/aqueduct-floods-methodology.

Ward, P. J., Jongman, B., Aerts, J.C.J.H., Bates, P.D., Botzen, W.J.W., DIaz Loaiza, A., Hallegatte, S., Kind, J.M., Kwadijk, J., Scussolini, P., Winsemius, H.C., 2017. A global framework for future costs and benefits of river-flood protection in urban areas. Nat. Clim. Chang. https://doi.org/10.1038/nclimate3350

Winsemius, H. C., Aerts, J. C., van Beek, L. P., Bierkens, M. F., Bouwman, A., Jongman, B., ... & Ward, P. J. (2016). Global drivers of future river flood risk. Nature Climate Change, 6(4), 381.

Yamagata, Y., Murakami, D., & Seya, H. (2015). A comparison of grid-level residential electricity demand scenarios in Japan for 2050. Applied Energy, 158, 255-262.